



Identifying a role for the  
*Dictyostelium discoideum*  $\gamma$ -  
secretase complex in endocytosis  
and autophagy

Devdutt Sharma

Royal Holloway, University of  
London

Ph.D. Biology

Declaration of Authorship I, Devdutt Sharma, hereby declare that this thesis and the work presented in it is entirely my own. Where I have consulted the work of others, this is always clearly stated.

Signed: \_\_\_\_\_

Date: \_\_\_\_\_

## Acknowledgements

There are many people I wish to extend my gratitude towards for their invaluable assistance during my Ph.D. I would like to begin by first thanking my supervisor Professor Robin Williams for giving me the opportunity to carry out this project and his help along the way. Secondly, I wish to thank my secondary supervisor Professor Philip Beesley for being an outside voice, and eye, during our countless meetings. I also would not have been able to complete this project without the aid of my parents, because of whom I was given the chance to do something I always wanted to.

Moving onto more personal acknowledgements. I thank my girlfriend, Christiane Hahn, for all her support, emotional, mental and sometimes physical during both the Ph.D. and the thesis writing period. The entire Williams' lab past and present, especially Dr. Grant Otto (whom I cannot ever thank enough), and Dr. Simona Ursu (likewise). The members of office 404, Rob Prouse, Dr. Enrique Lopez, Pavlos Alifragis, for their scientific insight and aid. My friends, Simon Green, Lauren Slater and Rachel Turner for putting up with my many cancellations, and delays to our plans because I was too tired to do anything. And Katrin Augustin and Marco Hahn for adopting me over two Christmases. Finally, no acknowledgements would be complete without mentioning my cats. Private Mittens and Mishka, for always being there and showing me unrequited love (or as much as cats are able to show).

I am sure I have missed some people who have been instrumental to my progress, and subsequent completion, and I apologise if I have, but know that I still thank you for everything.

## Abstract

The  $\gamma$ -secretase complex is a proteolytic protein complex required for normal mammalian development, consisting of the components Presenilin-1/2, Aph-1, Nicastrin and Pen-2. Mutations in the genes encoding the proteins that form this complex have been linked to familial Alzheimer's disease. It has been known that this protein complex possesses proteolytic and non-proteolytic activity, but how these processes contribute towards the pathogenicity of Alzheimer's disease is not well understood. The social amoeba, *Dictyostelium*, has been used to research the Presenilin-1 component of the complex in *Dictyostelium* development and phagocytosis. However, results regarding Aph-1, and Nicastrin have been controversial. Here, we utilise *Dictyostelium* to investigate the function of the  $\gamma$ -secretase complex. We investigate the homology between mammalian and *Dictyostelium*  $\gamma$ -secretase components, and the localisation of these components. We then describe the ablation of the *Dictyostelium aph-1* gene, and demonstrate that Aph-1 and Nicastrin play functional roles in *Dictyostelium* development, and show that this role is dependent upon cell substrate. We also implicate the presenilin proteins as playing a role in *Dictyostelium* growth in liquid media. We go on to show that mutants lacking Presenilin, Aph-1 or Nicastrin show reduced fluid phase uptake by macropinocytosis. We propose that these defects may be due to dysfunctional vesicle acidification as  $\gamma$ -secretase mutant cells are highly sensitive to pH changes when undergoing development. Furthering this, we demonstrate that cells lacking Presenilin, Aph-1 or Nicastrin show aberrant autophagy, accumulation of high molecular weight ubiquitin aggregates, and dysfunctional phagocytosis. Additionally, we show that the acidification defects

observed upon Presenilin ablation can be rescued through expression of a human Presenilin 1 protein in *Dictyostelium*. Finally, we show that these processes are not dependent upon catalytic activity. This work demonstrates a role for the  $\gamma$ -secretase complex in vesicle acidification, through a non-catalytic mechanism, that is evolutionarily conserved from *Dictyostelium* to humans.

## Table of Contents

Abstract.....	4
Chapter I.....	10
Introduction .....	10
1.1 Alzheimer's Disease .....	11
1.2 The $\gamma$ -secretase complex.....	12
1.2.1 Formation of the $\gamma$ -secretase complex .....	13
1.2.2 Presenilin.....	15
1.2.3 Anterior Pharynx Defective 1 .....	17
1.2.4 Nicastrin .....	19
1.2.5 Presenilin Enhancer 2.....	20
1.2.6 $\gamma$ -secretase protease activity .....	21
1.2.7 Scaffolding activity of $\gamma$ -secretase .....	24
1.3 Alzheimer's Disease Theories .....	25
1.3.1 Amyloid cascade hypothesis .....	26
1.3.2 Tau Phosphorylation Hypothesis .....	27
1.3.3 Glycogen Synthase Kinase 3.....	28
1.3.4 Endo-lysosomal and Vesicle Trafficking System .....	29
1.4 Models used for AD research.....	32
1.5 <i>Dictyostelium discoideum</i> .....	33
1.6 <i>Dictyostelium discoideum</i> as a biomedical model .....	34
1.6.1 <i>Dictyostelium discoideum</i> in $\gamma$ -secretase research .....	35
1.7 Aims of this Study .....	38
Chapter II.....	39
Materials and Methods.....	39
2.1 Materials .....	40
2.1.1 General Reagents.....	40
2.1.2 Antibiotics .....	41
2.1.3 Molecular Weight Standards .....	41
2.1.4 Restriction Enzymes .....	41
2.1.5 Other Enzymes .....	41
2.1.6 Antibodies .....	41
2.1.7 Kits.....	42
2.1.8 <i>Escherichia coli</i> Strains .....	42
2.1.9 Primers .....	42

2.1.10 Equipment.....	42
2.2 Methods.....	43
2.2.1 <i>Dictyostelium</i> Methods.....	43
2.2.1.1 Cell Culture.....	43
2.1.1.2 Immunofluorescence Microscopy .....	44
2.1.1.3 Development Assays .....	44
2.2.1.4 Growth Curve Assay.....	45
2.2.1.5 Macropinocytosis Assay.....	46
2.2.1.6 Autophagosome Maturation .....	46
2.2.1.7 Autophagosome Measurement.....	47
2.2.1.8 Phagosomal Proteolysis Assay (Carried out by Dr. Jason King, University of Sheffield) .....	47
2.2.2 Molecular Biology Techniques .....	47
2.2.2.1 Polymerase Chain Reaction .....	47
2.2.2.2 Gel Electrophoresis .....	48
2.2.2.3 Transformation of Competent <i>E. coli</i> .....	48
2.2.2.4 Plasmid Preparation.....	49
2.2.2.5 Restriction Digests .....	49
2.2.2.6 Construction of Knockout Vectors .....	50
2.2.2.7 Construction of Overexpression Vectors .....	51
2.2.2.8 Transformation of Vector Constructs into <i>Dictyostelium</i> .....	51
2.2.2.9 Extraction of DNA from Potential Transformants.....	52
2.2.2.9 Screening for Homologous Recombinants.....	52
2.2.2.11 Sub Cloning of Correct Transformants.....	53
2.2.2.12 RNA Extraction and Reverse Transcriptase PCR .....	53
2.2.3 Proteomics .....	54
2.2.3.1 Western Blot Analysis .....	54
2.3 Software.....	55
2.4 Websites.....	56
Chapter III.....	58
The <i>Dictyostelium</i> $\gamma$ -secretase Complex .....	58
3.1 Introduction .....	59
3.2 <i>Dictyostelium</i> and human Aph-1.....	60
3.3 <i>Dictyostelium</i> and human Nicastrin.....	62
3.4 <i>Dictyostelium</i> and human Pen-2.....	64
3.5 Localisation of the $\gamma$ -secretase complex components .....	66

3.5.1 Generation of overexpression constructs.....	67
3.5.1.1 Generation of an Aph-1 overexpression construct.....	67
3.5.1.2 Generation of a Nicastrin overexpression construct .....	68
3.5.1.3 Generation of a Pen-2 overexpression construct .....	70
3.5.2 Localisation of the $\gamma$ -secretase complex components in <i>Dictyostelium</i> .....	72
3.6 Discussion.....	74
Chapter IV .....	78
Genetic manipulation of $\gamma$ -secretase components and characterisation of mutants .....	78
4.1 Introduction .....	79
4.2 Creating an aph-1 knock-out mutant.....	81
4.3 Creating a pen-2 knock-out mutant.....	85
4.4 Development of aph-1 <sup>-</sup> and nicastrin <sup>-</sup> mutants .....	89
4.5 Growth rates of $\gamma$ -secretase deficient <i>Dictyostelium</i> mutants .....	92
4.6 $\gamma$ -secretase localisation in null mutants.....	94
4.7 Discussion.....	96
Chapter V .....	101
The Role of the <i>Dictyostelium</i> $\gamma$ -Secretase Complex in Macropinocytosis and Autophagy .....	101
5.1 Introduction .....	102
5.2 Macropinocytosis in $\gamma$ -secretase Component Null Mutants.....	105
5.3 The Effects of pH on $\gamma$ -secretase Mutant Development.....	107
5.4 The Effects of $\gamma$ -secretase Ablation on Autophagy and Protein Ubiquitination .....	111
5.5 $\gamma$ -secretase Ablation Causes Vesicle Acidification Defects .....	117
5.6 Discussion.....	120
Chapter VI .....	126
Discussion.....	126
6.1 Confirming Previous Research in <i>Dictyostelium</i> .....	127
6.2 The Role of <i>Dictyostelium</i> $\gamma$ -secretase in Vesicular Trafficking.....	129
References .....	132
Appendices.....	144



Figure 1.1 The $\gamma$ -secretase complex.....	12
Figure 1.2 Formation of the $\gamma$ -secretase complex. ....	15
Figure 1.3. A schematic of $\gamma$ -secretase proteolytic activity. ....	27
Table 2.1. Percentages of K <sub>2</sub> HPO <sub>4</sub> and KH <sub>2</sub> PO <sub>4</sub> to acquire required pH levels for development. ....	455
Figure 3.1 Bioinformatic analysis of <i>Dictyostelium</i> Aph-1.....	61
Figure 3.2 Bioinformatic analysis of <i>Dictyostelium</i> Nicastrin.....	63
Figure 3.3 Bioinformatic analysis of Pen-2. ....	655
Figure 3.4 Generation of an Aph-1 overexpression construct.....	688
Figure 3.5 Generation of a Nicastrin overexpression construct. ....	699
Figure 3.6 Generation of an RFP-Pen-2 construct. ....	71
Figure 3.7 Localisation of Aph-1 and Ncstn in <i>Dictyostelium</i> .....	73
Figure 3.8 Localisation of $\gamma$ -secretase components, PsenB, Aph-1 and Ncstn in <i>Dictyostelium</i> . ....	74
Figure 4.1 Genetic modification through homologous recombination. ....	81
Figure 4.2 Generation of an aph-1 knockout cassette.....	82
Figure 4.3. PCR Screening for homologous recombinants of <i>aph-1</i> <sup>-</sup> .....	84
Figure 4.4 Vector generation for a pen-2 knockout cassette. ....	86
Figure 4.5. PCR Screening for homologous recombinants of pen-2 <sup>-</sup> . ....	87
Figure 4.6 Vector generation of second pen-2 <sup>-</sup> construct and PCR screening for homologous recombinants. ....	88
Figure 4.7 Effects of aph-1 and nicastrin ablation on <i>Dictyostelium</i> development.....	91
Figure 4.8 Growth rates of $\gamma$ -secretase null <i>Dictyostelium</i> in liquid media. ....	93
Figure 4.9 Localisation of $\gamma$ -secretase components in $\gamma$ -secretase null mutants. ....	95
Figure 5.1 The Effects of Presenilin Ablation on Autophagy. ....	104
Figure 5.2 Macropinocytosis in <i>Dictyostelium</i> $\gamma$ -secretase mutants. ....	106
Figure 5.3 Development of <i>Dictyostelium</i> $\gamma$ -secretase null mutants under basic pH.....	109
Figure 5.4 Development of <i>Dictyostelium</i> $\gamma$ -secretase null mutants under acidic pH. ....	110
Figure 5.5 Localisation and size measurement of GFP-Atg8 positive vesicles in <i>Dictyostelium</i> .....	113
Figure 5.6 High molecular weight ubiquitin aggregation and localisation in <i>Dictyostelium</i> $\gamma$ -secretase mutants.....	115
Figure 5.7 Quantification of high molecular weight ubiquitin in <i>Dictyostelium</i> $\gamma$ -secretase mutants.....	116
Figure 5.8 Acidification of autophagosomes in <i>Dictyostelium</i> $\gamma$ -secretase null mutants.....	119

# Chapter I

## Introduction

---

## 1.1 Alzheimer's Disease

Alzheimer's disease (AD) is a neurodegenerative condition that results in cognitive decline, dementia decreased quality of life, and eventually death (Berchtold and Cotman, 1998). The disease affects roughly 46 million people worldwide (Anders et al., 2015), and as the ageing population increases the number of AD cases are also expected to rise with an estimated 131.5 million people affected by 2050 (Anders et al., 2015). AD cases can be categorised into two different etiologies, sporadic AD where the patient exhibits no family history (Rebeck et al., 1993, Saunders et al., 1993), or familial AD where familial history, and target gene mutations are present (Citron et al., 1992, Scheuner et al., 1996). In 2013 dementia in the UK affected 1.3%, or 815,827 persons, with 62% of this due to AD, of these cases only 8% were due to familial Alzheimer's disease (FAD) with the remainder being sporadic (Prince et al., 2014). These numbers are predicted to rise to 1.1 million people by 2025, and 2.2 million people by 2051 if the prevalence rates are steady (Prince et al., 2014, Anders and Prince, 2010)

The total estimated costs of AD worldwide in 2015 were calculated to be \$818 billion, and would be the 18<sup>th</sup> largest economy in the world (Anders et al., 2015). In 2010, the highest costs are in high income countries such as Western Europe (\$210.12 billion) and North America (\$213.04 billion) or \$30,122 per patient and \$48,605 per patient respectively (Anders and Prince, 2010). In the UK, the cost for 2013 were calculated at a total cost of £25.3 billion or £32,250 per patient with £4.3 billion on healthcare costs, £10.3 billion on social care and £11.6 billion in unpaid carers (Prince et al., 2014). The disease poses a significant burden to both, the ageing population, and the healthcare system worldwide.

## 1.2 The $\gamma$ -secretase complex

The  $\gamma$ -secretase complex is a protein complex consisting of four subunits: Presenilin (Psen); Anterior pharynx defective 1 (Aph-1); Nicastrin (Ncstn); and Presenilin enhancer 2 (Pen-2). The name  $\gamma$ -secretase was first used in 1993 when describing the proteolytic activity that cleaves amyloid precursor protein (APP) in the transmembrane domain (Haass and Selkoe, 1993), and it wasn't until 2003 when all of the components were identified (Strooper, 2003). The complex is responsible for the cleavage of a variety of single pass membrane proteins including amyloid precursor protein (APP) (De Strooper et al., 1998), Notch (De Strooper et al., 1999), erbB-4 (Ni et al., 2001), and E-cadherin (Marambaud et al., 2002).

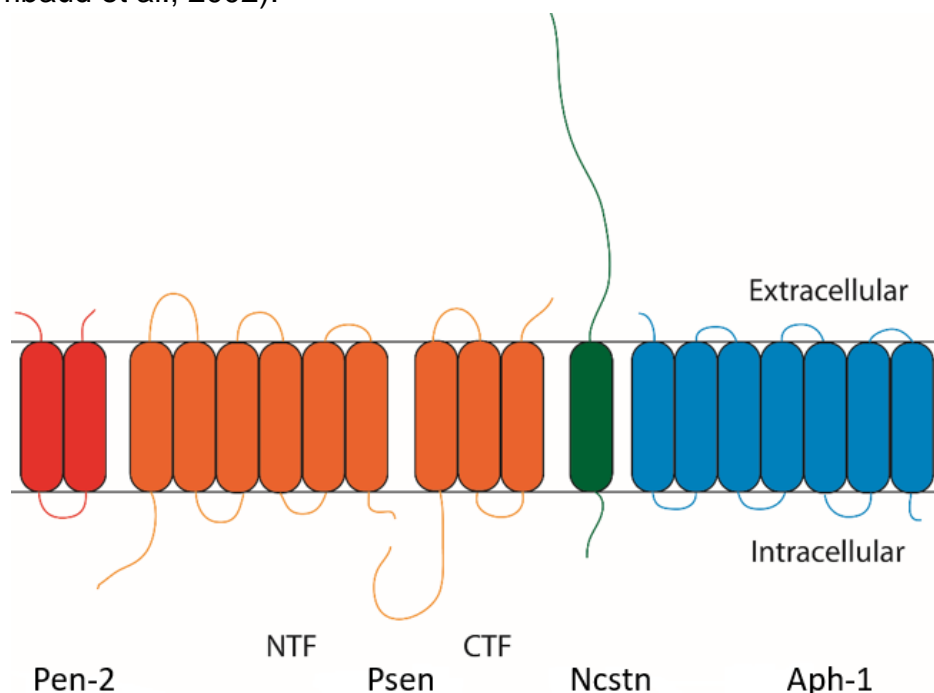


**Figure 1.1 The  $\gamma$ -secretase complex.** The intramembranous  $\gamma$ -secretase complex, showing the four subunits: The two transmembrane domain protein Pen-2 (red); the mutlipass protein Presenilin (orange) which undergoes endoproteolytic cleavage and subsequent activation; the single pass protein Nicastrin (green); and the mutlipass protein Aph-1 (blue).

The substrates of the  $\gamma$ -secretase complex are involved in multiple processes and pathways within an organism (Parks and Curtis, 2007), such as the role of Notch

in neuron cell differentiation which is necessary for development of the brain and maintenance of neuronal progenitor cells (Bolos et al., 2007, Feller et al., 2008, Androutsellis-Theotokis et al., 2006). The role of other substrates such as APP is not fully understood but there is a substantial amount of evidence suggesting it plays a role in synaptic formation and repair where APP is upregulated during neuronal differentiation, and during neuronal repair (Phinney et al., 1999, Priller et al., 2006).

Due to the large number of roles that  $\gamma$ -secretase substrates play in organisms, any mutations to complex components may disrupt not just embryonic development but also adult neuronal function, leading to disruption in a large number of vital processes. Therefore, it is important to understand the role of each component in this complex.

### 1.2.1 Formation of the $\gamma$ -secretase complex

The complete formation of the  $\gamma$ -secretase complex has not yet been fully understood, however it is widely believed that all of the subunits of the complex are synthesised in the endoplasmic reticulum (ER) before being shuttled to the Golgi apparatus (Smolarkiewicz et al., 2013, De Strooper, 2003, Strooper, 2003). The synthesis and the formation of the complex has multiple different stages as each subunit joins the forming complex. Initially, nicastrin in a non-glycosylated form, referred to as immature nicastrin (imNcstn) binds to Aph-1 to assemble a stable heterodimer in the ER, Presenilin then joins this complex to form a three-subunit protein complex before the final integration of Pen-2 (Mao et al., 2012, Fassler et al., 2011, Luo et al., 2003, Niimura et al., 2005). Once Pen-2 joins the complex Presenilin undergoes autoproteolysis therefore activating its catalytic

activity (Smolarkiewicz et al., 2013, Mao et al., 2012). Upon completion of the complex up to 5% of the complex is shuttled to the Golgi apparatus where Nicastrin then matures through glycosylation to form mature Nicastrin (mNcstn), the remainder stays within the endoplasmic reticulum as a reserve pool (Smolarkiewicz et al., 2013). Any components not part of this stable complex are degraded by lysosomes and endosomes. The final step involves the shuttling of active complexes (~5%) from the Golgi apparatus to the plasma membrane; inactive complexes remain shuttled between the Golgi apparatus and the ER (Smolarkiewicz et al., 2013). When positioned in the plasma membrane the catalytic domains are located within the plasma membrane itself allowing for intramembranous cleavage, the complex when localised to the ER is inactive, and active complexes are immediately shuttled out of the Golgi towards the plasma membrane (Smolarkiewicz et al., 2013). It is important to note that although a large portion of the complex is stored in the endoplasmic reticulum there are no known catalytic functions for  $\gamma$ -secretase in this sub-cellular compartment, but rather only on the plasma membrane and endosomes upon internalisation (Beel and Sanders, 2008). Additionally, although the complex does not have any catalytic activity in the endoplasmic reticulum it is proposed that it localises to the mitochondrial associated membrane and may affect mitochondrial function, however, this is not yet fully understood (Area-Gomez et al., 2009, Schon and Area-Gomez, 2010).

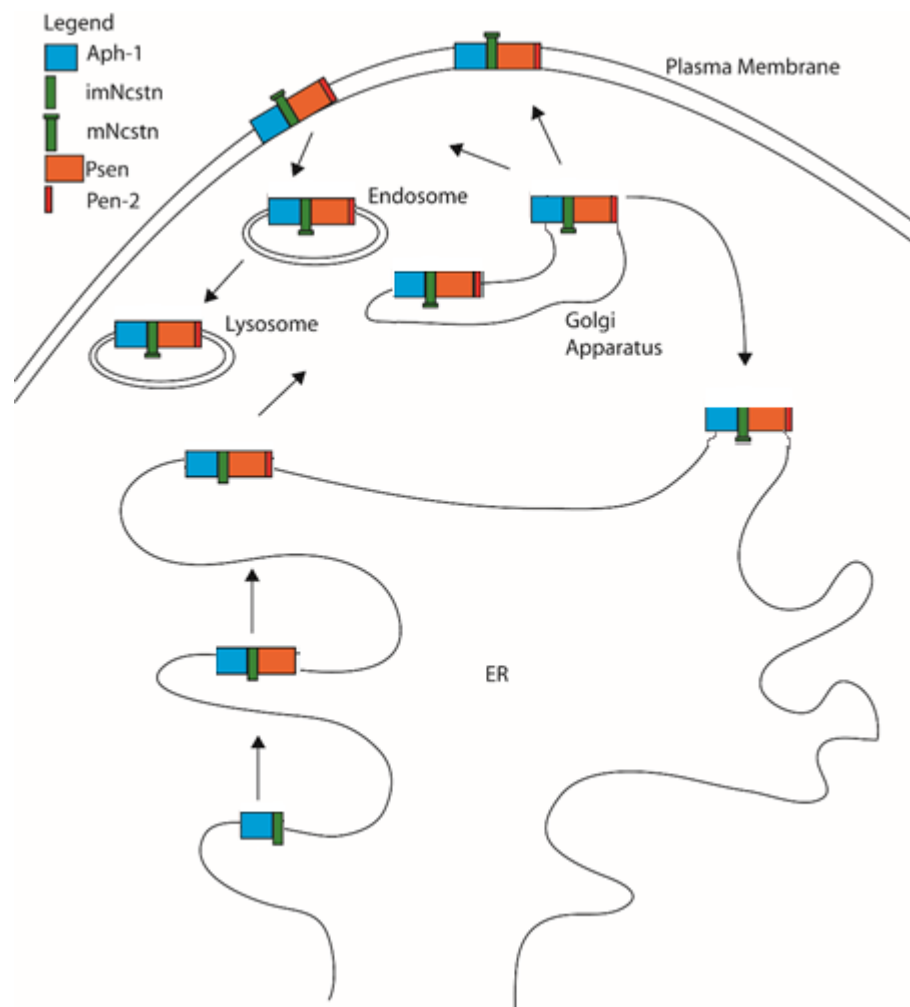


**Figure 1.2 Formation of the  $\gamma$ -secretase complex.** The four subunits of the  $\gamma$ -secretase complex are synthesised in the endoplasmic reticulum (ER), where Aph-1 (blue) and immature Nicastrin (imNcstn, green) form a subcomplex before being joined by presenilin (orange) and finally Pen-2 (red) before being shuttled to the Golgi where nicastrin matures (mNcstn). This completed, matured, complex is then shuttled to the plasma membrane or broken down in endosomes and lysosomes. Some complex is recycled to the ER. Figure adapted from Smolarkiewicz et al. (2013)

### 1.2.2 Presenilin

In 1995 analysis of mutations present in patients with familial AD discovered two nine-transmembrane proteins with a large number of mutations giving rise to AD, that were then named Presenilin 1 (Sherrington et al., 1995) and Presenilin 2 (Levy-Lahad et al., 1995). At the same time, a separate group

showed the involvement of presenilin in regulating the Notch signalling pathway in *Caenorhabditis elegans* (Levitan and Greenwald, 1995), therefore implicating the presenilin proteins not only in AD pathogenesis but also in embryonic and neural development via its interaction with Notch. The exact mechanism in which these two pathways were linked however was not fully understood.

The role of the presenilin proteins in AD was not clear until experiments in patient derived fibroblasts demonstrated that Presenilin mutations found in familial Alzheimer's disease (FAD) resulted in abnormal amyloid precursor protein (APP) cleavage and subsequent neurotoxic Amyloid- $\beta$  (A $\beta$ ) generation (Scheuner et al., 1996) and their function was further elucidated through overexpression of mutant presenilin proteins in cultured cell lines and *in vivo* mouse models (Borchelt et al., 1997, Borchelt et al., 1996). Further support for this was shown using neurons derived from Psen1 knockout mice to show that the generation of all A $\beta$  peptides, and not just abnormal forms was disturbed (De Strooper et al., 1998). The role of the presenilin proteins in both Notch signalling and APP cleavage was discovered when it was shown that  $\gamma$ -secretase inhibitors blocked both APP processing and Notch cleavage suggesting the complex was responsible for both effects, and therefore simply inactivating the complex as a treatment for AD was not possible due to resultant defects in Notch signalling (De Strooper et al., 1999).

The presenilins were first identified as the catalytic core of the  $\gamma$ -secretase complex, after undergoing endoproteolytic cleavage, when aspartyl residues within transmembrane domain 6 and transmembrane domain 7 were mutated resulting in abolished protein cleavage (Wolfe et al., 1999) demonstrating that the presenilins function as an aspartyl protease within the  $\gamma$ -secretase complex. It is



also worth noting that the aspartyl residues present in the human presenilins TMD 6 and 7 are conserved across different species including *P. patens* and *Dictyostelium* (Khandelwal et al., 2007, Ludtmann et al., 2014, Otto et al., 2016). Mutation of these key catalytic residues does not change the expression or incorporation of Presenilin into the  $\gamma$ -secretase complex (Nyabi et al., 2003), as catalytically inactive Presenilin is still able to incorporate into the complex suggesting that the catalytic activity is not necessary for Presenilin integration into the  $\gamma$ -secretase complex.

Although the main function of the presenilins is believed to provide the catalytic subunits of the  $\gamma$ -secretase complex, a number of different roles have also been suggested, such as roles in protein trafficking (Zhang et al., 2006), calcium homeostasis (Lee et al., 2015) and  $\beta$ -catenin signalling (De Strooper et al., 2012). These roles have been shown using presenilins with substituted aspartyl residues or non-catalytic presenilin mutants demonstrating that certain presenilin functions are not dependent on the catalytic activity.

### 1.2.3 Anterior Pharynx Defective 1

It was not until 2002 that the 7-transmembrane domain Anterior Pharynx Defective 1 (Aph-1) was implicated in the Notch signalling pathway in *C. elegans*. Aph-1 showed similar function and localisation to the presenilin genes, being required for the proper cell surface localisation of Nicastrin (Goutte et al., 2002). In 2003, it was shown that Aph-1 was required to enable a fully matured and active  $\gamma$ -secretase complex, where overexpression causes an accumulation of full-length presenilin and loss of function showed downregulated presenilin and

nicastrin (*in vitro*), and a Notch phenotype in *C. elegans* (Goutte et al., 2002, Strooper, 2003).

There are two different genes encoding for Aph-1 in humans, Aph-1A and Aph-1B, with a duplication of the B-type in mice giving rise to a third, Aph-1C (Serneels et al., 2005). These different Aph-1 proteins, whilst sharing a name and potential common function, do have some differences in the way that they contribute to the function of the  $\gamma$ -secretase complex *in vivo*. Analysis of Aph-1A<sup>-/-</sup>, B<sup>-/-</sup>, C<sup>-/-</sup> and BC<sup>-/-</sup> mice show that although the proteins are extremely similar in sequence the phenotypes in respective deficient mice differ (Serneels et al., 2005). Aph-1 A<sup>-/-</sup> mice were embryonically lethal showing defective angiogenesis in the yolk sac, neuronal tube malformations and somitogenesis defects, the remaining deficient mice (B<sup>-/-</sup>, C<sup>-/-</sup>, BC<sup>-/-</sup>) survived until adulthood but showed decreased APP processing in the adult brain.

Aph-1A and Aph-1B share a number of conserved domains and residues that are important for protein function. The GxxxGxxxG motif has been shown to be important for the binding and incorporation of Aph-1 to nicastrin and the  $\gamma$ -secretase complex (Lee et al., 2004b). Mutations in any of the glycine residues at positions 122, 126 and 130 in humans results in an unstable Aph-1-Nicastrin holocomplex and suggests that Aph-1 has a scaffolding role in the initial assembly and maturation of an active  $\gamma$ -secretase complex (Lee et al., 2004b). Mutations in the GxxxG domain in *C. elegans*, at position 123 leads to a complete Notch loss of function phenotype suggesting that the  $\gamma$ -secretase complex is not able to form if this motif is mutated (Goutte et al., 2002).

The role that Aph-1 plays within the  $\gamma$ -secretase complex however is still not fully understood. Aph-1 has been suggested to have an active role, responsible for regulation of the endoproteolysis of presenilin (Luo et al., 2003). Aph-1 has also been suggested to have a non-active, role in stabilising the  $\gamma$ -secretase complex (Takasugi et al., 2003). As recently as 2010 a new role was suggested for Aph-1 in directly associating with both full-length and C-terminal fragments of  $\gamma$ -secretase substrates in both Chinese hamster ovary and human embryonic kidney cells, even under complex denaturing conditions (Chen et al., 2010). This study further showed that mutation of conserved histidine residues in either positions 171 or 197 resulted in association with less APP, and the double mutant showed an even greater deficiency despite all three histidine mutants binding and incorporating to the  $\gamma$ -secretase complex (Chen et al., 2010).

#### 1.2.4 Nicastrin

Nicastrin is the largest component of the  $\gamma$ -secretase complex. It is a single pass membrane protein that initially forms a holocomplex with Aph-1 in its immature 110kDa form before maturing to a highly glycosylated 130 kDa form when the  $\gamma$ -secretase complex matures (De Strooper, 2003, Smolarkiewicz et al., 2013). First found to modulate presenilin-mediated notch signalling in *C.elegans*, nicastrin null mutations resulted in a notch deficient phenotype in *C. elegans*, as well as an increase in A $\beta$ 42/40 secretion in human embryonic kidney (HEK) cells (Yu et al., 2000).

The function of Nicastrin within the  $\gamma$ -secretase complex is a research area full of conflicting theories. It has been suggested that Nicastrin functions as a substrate recognition component prior to cleavage, with glutamate at position 333 providing

an amino acid for this function (Shah et al., 2005). However, this role was disputed as the same glutamate (Glu332 in mouse Nicastrin) was required for maturation of the  $\gamma$ -secretase complex, but played no role in the recognition of substrates (Chavez-Gutierrez et al., 2008). Further complications then arose as it was found that nicastrin  $^{-/-}$  mutants were able to cleave Notch and APP in two separate independent mouse embryonic fibroblast (MEF) lines in the presence of proteasome inhibitors, suggesting a potential stabilisation role rather than an active role within the complex in either substrate recognition or maturation (Zhao et al., 2010). Finally, nicastrin may play a role in synaptic function in hippocampal neurons independent of the  $\gamma$ -secretase complex. Conditional nicastrin mouse knockouts have deficiencies in presynaptic plasticity, a phenotype blocked by the depletion of  $\text{Ca}^{2+}$  suggesting that calcium homeostasis underlies these presynaptic deficits (Lee et al., 2014). These findings suggest that nicastrin may have a role independent of  $\gamma$ -secretase in regulation of synaptic function, however its role within the complex is still an area of debate.

#### 1.2.5 Presenilin Enhancer 2

Pen-2 is the smallest component of the  $\gamma$ -secretase complex, and the final member to be incorporated into the complex (Mao et al., 2012). Pen-2 is a multipass membrane protein with two transmembrane domains and the function of the protein remains unclear. In 2003 Pen-2 was shown to regulate the proteolytic processing of the presenilins as reduced Pen-2 levels resulted in reduced production of Presenilin CTF, showing only full length Presenilin (Luo et al., 2003). More recent research has demonstrated that Pen-2 is dispensable for presenilin endoproteolysis as in the presence of proteasome inhibitors, Presenilin

was capable of endoproteolysis in MEFs independently of Pen-2 (Mao et al., 2012).

Mutations in different regions of the Pen-2 protein result in different effects on the  $\gamma$ -secretase complex, showing conserved regions across several species (Holmes et al., 2014). These conserved regions include, within the N-terminal domain N8 where a mutation results in an increase of A $\beta$ 40/42 production by 300% and 180% respectively; and amino acid mutations K11A/K17A which results again in increased A $\beta$  production. Mutations within the first half of TMD1 reduced A $\beta$  production with the greatest effects from mutations of F25/L26, resulting in a decrease by 30-50% compared to wild type. Mutations in the second half of TMD1 elevated A $\beta$  production by up to two-fold compared to wild type. Mutations in the loop region, I53A, V57A and K54A reduced A $\beta$ 40 production with no changes to the 42 form. TMD2 mutations however seemed to have moderate effects causing only slight decreases in both forms of A $\beta$ . Finally, in the C-terminal domain a loss of D90 results in both A $\beta$  forms increasing in secretion by 160%, whilst converting it to a positively charged amino acid results in reduced secretion of both species to about 50% (Holmes et al., 2014). In the absence of any detectable Pen-2 there is still a minor amount of presenilin endoproteolysis in the presence of proteasome inhibitors (Holmes et al., 2014). These data taken together suggest that Pen-2 may act as a catalyst for presenilin endoproteolysis, and as a stabilisation factor that allows for full assembly and complete trafficking.

### 1.2.6 $\gamma$ -secretase protease activity

The protease activity of  $\gamma$ -secretase is dependent on catalytic aspartyl residues in the presenilin proteins which proteolytically process single

transmembrane domain substrates which are implicated in a number of different processes within a cell, and number up to 91 different proteins (Haapasalo and Kovacs, 2011). These processes include transcriptional regulation, regulation of cell fate, cell death, neurite outgrowth and cell adhesion, regulation of angiogenesis and tumorigenesis (Haapasalo and Kovacs, 2011).

Several  $\gamma$ -secretase substrates have been implicated in transcriptional regulation. The transcriptional function of these substrates is most often suggested due to their nuclear localisation and ability to affect transcription in assays, these include: alcaidens (Araki et al., 2004); CD44 (Okamoto et al., 2001); Notch (Schroeter et al., 1998) and its ligands Delta and Jagged (Ikeuchi and Sisodia, 2003), E-cadherin (Marambaud et al., 2002) and receptor-like protein tyrosine phosphatases (Anders et al., 2006). The intracellular domains of all of these substrates generated by cleavage by  $\gamma$ -secretase serve as regulatory switches in their downstream activity (Haapasalo and Kovacs, 2011). This has been demonstrated in the full-length forms of E-cadherin which is usually involved in cell-cell adhesion whereas the intracellular domain generated has been shown to regulate transcription after nuclear localisation (Marambaud et al., 2002). Notch, a  $\gamma$ -secretase substrate, has been shown to regulate cell fate through its transcriptional activity (Fiuza and Arias, 2007). Notch achieves transcriptional regulation by releasing the Notch intracellular domain (NICD) after ligand binding which then localises to the nucleus and targets the recombining binding protein suppressor of hairless (RBP-J) thereby activating previously suppressed transcription (Shawber et al., 1996, Castel et al., 2013). Other substrates regulated with cell fate regulation include receptor tyrosin-protein kinase ErbB4 (ErbB4), which upon cleavage releases the ErbB4-ICD implicated in nuclear

translocation and pro-apoptotic activity, whereas the ErbB4 protein has been shown to have a role in cell fate determination in the brain (Linggi et al., 2006).

Neuronal cell death is considered a cause of Alzheimer's disease progression, and the intracellular domain of p75 neurotrophin receptor, a  $\gamma$ -secretase substrate, has been implicated in neurotrophin-mediated death signalling in neurons where it was shown that brain-derived neurotrophic factor induces the generation of the p75 neurotrophin receptor intracellular domain by  $\gamma$ -secretase and subsequent apoptotic signalling (Majdan et al., 1997).

The proteolytic activity of  $\gamma$ -secretase has also been implicated in human disease, most notably Alzheimer's disease through the cleavage of APP to generate the small 36 – 43 peptide Amyloid  $\beta$  proteins including the two toxic 42 and 43 forms (Scheuner et al., 1996, Borchelt et al., 1996). This proteolytic pathway is the basis of the amyloid cascade hypothesis in AD progression which states that the toxic A $\beta$  fragments aggregate upon generation and cause senile plaques indicative of the condition which are thought to arise due to mutations in the catalytic presenilin proteins (Scheuner et al., 1996). A second pathway is present for the processing of APP, known as the non-amyloidogenic pathway as it does not culminate with the production of A $\beta$  fragments, in this pathway the initial cleavage of APP is carried out by  $\alpha$ -secretase as opposed to  $\beta$ -secretase therefore exposing different CTF cut sites to  $\gamma$ -secretase resulting in the generation of p3 instead of A $\beta$ .

### 1.2.7 Scaffolding activity of $\gamma$ -secretase

Aside from the well-established proteolytic role of the  $\gamma$ -secretase complex there have been a number of studies investigating the non-proteolytic functions of the complex. These functions include roles in protein trafficking and turnover (Esselens et al., 2004), calcium homeostasis (Lee et al., 2015, Begley et al., 1999, Keller et al., 1998) and in the regulation of  $\beta$ -catenin (Kang et al., 1999). These non-proteolytic roles have been shown in a number of different studies. Presenilin 1 has been shown to bind to  $\beta$ -catenin, which is not a proteolytic substrate of  $\gamma$ -secretase, in both transfected EcR293 cells and in the brains of transgenic mice (Kang et al., 1999). This interaction between PS and  $\beta$ -catenin lead to an increased association of  $\beta$ -catenin with GSK3 $\beta$  when PS1 was overexpressed which subsequently resulted in increased turnover of  $\beta$ -catenin as GSK3 $\beta$  is a negative regulator (Kang et al., 1999). Further, the half-life of  $\beta$ -catenin was greatly increased in fibroblasts that were PS1 deficient which was overcome by reconstitution of catalytically inactive PS1 demonstrating a non-catalytic protein turnover function of PS1 in the  $\gamma$ -secretase complex (Kang et al., 1999).

Two independent studies in 1999 and 1998 demonstrate that  $\gamma$ -secretase functions in calcium homeostasis and dysfunctional calcium homeostasis resulted in mitochondrial dysfunction and toxin-induced apoptosis in neuronal cells. In rat adrenal medulla (PC12) cells expressing FAD mutant Psen1 (L286V) are more sensitive to apoptosis induced by 3-nitropropionic acid and oxyradical production than wild-type cells, which is associated with elevated levels of Ca<sup>2+</sup>, and subsequent mitochondrial failure which could be reversed through reduction



of cytoplasmic calcium levels (Keller et al., 1998), suggesting that these presenilin mutations are involved in aberrant calcium regulation and oxidative stress. Additionally, synaptosomes prepared from FAD Psen1 mutation harbouring mice showed elevated levels of cytoplasmic calcium compared with synaptosomes from nontransgenic mice and mice overexpressing wild-type Psen1 (Begley et al., 1999). The mitochondrial dysfunction after metabolic insults was more potent in these FAD Psen1 mutant mice synaptosomes when compared to wild type mice and, once again, these results could be reversed through the use of buffered cytoplasmic calcium or using agents that prevented the release of  $\text{Ca}^{2+}$  from the endoplasmic reticulum (Begley et al., 1999).

These various studies suggest that the  $\gamma$ -secretase complex does not just have a proteolytic role but also a variety of non-proteolytic roles as catalytically inactive complexes are capable of restoring wild-type phenotypes. These studies further demonstrate that mutations in Psen1 that affect the cleavage of APP may not be the only way in which the  $\gamma$ -secretase complex can contribute to the pathogenesis of AD. Finally, a number of these roles are conserved across various species and organisms (Otto et al., 2016).

### 1.3 Alzheimer's Disease Theories

Numerous theories have been proposed for the causes of AD, each with a substantial amount of evidence to lend credence to them. There are four major theories which will be discussed here, these are the amyloid cascade hypothesis (Borchelt et al., 1997), the tau hypothesis (Ittner and Gotz, 2011), the Glycogen Synthase Kinase 3 hypothesis (Hooper et al., 2008), and the dysfunctional endo-lysosomal system hypothesis (Hu et al., 2015, Menzies et al., 2015). However,

despite these four hypotheses being seemingly independent, it is important to note that AD is most likely a multifactorial condition and each of these conditions may contribute to the overall disease.

### 1.3.1 Amyloid cascade hypothesis

The most common theory for Alzheimer's disease pathology is the amyloid cascade hypothesis, where aberrant cleavage of the protein amyloid precursor protein results in neurotoxic plaque formation in the brain (Citron et al., 1992). Amyloid Precursor Protein is a single pass transmembrane protein that is cleaved sequentially by two proteases,  $\beta$ -secretase, generating a fragment known as CTF- $\beta$ , and  $\gamma$ -secretase which generates a small 36 – 43 amino acid protein known as Amyloid- $\beta$ , A $\beta$  (Nunan and Small, 2000). Two forms of A $\beta$  are thought to be toxic, these are the 42 and 43 amino acid forms (A $\beta$ 42 and A $\beta$ 43). The exact reason behind the production of these two toxic forms of A $\beta$  is not fully understood, but is thought to be due to mutations in the  $\gamma$ -secretase that cleaves CTF- $\beta$  (Zhang et al., 2011).

The amyloid cascade hypothesis follows the production of these two toxic forms of A $\beta$  and suggests that A $\beta$ 42 and A $\beta$ 43 may aggregate and self-polymerise to form extracellular plaques in AD patient brains (termed senile plaques) (Tanzi, 2005). This theory has been successfully demonstrated in the brains of mouse and fruit fly models (Iijima et al., 2004) and in human AD patients where plaque formation results in neuronal death (Gregory and Halliday, 2005).

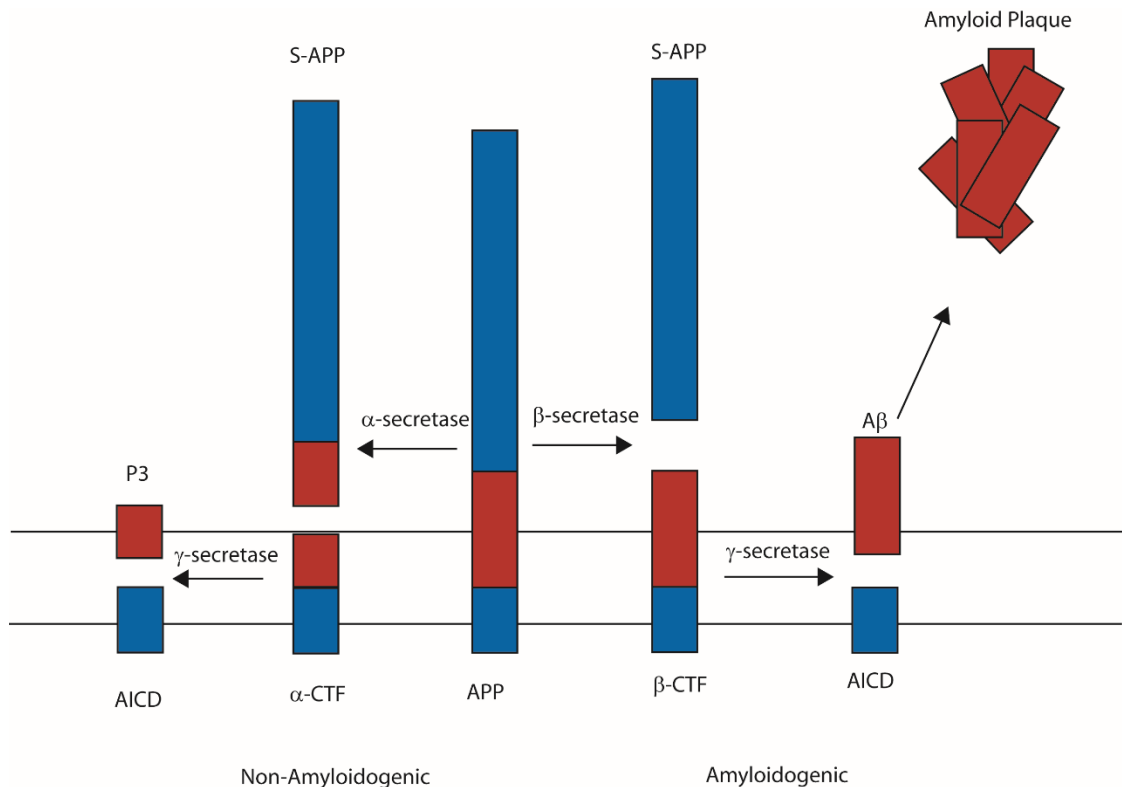


**Figure 1.3. A schematic of  $\gamma$ -secretase proteolytic activity.** When amyloid precursor protein (APP) undergoes proteolytic processing, there are two separate pathways depending on the initial cleavage. The amyloidogenic pathway (right) arises from a cleavage of APP by  $\beta$ -secretase generating secreted APP (S-APP) and a  $\beta$ -CTF. This is then subsequently cleaved by  $\gamma$ -secretase to generate an amyloid intracellular domain (AICD) and amyloid  $\beta$  ( $A\beta$ ) fragments which aggregate to form characteristic senile plaques in Alzheimer's disease patient brains. The second pathway is the non-amyloidogenic pathway (left) which arises from APP cleavage by  $\alpha$ -secretase and subsequent cleavage by  $\gamma$ -secretase generating an AICD and p3.

It is worth noting however that not all studies support the senile plaques as a cause of AD. Evidence has suggested that the deposition of  $A\beta$  may be a neuroprotective response to AD (Lee et al., 2004a).

### 1.3.2 Tau Phosphorylation Hypothesis

Tau is a protein associated with microtubules in neurons in humans. These proteins are responsible for the stability of the axon microtubules and play an important role in the human brain (Harada et al, 1994). Upon

hyperphosphorylation Tau is no longer able to stabilise axonal microtubules leading to neuronal death (Trojanowski and Lee, 2005). Histopathological studies of AD patient brain samples showed hyperphosphorylated tau aggregates termed neurofibrillary tangles (NFTs) (Ittner and Gotz, 2011). These hyperphosphorylated NFTs are spread throughout the brain and appear to show the progression and severity of AD in the patient, they also show synaptic loss in the patient brain (Ittner and Gotz, 2011).

### 1.3.3 Glycogen Synthase Kinase 3

Deregulation of the kinase Glycogen Synthase Kinase 3 (GSK3) may also be a causative factor for the pathogenesis of AD (Hooper et al., 2008). This model suggests that the deregulation of GSK3 results in the hyperphosphorylation of tau, memory impairment and increased production of A $\beta$ . The rationale behind this is due to the evidence that GSK3 has been shown to colocalize with dystrophic neurites and the characteristic neurofibrillary tangles observed in AD patient brains as well as the presence of GSK3 in pre-tangle neurons, hippocampus and frontal cortex of AD patients (Hooper et al., 2008). In addition, a polymorphism in the GSK3 promoter has also identified as a risk factor for AD (GSK3 -50TT genotype) (Mateo et al., 2006). Finally, GSK3 inhibitors show benefits in AD model neurodegeneration, reducing amyloid inflammation and neurotoxicity in hippocampal neuronal cultures (Hu et al., 2009), however more research has to be done into this pathway before anything conclusive can be said.

#### 1.3.4 Endo-lysosomal and Vesicle Trafficking System

The Presenilin proteins and  $\gamma$ -secretase complex have been implicated in mediating mammalian endocytosis and autophagy, potential contributing factors in Alzheimer's disease (Lee et al., 2015, Lee et al., 2010, Neely et al., 2011, Cataldo et al., 2000, Tamboli et al., 2008, Zhang et al., 2006). Mammalian cells lacking Presenilin proteins show decreased endocytosis, taking up lower levels of lipoprotein transporters and subsequent increased levels of apolipoprotein E (Tamboli et al., 2008). Additionally, cells have decreased clearance from endocytic compartments and increased protein deposition (Zhang et al., 2006). Presenilin has also been implicated in autophagy, the process through which cells break down intracellular components. Mammalian cells lacking Presenilin, or with AD-causing mutations, demonstrate increased autophagosome accumulation, and decreased protein clearance (Lee et al., 2010, Neely et al., 2011). It has been proposed that these defects in protein clearance result in the accumulation and aggregation of  $A\beta$ , and that these defects precede the characteristic neurofibrillary tangles, and amyloid plaques (Ghavami et al., 2014, Hu et al., 2015, Wolfe et al., 2013).

It has been suggested that defects in the endocytic and autophagic pathway are due to more basic lysosomal pH conditions (Dobrowolski et al., 2012, Lee et al., 2015, Lee et al., 2010, Wolfe et al., 2013). Ablation of presenilin results in a more basic lysosomal pH suggesting that presenilin mediates lysosomal pH through calcium regulation and homeostasis (Lee et al., 2015). Additionally, these studies are unable to differentiate between effects observed upon presenilin ablation or due to lack of  $\gamma$ -secretase activity as a whole.

### 1.3.5 Other theories

There are several other potential AD causing theories than the ones mentioned above. These include the cholinergic hypothesis, biometals hypothesis, retrogenesis hypothesis and the spirochetosis theory which shall all be discussed below.

The cholinergic hypothesis is one of the oldest theories for AD and has a number of treatments based upon it (Francis et al., 1999). This theory suggests that deficits in excitatory amino acid neurotransmission and in cholinergic system processing, due to cholinergic neuronal loss, result in the observed decline of memory and learning in AD patients (Davies and Maloney, 1976, Perry et al., 1978, Bartus et al., 1982). Several therapies have been based upon the cholinergic hypothesis especially the use of acetylcholinesterase inhibitors (Martorana et al., 2010), however, the efficacy of these drugs leaves much to be desired. Currently, these treatments do show some improvement in memory and cognitive function throughout AD progression, however these changes are unlikely to be solely due to acetylcholine upregulation suggesting that decline in memory and cognitive function are due to a complex interaction of several different neurotransmitters (Martorana et al., 2010).

The biometals theory is a more controversial theory than those previously discussed. This theory posits that the cellular homeostasis of biometals is disrupted in cases of AD, especially exposure to and the levels of aluminium (Exley, 2007, Rodella et al., 2008, Bondy, 2016, Kandimalla et al., 2016, Kastenholz et al., 2009, Xu et al., 2014). The biometals theory proposes that these metal ions affect, and are in turn, affected by several other AD related proteins such as apolipoprotein E (Xu et al., 2014), and tau (Exley, 2007)

thereby causing oxidative stress that may contribute to AD progression (Su et al., 2008). This theory does however have several opponents (Lidsky, 2014) with the quality of the research being criticised (Lidsky, 2014, Santibanez et al., 2007).

The retrogenesis hypothesis is based upon the idea that as fetuses undergo neurodevelopment people with AD undergo a reverse process resulting in progressive cognitive decline first suggested by Reisberg (Reisberg et al., 1999a, Reisberg et al., 1999b, Alves et al., 2015). However, the retrogenesis theory has not been extensively investigated.

The final AD causing theory to be discussed here is the spirochetosis theory. It has been established that spirochetal infection may be a causative factor of progressive dementia, brain atrophy and amyloid deposition, especially in cases such as syphilis or Lyme disease (MacDonald, 1986, Dupuis, 1988, Schaeffer et al., 1994, Miklossy, 1993). More recently, research has begun to implicate spirochetosis and AD, as spirochetes may be present in the brains of AD patients (Miklossy, 2011, Riviere et al., 2002, MacDonald, 2006). Additionally, within the senile plaques characteristic of AD progression researchers have discovered the presence of biofilms (Allen, 2016), this theory postulates that the innate immune system cannot penetrate the biofilm and destroy the spirochetes forming these biofilms and instead destroy the surrounding tissue (Allen, 2016). The destruction of the surrounding brain tissue results in the characteristic neurodegeneration and brain atrophy found in AD patient brains.

## 1.4 Models used for AD research

Current models used in Alzheimer's disease include the usual model organisms such as transgenic mice (Begley et al., 1999, Majdan et al., 1997, Borchelt et al., 1997, Meckler et al., 2010), mammalian cell lines, e.g. HEKs and MEFs (Nyabi et al., 2003, Chavez-Gutierrez et al., 2008, De Strooper et al., 1999, Strooper, 2003) and other slightly unusual model organisms such as the moss *Physcomitrella patens* (Khandelwal et al., 2007).

With the use of each model organism there are a number of advantages and disadvantages, for example in mouse models it is necessary to note that animals do not present neuronal loss observed in AD patients, but show a loss of synapses which precedes the neuronal loss (Cuadrado-Tejedor and Garcia-Osta, 2014). Additionally, in mouse models you cannot generate a complete  $\gamma$ -secretase complex null line in mice, or other whole animal models such as *C. elegans*, as any non-functional complex results in embryonic lethality due to the importance of Notch, a vital component of embryonic development (Serneels et al., 2005, Goutte et al., 2002). This means that no true null lines can be generated and only knock downs, or conditional knock outs, which may lead to residual levels of these components that may still be able to carry out their required function. Mammalian cell lines are also diploid in nature, with two copies of each gene, making genetic manipulation and gene ablation much more difficult than in haploid model organisms. Plant models such as *P. patens* used by Khandelwal et al in 2007 do have some advantages over animal models. *P. patens* does not express Notch, APP or ErbB4 and so are not affected by the dominant loss of Notch lethal phenotype seen in animal models, but do demonstrate a non-proteolytic loss of  $\gamma$ -secretase activity phenotype with regards to an inability to



respond light which can be rescued by expression of human presenilin (Khandelwal et al., 2007) indicating conservation of function between these two organisms.

### 1.5 Dictyostelium discoideum

*Dictyostelium discoideum* is a single celled amoeba first discovered in 1935 by K.B. Raper (Raper, 1935). The organisms inhabits forest floors and survives by ingesting bacteria through phagocytosis (Boeckeler and Williams, 2001). Upon starvation *Dictyostelium* begin to undergo multicellular development. This development process begins when starving cells begin to secrete cyclic AMP (cAMP) and chemotax towards the secreted cAMP where they form a mound and then the final developmental structure, a fruiting body. This fruiting body will contain a spore head filled with viable *Dictyostelium* spores to ensure survival (Williams et al., 2006).

This developmental process can be broken down into several stages, the first of which is aggregation. In this stage, the single cells will begin to chemotax towards cells secreting cAMP through G-protein coupled receptor activation (McMains et al., 2008) until  $\sim 10^5$  cells have come together at a central point called the mound, the second stage. Once the mound has been formed cells begin to undergo differential gene expression becoming either pre-spore or pre-stalk cells (Williams et al., 2006). The third stage, the slug, occurs after the differentiation of pre-spore and pre-stalk cells is completed. Cells with pre-determined cell fates will form a multicellular slug consisting of pre-stalk cells in the anterior and pre-spore cells in the posterior (MacWilliams and Bonner, 1979). Culmination is the final step in *Dictyostelium* development and consists of the pre-stalk cells forming

a stalk of non-viable cells, and the pre-spore cells forming a spore head atop the stalk (Jang and Gomer, 2011). The ultimate structure is the *Dictyostelium* fruiting body which is approximately 1mm in height and consists of three separate structures: the basal disc, the stalk and the spore head (Williams et al., 2006).

### 1.6 *Dictyostelium discoideum* as a biomedical model

Whilst its natural habitat is damp forest floors, *Dictyostelium* has also been used as a biomedical model. The cells are able to be easily maintained at a constant 22°C in liquid media ingesting nutrients through macropinocytosis and double approximately every 8 hours in laboratory conditions, allowing for high throughput research.

The development of DNA-transformation techniques using *Dictyostelium* (Nellen et al., 1984) was a major step forward for the use of this organism as a biomedical model, and the full sequencing of the 34Mb, 6 chromosome, genome has only aided this (Eichinger et al., 2005). Upon sequencing of the genome, it was discovered that 64 of 287, or ~32%, of queried human disease genes share homology to *Dictyostelium* counterparts and has allowed the organism to be used in a variety of studies relating to human drug target, and intracellular pathway analysis (Eichinger et al., 2005, Williams et al., 2006). One major advantage of using *Dictyostelium* as a model as opposed to other single celled biomedical models is the possession of several genes and targets that are lacking in other biomedical models, such as *Saccharomyces cerevisiae* (Eichinger et al., 2005).

A wide variety of methodologies has allowed *Dictyostelium* to be used to investigate a multitude of human diseases. These include, gene manipulation through ablation and overexpression in isogenic cell lines, developmental assays,

chemotaxis studies, and mutant library screening. All of these methods can be used to determine the effects of compounds of interest on the organism, therefore finding potential targets, or for the effects of gene ablation or overexpression and the resulting phenotypic defects in the model (Boeckeler and Williams, 2001).

The organism has been used until now to investigate the effects of valproic acid and lithium bipolar disorder and epilepsy (Terbach et al., 2011, Chang et al., 2012, King et al., 2009), and to help further the understanding of Alzheimer's disease (McMains et al., 2010, Ludtmann et al., 2014), mitochondrial disease (Francione et al., 2011), and Schwachman-Diamond syndrome (Wong et al., 2011).

#### 1.6.1 *Dictyostelium discoideum* in $\gamma$ -secretase research

*Dictyostelium* has been used to better determine the basal function of the complex and its components despite lacking any known  $\gamma$ -secretase substrates. The organism has been used to investigate the entire  $\gamma$ -secretase complex showing that the *Dictyostelium* complex is able to cleave a truncated version of human APP (consisting of only the C-terminal 240 amino acids) expressed in *Dictyostelium* and release A $\beta$  peptides (McMains et al., 2010). Additionally, inhibitors of  $\gamma$ -secretase activity are able to partially inhibit the processing of APP by *Dictyostelium*  $\gamma$ -secretase (McMains et al., 2010). The *Dictyostelium*  $\gamma$ -secretase complex is also able to cleave the human Notch protein (Ludtmann et al., 2014). The ability of the *Dictyostelium* complex to cleave human substrates, but not have any known endogenous substrates, may suggest that the  $\gamma$ -secretase complex and its function has been evolutionarily conserved, and so

may have a different role perhaps in one of the other areas such as scaffolding, protein trafficking or calcium homeostasis.

The *Dictyostelium*  $\gamma$ -secretase complex has also been implicated in *Dictyostelium* phagocytosis and development. Psen1<sup>-</sup>, and Psen1<sup>-</sup>/2<sup>-</sup> mutants showed defective growth on bacteria under laboratory conditions when compared to wild type strains with double mutants showing more severe growth defects when compared to single mutants demonstrated by smaller cleared plaques (McMains et al., 2010), however, it is also important to note that these defects may be observed as a result of decreased cell motility. Cell lines lacking  $\gamma$ -secretase components also showed development defects, each mutant showed different phenotypes depending on which component was ablated, Psen2<sup>-</sup>, Aph-1<sup>-</sup> and Ncstn<sup>-</sup> cells all exhibited defects in late development extending the amount of time spent in the migratory slug stage, and a decreased amount of viable spores whilst Psen1<sup>-</sup> null cells completed development along with wild type within ~24 hours (McMains et al., 2010). Double mutants consisting of Psen1<sup>-</sup>/2<sup>-</sup>, Aph-1<sup>-</sup>/Psen2<sup>-</sup> and Ncstn<sup>-</sup>/Psen2<sup>-</sup> lines showed a similar phenotype to their corresponding single knock outs with the double Psen1<sup>-</sup>/2<sup>-</sup> knockout being the most drastic suggesting that the  $\gamma$ -secretase complex plays a role in late development of *Dictyostelium* (McMains et al., 2010). However, the roles of the  $\gamma$ -secretase components in *Dictyostelium* development are controversial, a subsequent study showed that single Psen mutants did not show any developmental defects, nor did a Ncstn<sup>-</sup> cell line suggesting a presenilin-only complex independent role in development (Ludtmann et al., 2014). Additionally, expression of the human Psen1 in the double Psen1<sup>-</sup>/2<sup>-</sup> mutant rescues this developmental defect suggesting that there may be a common function shared between the presenilin proteins between

these two distantly related species (Ludtmann et al., 2014). Finally, *Dictyostelium* development is not dependent upon Presenilin catalytic activity as mutants lacking catalytic activity formed normal morphology fruiting bodies when compared to wild-type cells (Ludtmann et al., 2014). The reasons behind these controversial results is not fully understood, but may be due to different developmental techniques or substrates used in these studies (McMains et al., 2010, Ludtmann et al., 2014).

The *Dictyostelium* presenilin proteins have also had their subcellular localisation examined using overexpressed Green fluorescent protein (GFP) tagged Presenilin proteins. The *Dictyostelium* Presenilin has been found to localise to the endoplasmic reticulum (Ludtmann et al., 2014), a similar localisation to that observed in mammalian cells (Smolarkiewicz et al., 2013, Fassler et al., 2011). This similarity in subcellular localisation further enforces the idea that these two presenilin proteins may behave in a similar fashion. The Presenilin proteins also function in calcium homeostasis in *Dictyostelium* as in mammalian cells and whole animal models (Begley et al., 1999, Keller et al., 1998, Lee et al., 2015). In *Dictyostelium* PsenB<sup>-</sup> and PsenA<sup>-</sup>/B<sup>-</sup> cells the magnitude of a cAMP-induced calcium response was 2-2.5 fold greater when compared to wild type cells (Ludtmann et al., 2014).

Despite *Dictyostelium* being far removed from humans evolutionarily it is important to note that there are a number of similarities in terms of proteins and signalling pathways that are present in the organism (Eichinger et al., 2005). Additionally, a number of mammalian Presenilin/ $\gamma$ -secretase functions are conserved in *Dictyostelium* (Ludtmann et al., 2014, McMains et al., 2010). This

similarity at a signalling level as well as the advantages that the organism lends to laboratory research provides an alternative, non-animal, model in which to investigate the roles of the  $\gamma$ -secretase complex, not just proteolytically but also non-proteolytic roles and the roles of each individual component of the complex.

## 1.7 Aims of this Study

This PhD thesis investigated the roles of the  $\gamma$ -secretase complex and its components in *Dictyostelium*, and conserved function with the human Presenilin protein. Chapter III will examine the homology between the *Dictyostelium* Aph-1, Nicastrin and Pen-2 proteins with their human orthologues and investigate the localisation of overexpressed GFP-tagged Aph-1 and Nicastrin. Chapter IV will demonstrate the process of ablating *Dictyostelium* Aph-1 and the resultant effects on *Dictyostelium* development, growth and component localisation. Chapter V studies the effects of single component null mutants in *Dictyostelium* to determine whether dysfunctional processes observed are a result of single component ablation or a result of the  $\gamma$ -secretase complex as a whole, and determine a potential underlying cause. Additionally, this study investigated whether defects observed are due to catalytic, or non-catalytic roles for the  $\gamma$ -secretase complex, and whether these functions are shared with the human Presenilin proteins.

## Chapter II

### Materials and Methods

---

## 2.1 Materials

### 2.1.1 General Reagents

#### Reagents purchased from Sigma Aldrich Co (Dorset, England)

Acrylamide (30%), ammonium persulphate (APS), bacteriological agar,  $\beta$ -mercaptoethanol, calcium chloride, glucose, horse serum, Luria-Bertani (LB) broth tablets, N,N,N',N'-tetramethyl-ethelene-1,2-diamine (TEMED), potassium chloride, sodium chloride, sodium dodecyl sulphate (SDS), sucrose, tris base, TRITC-Dextran, triton-100, Trypan Blue powder, TWEEN20.

#### Reagents purchased from Bioline (London, England)

Agarose, deoxynucleotide triphosphates (dNTPs), 5x DNA Loading dye

#### Reagents purchased from Formedium (Norfolk, England)

HL-5 Medium without glucose, SM Agar.

#### Reagents purchased from ThermoFisher Scientific (Loughborough, England)

Glycine, tris-acetate EDTA buffer.

#### Reagents purchased from VWR International (Leicestershire, England)

Acetic acid, acetone, bromophenol blue, ethanol, glycerol, hydrochloric acid, methanol, potassium dihydrogen phosphate.

#### Reagents purchased from Kisker Biotech (Steinfurt, Germany)

DQgreen/Alexa 594 co-labelled 3  $\mu$ m silica beads.



### 2.1.2 Antibiotics

Geneticin (Invitrogen, Groningen, Netherlands).

Blasticidin (Apollo Scientific, Stockport, United Kingdom).

Penicillin/Streptomycin (Loughborough, England).

Hygromycin (ForMedium, Norfolk, England).

Ampicillin (Sigma-Aldrich, Dorset, England).

### 2.1.3 Molecular Weight Standards

Hyperladder 1kb DNA Ladder (Bioline, London, England).

PageRuler Plus Prestained Protein Ladder (Fermentas, Sunderland, England).

### 2.1.4 Restriction Enzymes

All restriction enzymes and buffers (ThermoScientific, Loughborough, England).

### 2.1.5 Other Enzymes

BioTaq Polymerase (Bioline, London, England).

Q5 DNA Polymerase (New England Biolabs, Ipswich, United States).

RNase A, DNase (Sigma-Aldrich, Dorset, England).

### 2.1.6 Antibodies

IRDye800 Goat Anti-Mouse (Licor Biotechnologies, Cambridge, England).

Mouse  $\alpha$ -ubiquitin (New England Biolabs, Ipswich, United States).

Rat  $\alpha$ -GFP, Rat  $\alpha$ -RFP (Chromotek, Martinsried, Germany).

Mouse  $\alpha$ -Calreticulin, mouse  $\alpha$ -PDI (A kind gift from Annette Muller-Taubenberger).

#### 2.1.7 Kits

DNAse treated with DNA-Free Kit (Ambion, England).

First Strand cDNA Synthesis Kit (Fermentas, Sunderland, England).

QIAFilter Plasmid Maxi kit, QIAQuick PCR purification kit, QIAQuick Gel Extraction Kit (QIAGEN, West Sussex, England).

High Pure RNA Isolation Kit (Roche, West Sussex, England).

GeneJET Plasmid Miniprep Kit (ThermoScientific, Loughborough, England).

#### 2.1.8 Escherichia coli Strains

TOP10 chemically competent *E. coli* (Invitrogen, Groningen, Netherlands).

#### 2.1.9 Primers

All primers were purchased from MWG Eurofins (Westway Estate, England) or Sigma-Aldrich (Dorset, England).

#### 2.1.10 Equipment

Bio-Rad gel casting system, PowerPac 300 Power Supply, GenePulser Xcell Electroporator (Bio-Rad Laboratories, Hemel Hempstead, England).

PeqLab Mini Blue gel casting system, PeqSTAR 2x thermocycler, PeqSTAR 96 universal thermocycler (VWR International, Leicestershire, England).

Centrifuge (ThermoFisher Scientific, Loughborough, England)

Neubauer improved haemocytometer (Hawksley, Sussex, England)

Odyssey Infrared Imaging System (Li-Core Biotechnologies, Cambridge, England)

Olympus IX71 Microscope, U-RFP-T, QImaging RetegaExi Fast1394 Digital camera (Olympus, Southend-on-sea, England)

GeneFlash gel documentation system (Syngene Bio Imaging)

Leica dissection microscope (Leica, Wetzlar, Germany)

Ultraview VoX Inverted spinning disk microscope, LS50B Spectrophotometer (Perkin-Elmer, Waltham, United States)

C9100-50-EM-CCD Camera (Hamamatsu, Japan)

## 2.2 Methods

### 2.2.1 *Dictyostelium* Methods

#### 2.2.1.1 Cell Culture

*Dictyostelium* stocks were maintained at -80°C in *Dictyostelium* freezing medium (7% dimethyl sulfoxide (DMSO), and horse serum). Every four weeks frozen cells were scraped onto SM Agar plates upon which 200 µL *Raoultella planticola* was plated. Colonies were allowed form at 22°C, and cells from the growth zone of these colonies were transferred into liquid HL5 with glucose media and 100 µg/mL penicillin/streptomycin. Liquid plates were washed and split three times per week and maintained in the log phase ( $1-2 \times 10^6$  cells/mL). Cell concentrations were calculated using a Neubauer improved haemocytometer.

### 2.1.1.2 Immunofluorescence Microscopy

To visualise *Dictyostelium*  $\gamma$ -secretase component protein localisation, cells were fixed using -80°C methanol. Cell lines overexpressing GFP/RFP-tagged  $\gamma$ -secretase components were seeded on 13mm, thickness 1, glass coverslips overnight to reach confluency in HL5 medium. Coverslips were dried on paper towels of excess media and submerged at a 40° angle from the vertical to limit cell shearing in -80°C methanol (Hagedorn et al., 2006). Coverslips were incubated in methanol on top of dry ice for 30 minutes to allow for adequate cell fixation and then submerged in room temperature phosphate buffered saline. Following fixation cells were stained using a 1:500 dilution  $\alpha$ -GFP/Red fluorescent protein (RFP) antibodies to visualise  $\gamma$ -secretase components, and a 1:5 dilution  $\alpha$ -calreticulin antibody to visualise the endoplasmic reticulum. Additionally, 4',6'-diamidino-2-phenylindole (DAPI) was added during the final wash stage at a 1:1000 dilution (final concentration 1  $\mu$ g/mL) for 5 minutes to visualise the nucleus. Cells were imaged on an Olympus IX71 wide-field fluorescence microscope and representative images were captured.

### 2.1.1.3 Development Assays

For development assays on nitrocellulose filters  $1 \times 10^7$  cells were harvested from cells grown in liquid media, washed and resuspended in 1 mL KK2 (16.2mM  $\text{KH}_2\text{PO}_4$ , 4mM  $\text{K}_2\text{HPO}_4$ ). Cells were evenly distributed over a 47mm black nitrocellulose filter soaked in KK2 and incubated at 22°C for 24 hours in a container with wet tissue paper to maintain a humid environment.

For development assays on 1% KK2 agar plates (5 mL KK2 and 0.05g bacteriological agar)  $5 \times 10^6$  cells were harvested from cells grown in liquid media,

washed and resuspended in 50  $\mu$ L KK2. Cells were spotted on 1% KK2 agar plates and allowed to dry and then incubated at 22°C for 24 hours in a container with wet tissue paper to maintain a humid environment.

For experiments requiring acidic or basic pH, levels of  $\text{KH}_2\text{PO}_4$  or  $\text{K}_2\text{HPO}_4$  were adjusted to reach the desired pH (Table 2.1). Cells were harvested as previously, but were washed and resuspended in the required pH KK2 buffer before incubation. All cells were incubated on pH7 soaked nitrocellulose filters for 24 hours.

pH	% $\text{K}_2\text{HPO}_4$	% $\text{KH}_2\text{PO}_4$
5.0	7.3	92.7
6.0	13.2	86.8
7.0	61.5	38.5
8.0	94.0	6.0
9.0	94.7	5.3

**Table 2.1. Percentages of  $\text{K}_2\text{HPO}_4$  and  $\text{KH}_2\text{PO}_4$  to acquire required pH levels for development.**

#### 2.2.1.4 Growth Curve Assay

For proliferation assays *Dictyostelium* cells were harvested and diluted in HL5 medium at  $2 \times 10^4$  cells/mL. Cells were distributed in 500  $\mu$ L aliquots in a well of a 24 well plates in triplicate and allowed to grow at 22°C for 7 days. Cell density was counted and calculated every from day 3 to day 7. *Dictyostelium* cells containing extrachromosomal plasmids were grown in the presence of 10 $\mu$ g/mL hygromycin.

#### 2.2.1.5 Macropinocytosis Assay

To measure macropinocytosis  $5 \times 10^7$  cells were harvested from liquid media and diluted in 5 mL of HL5 medium at  $1 \times 10^7$  cells (Hacker et al., 1997). Cells were incubated in shaking culture for 15 minutes to recover after which 100  $\mu$ L of 100  $\mu$ g/mL TRITC-Dextran was added to the cells. 500  $\mu$ L of cells were aliquoted and extracellular TRITC-Dextran was quenched in 50  $\mu$ L trypan blue solution (0.4% w/v trypan blue in KK2) at time points 0, 15, 30, 45, 60, 90, 120 minutes. Immediately upon quenching cells were washed two times in KK2 buffer and resuspended in a final volume of 1 mL KK2 and average intracellular fluorescence was measured at emission wavelength 577 nm (excitation 468nm) over 3 readings using a Perkin Elmer LS50B Spectrophotometer.

#### 2.2.1.6 Autophagosome Maturation

To analyse autophagosome formation and maturation the autophagy reporter GFP-Atg8 was utilised (King et al., 2011). In order to minimise vesicle movement in the Z-plane, and stimulate the autophagosome formation cells were compressed under a thin layer of 1% agarose in HL5 medium. Cells were seeded in a glass-bottomed microscopy dish and covered by a ~2 mm agarose slab, excess media was removed by capillary action using blotting paper. After 10 minutes, cells were imaged using a 100x objective and a 488 nm excitation laser, 4 z-plane images were taken every 2 seconds at a distance of 1  $\mu$ M spacing. The point of autophagosome completion was determined by the enlargement and dimming of GFP fluorescence. The time until GFP-fluorescence was undetectable was measured from blinded movies captured from at least three independent experiments.

### 2.2.1.7 Autophagosome Measurement

To measure the size of GFP-Atg8 tagged autophagosomes cells were imaged after compression under a thin layer of 1% agarose in HL5 medium using a 60x oil immersion objective and GFP filter. After imaging, autophagosome size was measured utilising the line tool in ImageJ. Measurements were taken manually from the widest point of the autophagosome from blinded images.

### 2.2.1.8 Phagosomal Proteolysis Assay (Carried out by Dr. Jason King, University of Sheffield)

Phagosomal proteolytic activity was measured through the use of DQgreen/Alexa594 labelled beads (Sattler et al., 2013).  $3 \times 10^5$  cells were seeded in each well of a 96 well plate, and 3  $\mu$ M labelled beads were subsequently added. Fluorescence was measured on a plate reader each minute in triplicate. Normalised Alexa594 fluorescence was used to normalise proteolytic activity, and differences in bead uptake and rates were normalised to wild-type cells to calculate relative activity.

## 2.2.2 Molecular Biology Techniques

### 2.2.2.1 Polymerase Chain Reaction

Amplification of DNA using polymerase chain reaction (PCR) followed the conditions for standard amplification reactions: 2 – 5  $\mu$ L DNA, 2  $\mu$ L 2 mM dNTPs, 2  $\mu$ L 5x  $\text{NH}_4$  reaction buffer, 0.8  $\mu$ L  $\text{MgCl}_2$ , 0.1  $\mu$ L BIOTAQ DNA Polymerase (5U  $\mu\text{L}^{-1}$ ), 2  $\mu$ L 10 pmol 5' primer, 2  $\mu$ L 10 pmol 3' primer and  $\text{dH}_2\text{O}$  to bring up to 20  $\mu$ L reaction volume. For amplification using a proof reading enzyme the following conditions were used: 2 – 5  $\mu$ L DNA, 2  $\mu$ L 2mM dNTPs, 5  $\mu$ L 5x Q5 Reaction

buffer, 0.1  $\mu\text{L}$  Q5 DNA Polymerase, 2  $\mu\text{L}$  10 pmol 5' primer, 2  $\mu\text{L}$  10 pmol 3' primer, dH<sub>2</sub>O up to 25  $\mu\text{L}$  total reaction volume.

The PCR reactions were carried out using the following thermocycler conditions: initial denature, 10 minutes at 95°C; 30 reaction cycles at 95°C for 30 seconds, 50°C – 68°C (depending on primer annealing temperature) for 30 seconds, extension at 30 seconds per kilobase at 68°C; final extension for 5 minutes at 68°C. Samples were stored at 4°C until they could be visualised by gel electrophoresis.

#### 2.2.2.2 Gel Electrophoresis

To visualise and separate DNA, 1% agarose gels containing ethidium bromide and 1x TAE buffer were used. 5x DNA loading dye was added at the appropriate volume to DNA samples and samples were run alongside a 1 kb DNA ladder to determine fragment size. Agarose gels were run in an electrophoresis tank for 30 – 50 minutes at 110V and visualised with a UV light using a GeneFlash gel documentation system.

To purify DNA Qiagen QIAquick Gel Extraction kits or Qiagen QIAquick PCR Purification kits were used following the manufacturer's guidelines.

#### 2.2.2.3 Transformation of Competent *E. coli*

Chemically competent *E. coli* cells were thawed on ice for bacterial transformations. ~10  $\mu\text{L}$  of ligated DNA was added to 50  $\mu\text{L}$  competent *E. coli*, cells were incubated on ice for 30 minutes before heat-shock treatment for 30 seconds at 42 °C. Cells were then transferred to ice for 2 minutes before the addition of 50  $\mu\text{L}$  Luria-Bertani (LB) broth followed by incubation at 37°C for 1



hour. After incubation cells were briefly mixed by pipetting, streaked onto LB agar plates (containing 20 µg/mL ampicillin) and incubated overnight at 37°C.

#### 2.2.2.4 Plasmid Preparation

Verification of positive *E. coli* transformants was carried out without the use of commercial plasmid preparation kits. 2mL of positive culture was spun down for 2 minutes at 15,000G, supernatant aspirated and resuspended in 200 µL P1 buffer (50 mM Tris-Cl pH 8.0, 10 mM EDTA, 100 µg/mL RNase A). Cells were lysed for 5 minutes in 200 µL P2 buffer (200 mM NaOH, 1%SDS (W/V)), and the lysis was neutralised by addition of 200 µL P3 buffer (3M potassium acetate pH 5.5). The neutralised lysis mixture was spun down at 15,000 G for 20 minutes and supernatant was transferred into a clean, fresh tube. DNA was precipitated by the addition of 420 µL isopropanol (70% reaction volume) and the mixture was vortexed and centrifuged for 15 minutes at 15,000 G. Supernatant was discarded, and 1mL 70% ethanol was added to remove residual salts. The DNA was vortexed and then centrifuged for 5 minutes at 15,000 G, supernatant discarded and residual ethanol removed by incubation at 50 °C for approximately 10 minutes. The resultant DNA was resuspended in 30 – 50 µL dH<sub>2</sub>O.

For preparations involving commercially available kits Qiagen QIAFilter Plasmid Maxi kits and ThermoScientific GeneJET Plasmid Miniprep Kits were used following the manufacturer's guidelines.

#### 2.2.2.5 Restriction Digests

All restriction digests followed standard restriction digest conditions: 5 µL DNA, 0.1 – 0.4 µL restriction digest enzyme(s) (100 U µL<sup>-1</sup>), 2 – 5 µL appropriate

restriction digest buffer (following manufacturer's guidelines), dH<sub>2</sub>O to 20 – 50 µL total reaction volume. Restriction digest mixtures were incubated at 37 °C for 1 – 2 hours to ensure complete DNA digestion.

#### 2.2.2.6 Construction of Knockout Vectors

Generation of knockout vectors utilised the following procedure. Two fragments of the gene of interest open reading frame were amplified using PCR. Primers used for PCR amplification used restriction sites corresponding to the cloning vector pLPBLP (Faix et al., 2004). PCR products were purified using the GeneJET plasmid miniprep kit and subsequently subjected to restriction enzyme digest alongside pLPBLP vector, BamHI and PstI for N-terminal cloning, and NcoI and KpnI for C-terminal cloning. Gene fragments were ligated into the pLPBLP vector backbone using 0.5 T4 DNA ligase (1 U µL<sup>-1</sup>), 1 µL T4 DNA ligase buffer at molar ratios of 1:5 vector: insert or 1:10 vector: insert. Ligation mixtures were either incubated at room temperature for 2 – 4 hours, overnight at 16°C or over 48 hours at 4°C depending on the size of the gene insert (larger sizes were incubated for longer times). Ligation mixtures were heat inactivated at 70°C for 20 minutes before transformation into chemically competent *E. coli* cells. Following colony formation on LB agar plates containing ampicillin single bacterial colonies were picked and grown in 5mL LB media containing 20 µg/mL ampicillin before plasmid preparation. To confirm insertion of fragment DNA restriction digests were performed using the previously used restriction enzymes. Confirmation of insertion for one gene fragment was followed by repeating the process with the second gene fragment into the same pLPBLP vector backbone. Once confirmation for both N- and C-terminal fragments was successful the

knockout construct was prepared using the QIAfilter Plasmid Maxi kit and subsequently electroporated into *Dictyostelium* cells.

#### 2.2.2.7 Construction of Overexpression Vectors

Overexpression vectors containing N-terminal GFP (pTX-GFP) (Levi et al., 2000), C-terminal GFP (pDM-450) (Veltman et al., 2009) or C-terminal RFP (389-2 RFP) (Fischer et al., 2004) tags were obtained from [www.dictybase.org](http://www.dictybase.org). Full length target gene cDNA was amplified by PCR using primers with appropriate restriction sites and a proof reading DNA polymerase. Overexpression constructs were restriction enzyme digested alongside vector backbones followed by ligation into the appropriate vector. Following confirmation of DNA fragment insertion by restriction digest and sequence verification by DNA sequencing plasmids were prepared using the QIAfilter Plasmid Maxi kits.

#### 2.2.2.8 Transformation of Vector Constructs into *Dictyostelium*

*Dictyostelium* knockout and overexpression vectors were transformed into *Dictyostelium* by electroporation (Gaudet et al., 2007). Knockout cassettes were prepared for transformation by excision from the vector backbone using the restriction enzymes BamHI and KpnI. 20µg of the excised knockout cassette was purified using isopropanol precipitation. Overexpression vectors were transformed as extrachromosomal vectors and unaltered.

For electroporation,  $5 \times 10^6$  cells were harvested and incubated on ice for 10 minutes before centrifugation at 1500g for 3 minutes. Cells were then washed twice with ice cold KK2 prior to a final wash with ice cold electroporation buffer (4.76g HEPES, 3.73g KCl, 0.58g NaCl, 0.12g MgSO<sub>4</sub>, 0.42g NaHCO<sub>3</sub> and 0.156g NaH<sub>2</sub>PO<sub>4</sub>, pH 7.0, make up to 1L with dH<sub>2</sub>O) and then resuspended in 100 µL

electroporation buffer. The final resuspended pellet was transferred to a 0.1mm cuvette and pulsed in a BIO-RAD GenePulser Xcell electroporator using 1 pulse at 850V and 25 $\mu$ F. Cells were incubated on ice for 10 minutes before being transferred into 10mL HL5 media containing 10 $\mu$ g/mL penicillin/streptomycin. Knockout transformants were transferred to each well of a 96 well plate, whilst overexpression transformants were transferred to a 10cm tissue culture dish. After 24 hours 100 $\mu$ L of 20 $\mu$ g/mL blasticidin in HL5 media was transferred to each well of the 96 well plate for knockout transformants, for overexpression transformants 10 $\mu$ L of 10 $\mu$ g/mL geneticin or hygromycin was added to the tissue culture plate.

#### 2.2.2.9 Extraction of DNA from Potential Transformants

In order to confirm successful transformation of the knockout cassette transformants growing in the presence of blasticidin after transformation were harvested once they reached confluence. Cells were centrifuged for 3 minutes at 1000g and resuspended in 48 $\mu$ L lysis buffer (50mM KCl, 10mM Tris pH 8.3, 2.5M MgCl<sub>2</sub>, 0.45% Nonidet P40, 0.45% TWEEN 20) and 2 $\mu$ L Proteinase K (822 U mL<sup>-1</sup>) and incubated for 5 minutes. Proteinase K was inactivated at 95°C for 1 minute following incubation, and the resultant DNA was used in PCR reactions to screen for correct homologous recombinant knockouts.

#### 2.2.2.9 Screening for Homologous Recombinants

Primers were designed to determine whether *Dictyostelium* cells transformed with the knockout construct underwent target gene ablation with a correctly incorporated knockout cassette. Genomic DNA was extracted from cells and used in PCR analysis based on 3 different primer combinations to screen for

the knockout cassette. Genomic control primers were designed to amplify DNA from 3' and 5' regions flanking the fragments used in the knockout cassette, these would amplify non-deleted regions of the gene. Vector control primers were designed to amplify DNA from within the DNA fragments used in the vector construction and in the blasticidin resistance gene, these would confirm the transformation of the knockout cassette. Knockout diagnostic primers used a flanking primer from the genomic control reaction and the blasticidin resistance cassette primer from the vector control reaction to determine whether the cassette was inserted into the correct region of the *Dictyostelium* genome. Primer combinations were designed to screen both the 3' and 5' fragments of the knockout cassette.

#### 2.2.2.11 Sub Cloning of Correct Transformants

To allow for isogenic cell line selection of correct knockout transformants cells were plated onto SM agar plates with 200 $\mu$ L *Raoultella planticola*. After incubation at 22°C single colonies were selected, genomic DNA was extracted and re-screened with the PCR primers previously described (Section 2.2.2.10).

#### 2.2.2.12 RNA Extraction and Reverse Transcriptase PCR

To confirm gene ablation  $1 \times 10^7$  *Dictyostelium* cells were harvested. These cells were washed and resuspended in KK2 before the RNA was extracted using a High Pure RNA Isolation Kit (Roche) according to manufacturer instructions.

Following RNA extraction cDNA was synthesised to allow for RT PCR. Extracted RNA was used at 1-4 $\mu$ g to synthesise cDNA using a First Strand cDNA synthesis kit following the manufacturer's instructions. Following this, 2 $\mu$ L cDNA was used in PCR amplification. Primers used in the PCR were designed to flank the

blastocidin resistance cassette in knockout cell lines giving a small ~400 base pair product in wild-type cells and a ~1800 base pair, or no product, for knockout cells.

## 2.2.3 Proteomics

### 2.2.3.1 Western Blot Analysis

To analyse high molecular weight ubiquitinated protein content  $5 \times 10^6$  cells were harvested and resuspended and incubated for 10 minutes in 100  $\mu$ L of PBS (10x – 14.4g  $\text{Na}_2\text{HPO}_4$ , 80g NaCl, 2g KCl, 2.4g  $\text{KH}_2\text{PO}_4$  made up to 1 L with  $\text{dH}_2\text{O}$ , pH 7.4) supplemented with 0.1% NP40 and 1% TritonX-100 and protease inhibitors (Calvo-Garrido and Escalante, 2010). Cells were then passed through a 30-gauge needle four times to allow for complete cell disruption. Extracts were centrifuged at 17500g for 5 minutes and the supernatant was decanted and mixed with 20 $\mu$ L 5x SDS loading buffer (0.8mL 2M Tris pH 6.8, 3mL 80% glycerol, 5mL 10% SDS, 1.25 mL  $\beta$ -mercaptoethanol, water to 10mL, bromophenol blue) before boiling at 95°C for 10 minutes. Protein samples were loaded into the stacking gel (stacking gel – 425  $\mu$ L 30% acrylamide solution, 157.5  $\mu$ L Tris pH 6.8, 1.875 mL  $\text{dH}_2\text{O}$ , 25 $\mu$ L 10% SDS, 25  $\mu$ L 10% ammonium persulphate, 7.5  $\mu$ L TEMED. Resolving gel – 2.215 mL 30% acrylamide, 0.95 mL Tris pH 8.8, 1.825 mL  $\text{dH}_2\text{O}$ , 100  $\mu$ L 10%SDS, 50  $\mu$ L 10% ammonium persulphate, 5  $\mu$ L TEMED) alongside a molecular marker, PageRuler Plus Prestained Protein Ladder. The gel was run at 200 V for 35 minutes in 1x running buffer (10x – 30g Trisma base, 144g glycine, 100 mL 10% SDS, made up to 1L with  $\text{dH}_2\text{O}$ ). The separated protein was blotted onto a PVDF membrane activated in methanol. All materials for blotting, blotting paper, sponges and activated membrane were soaked in ice cold transfer buffer containing 10% ETB buffer (10x – 75g Trisma base, 360g glycine, 25 mL 10%

SDS) with 10% methanol. The transfer blot was added to a tank containing ice cold transfer buffer placed inside a filled ice box and run at 200 mA for 2 hours.

Once blotting was completed the PVDF membrane was incubated using 5mL 5% skimmed milk in PBST (1x PBS + 1% TWEEN 20) for 1 hour. The  $\alpha$ -ubiquitin antibody was prepared at 1:1000 dilution, and  $\alpha$ -PDI as a loading control at 1:10 in skimmed milk in PBST and incubated at 4°C overnight. Primary antibody was then washed away with 1x PBS followed by 3 x 10 minute washes in PBST. The appropriate secondary antibodies were then added at a 1:10,000 dilution in skimmed milk + PBST before imaging on an Odyssey Infrared Imaging System.

Following imaging western blots were analysed using the LiCor Image Studio software. Total ubiquitinated protein content was calculated against the appropriate loading control, and normalised against wild-type.

#### 2.2.4 Bioinformatic Analysis

In order to determine evolutionary conservation of the target proteins Aph-1, Pen-2 and Ncstn, phylogenetic trees were generated using the program Mega 5.1 (Kumar et al., 2008). Briefly, amino acid sequences were gathered from Uniprot for proteins of interest from several different organisms spanning the animal and plant clades (The UniProt, 2017). These sequences were then aligned using ClustalW alignment (Goujon et al., 2010). After alignment a Neighbour-Joining tree was generated using the Bootstrap method and 500 Bootstrap replications, the substitution model used was the Poisson model. Outgroups were chosen by selecting distantly related proteins.

## 2.3 Statistical Analyses

To determine statistical significance tests varied depending upon the criteria. First, data was determined to be normally distributed as shown by the D'agostino & Pearson normality test. For experiments comparing mean values from several data sets (growth assays, macropinocytosis assay, GFP-Atg8 measurement and quenching assays) a two-way ANOVA was used with the Bonferroni post-hoc test to compare multiple data sets to each other. For data comparing values to a normalised value (ubiquitinated protein western blot) a one sample T-test was utilised. In all graphical representations of data error bars shown are standard error of the mean. \* denotes  $p < 0.05$ , \*\* denotes  $p < 0.01$ , \*\*\* denotes  $p < 0.0001$ .

## 2.4 Software

Microscopy analysis for Atg8 quenching was carried out using Fiji (Schindelin et al., 2012). GraphPad was used for statistical analysis (GraphPad Software Inc, California, United States). Western blot analysis used Image Studio Lite (LiCor Biotechnologies, Cambridge, United Kingdom). Mega 5.1 software was used for phylogenetic analysis (Kumar et al., 2008).

## 2.5 Websites

### *Dictyostelium* gene and protein information

[www.dictybase.org](http://www.dictybase.org)

### *Dictyostelium* gene expression information

[www.dictyexpress.biolab.si](http://www.dictyexpress.biolab.si)

### Basic Local Alignment Search Tool (BLAST) Analysis



[www.dictybase.org/tools/blast](http://www.dictybase.org/tools/blast)

[www.ncbi.nlm.nih.gov/BLAST](http://www.ncbi.nlm.nih.gov/BLAST)

#### Protein sequence alignment

[www.ebi.ac.uk/tools/msa/clustalo](http://www.ebi.ac.uk/tools/msa/clustalo)

#### Protein domain prediction

<http://www.cbs.dtu.dk/services/TMHMM/>

#### Protein information

[www.uniprot.org](http://www.uniprot.org)

## Chapter III

### The *Dictyostelium* $\gamma$ -secretase Complex

---

### 3.1 Introduction

The  $\gamma$ -secretase complex has been studied in *Dictyostelium* to advance our knowledge of its cellular and developmental function showing roles for the complex in development, exogenous substrate cleavage, phagocytosis and calcium homeostasis (McMains et al., 2010, Ludtmann et al., 2014). These studies, however, have not included detailed research into the homology between *Dictyostelium* and human components apart from Presenilin (Ludtmann et al., 2014). In order to better understand the role of the other components of the complex it is necessary to investigate these components, and compare the *Dictyostelium* components with their human orthologues

*Dictyostelium* has been successfully used as a model organism to investigate the roles and functions of Presenilin (McMains et al., 2010, Ludtmann et al., 2014). These studies have found roles for this protein in *Dictyostelium* development, intracellular calcium signalling, phagocytosis and an evolutionary conservation of catalytic activity (McMains et al., 2010, Ludtmann et al., 2014). However, with regards to the remaining components of this protein complex there has been some conflicting evidence. One study, for example, shows a role for presenilin, Aph-1 and Nicastrin in *Dictyostelium* development (McMains et al., 2010), whilst another shows that Nicastrin null cell lines develop comparable to wild-type cells (Ludtmann et al., 2014). Studies in *Dictyostelium* have also shown that the presenilin proteins localise to the endoplasmic reticulum (Ludtmann et al., 2014), a localisation also found in mammalian model organisms used to investigate this protein, and the  $\gamma$ -secretase complex (Xia et al., 1998, Smolarkiewicz et al., 2013).

In this chapter, we will compare the human and *Dictyostelium*  $\gamma$ -secretase components Aph-1, Nicastrin and Pen-2 against their human counterparts. Using bioinformatic tools (Altschul et al., 1990, Pasquier et al., 1999) we will investigate similarities in size, as well as conservation of important domains and motifs in these proteins. Additionally, we will investigate the localisation of these components and compare their localisation in *Dictyostelium* with mammalian model organisms.

### 3.2 *Dictyostelium* and human Aph-1

In order to determine whether *Dictyostelium* is a viable model organism to investigate the function of Aph-1 a number of bioinformatic analyses were carried out. The aim of these was to use a bioinformatics approach to improve our understanding of the *Dictyostelium* Aph-1 protein and to establish similarities to the orthologous mammalian protein.

Upon bioinformatic analysis of Aph-1 between *Dictyostelium* and humans several similarities are observed. The Aph-1 orthologues are closely related in size with the *Dictyostelium* Aph-1 containing 328 amino acids and the human Aph-1A and Aph-1B containing 265 and 257 amino acids respectively (Figure 3.1A). Additionally, these orthologues possess 7 conserved transmembrane domains of similar length and position, containing similar hydrophobic amino acids and by using the TMHMM Server (Krogh et al., 2001), (Figure 3.1 A, D), and a conserved GxxxGxxxG motif in transmembrane domain 4 (Figure 3.1 A, C) (Appendix 1). The *Dictyostelium* Aph-1 when visualised on a phylogenetic tree is more similar to the animal clade than plant Aph-1 proteins (Figure 3.1B).

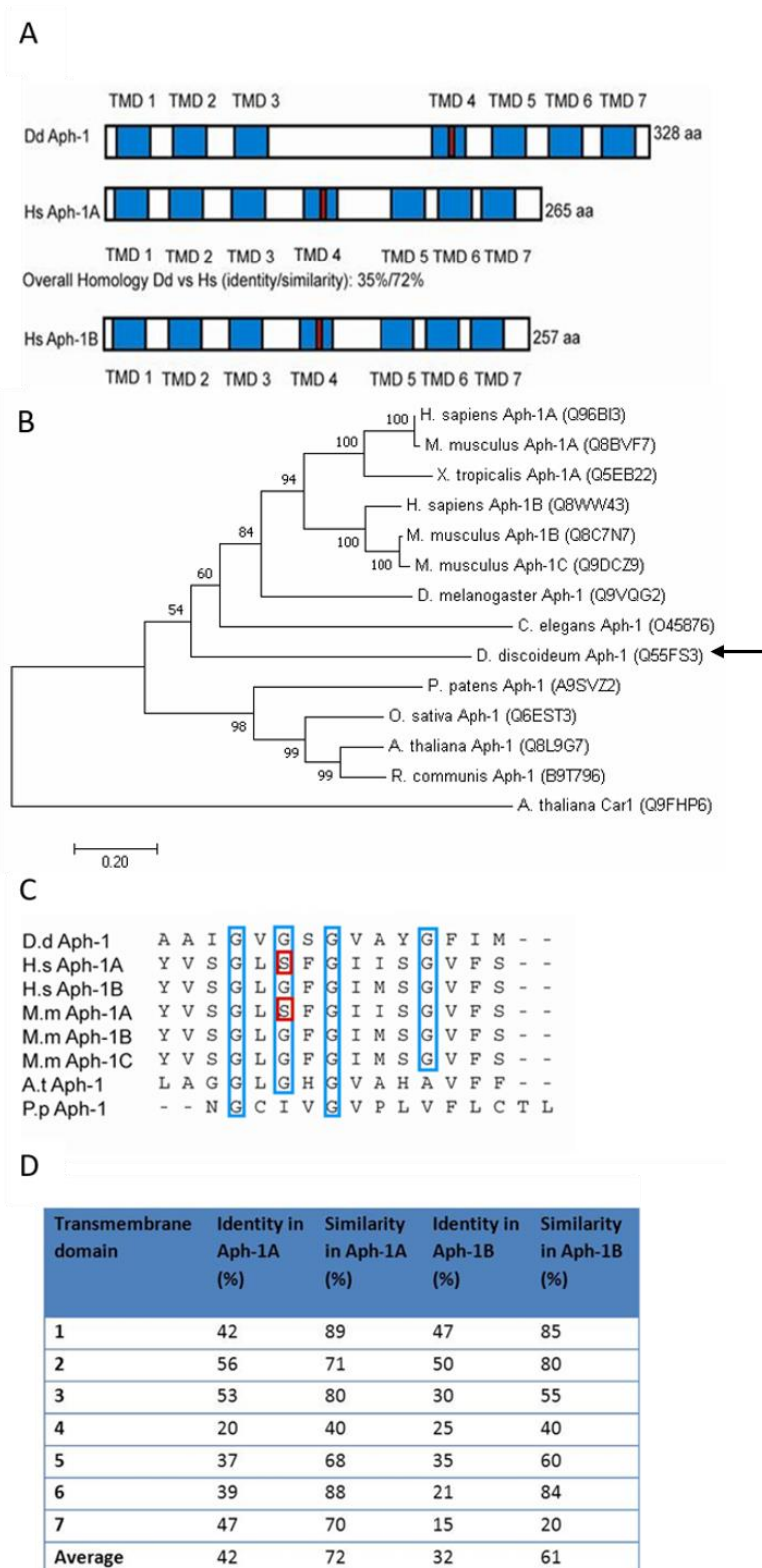


**Figure 3.1 Bioinformatic analysis of *Dictyostelium* Aph-1.** A) Schematic representations of *Dictyostelium* Aph-1, and human Aph-1A and Aph-1B. The relative lengths of Aph-1 is similar between *Dictyostelium* and the two human Aph-1 proteins, as well as location, size and number of transmembrane domains (Blue). Additionally, there is a conserved GxxxGxxxG motif across all three proteins in transmembrane domain 4 (Red). B) Phylogenetic analysis between human, mouse, *Xenopus*, *Drosophila*, *Dictyostelium*, *C. elegans*, *Arabidopsis*, *Physcomitrella*, *R. communis* and *Oryza* Aph-1 proteins. The *Dictyostelium* protein clusters more closely to the animal proteins than the plant or *C. elegans* proteins. C) Alignment of the conserved GxxxGxxxG motif across a number of species including *Dictyostelium*, human, and mouse. Blue boxes indicate conserved glycine residues in the GxxxGxxxG motif, red boxes indicate deviations from conserved glycine. D) A table demonstrating the identity, and similarity of each of the 7 transmembrane domains across *Dictyostelium* and human proteins including the average identity and similarity.

An important domain within the Aph-1 protein is the GxxxGxxxG motif located in transmembrane domain 4 (Lee et al., 2004b). This motif is required for Aph-1 to integrate into, and potentially stabilise, the  $\gamma$ -secretase complex (Lee et al., 2004b). This motif is highly conserved between human and mouse Aph-1 isoforms, and is also present in *Dictyostelium*. However, in the plant model organisms *A. thaliana* and *P. patens* the motif is reduced to GxxxG (Figure 3.1 C).

### 3.3 *Dictyostelium* and human Nicastrin

Nicastrin was analysed in order to determine similarity between the human and *Dictyostelium* proteins. The aim of this was to compare domains and motifs of the proteins, and to compare the size, placement and identity with the human and rodent proteins.

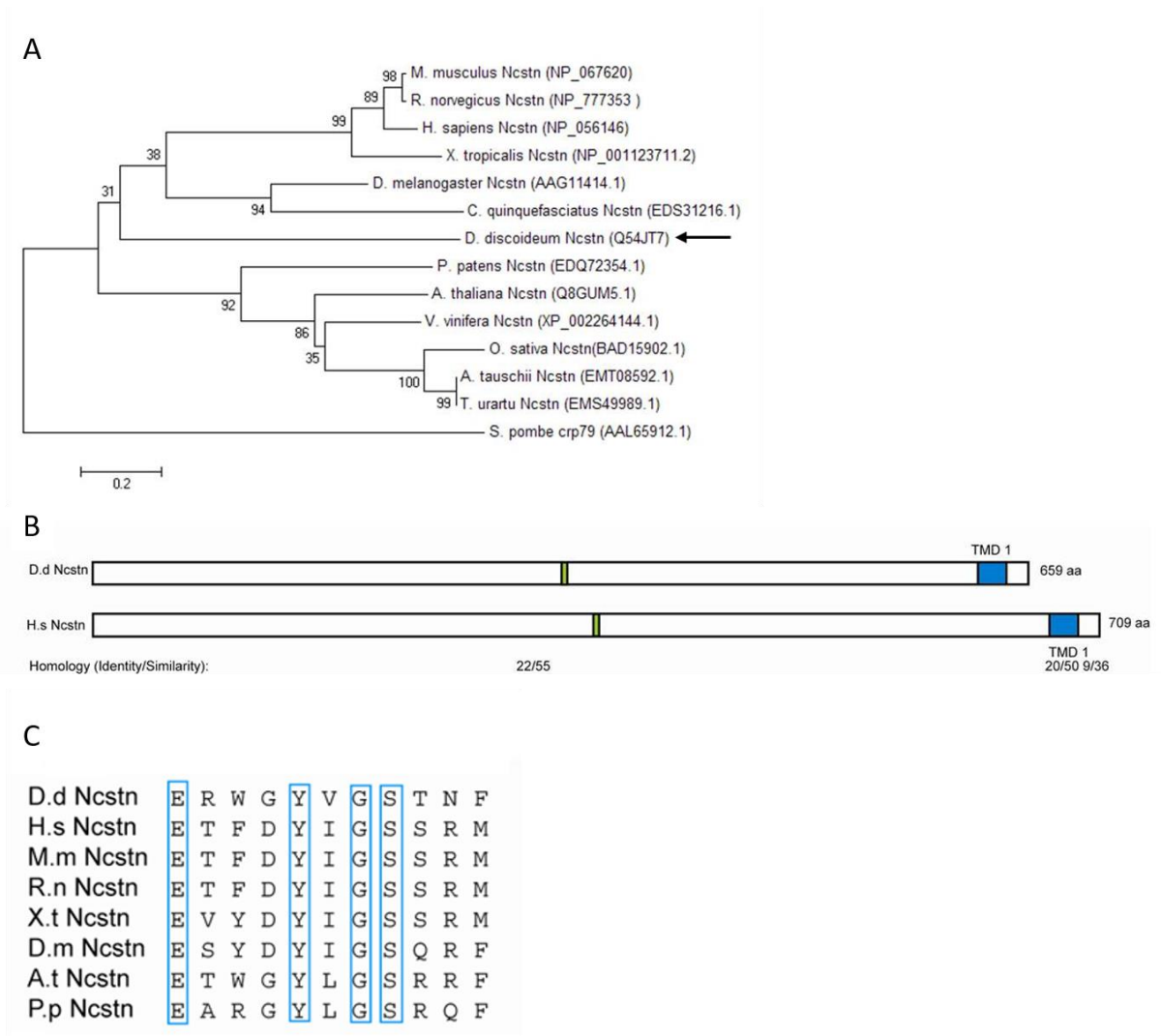


**Figure 3.2 Bioinformatic analysis of *Dictyostelium* Nicastrin.** A) Phylogenetic analysis between human, rat, mouse, *Xenopus*, *Drosophila*, *C. quinquefasciatus*, *Dictyostelium*, *Arabidopsis*, *Physcomitrella*, *V. vinifera*, *A. tauschii*, and *T. urarfu* Nicastrin proteins. The *Dictyostelium* protein clusters more closely to the animal proteins than the plant proteins. B) Schematic representations of *Dictyostelium* Nicastrin, and human Nicastrin. The relative lengths of the protein is similar between *Dictyostelium* and the human protein, as well as location, size and number of transmembrane domains (Blue). Additionally, there is a conserved DYIGS motif across both proteins in the extracellular domain 4 (Green). C) Alignment of the conserved DYIGS motif across a number of species including *Dictyostelium*, human, mouse, *A. thaliana* and *P. patens*. Blue boxes indicate conserved amino acids across species.

In *Dictyostelium* and other model organisms there is only one copy of the Nicastrin protein (Smolarkiewicz et al., 2013, De Strooper, 2003, Ludtmann et al., 2014). Through phylogenetic analysis the *Dictyostelium* Nicastrin protein clusters more towards the mammalian, and animal clade than the plant clade (Figure 3.2A). Additionally, the overall size between the proteins is quite similar, the *Dictyostelium* protein measures 659 amino acids, whilst the human protein measures 709 amino acids. Both orthologues share one transmembrane domain, and a common DYIGS motif (Figure 3.2B). The DYIGS motif in Nicastrin is required for integration into, and stability or substrate recognition in the  $\gamma$ -secretase complex (Lim et al., 2015) (Appendix 2).

### 3.4 *Dictyostelium* and human Pen-2

Pen-2 was analysed to determine homology between the human and *Dictyostelium* proteins. Orthologues were compared to determine similarity in size, and conservation of important motifs and domains within the protein.



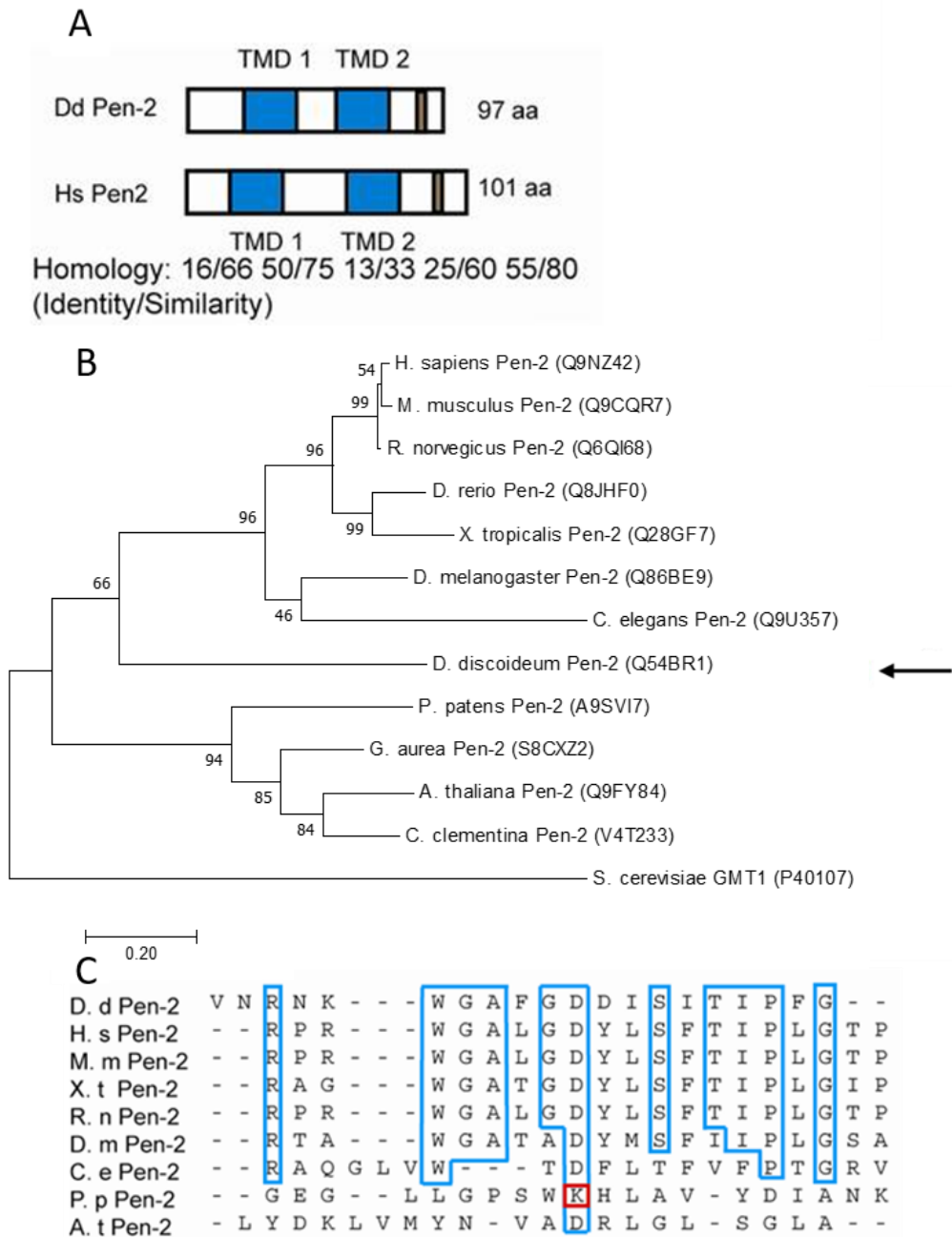


**Figure 3.3 Bioinformatic analysis of Pen-2.** A) Schematic representations of *Dictyostelium* and human Pen-2 comparing *Dictyostelium* and human Pen-2. The overall length between *Dictyostelium* and human Pen-2 is highly similar, with only four amino acid difference between orthologues. Transmembrane domains (blue) are localised to similar positions within the two proteins and are of similar size. Additionally, the C-terminal domains share a conserved DYLSF (brown) motif. B) Phylogenetic analysis of human, mouse, rat, zebrafish, frog, fruit fly, *C. elegans*, *Dictyostelium*, *P. patens*, *G. aurea*, *Arabidopsis*, and *C. clementina* Pen-2 proteins show that the *Dictyostelium* protein clusters more closely to the animal clade than the plant proteins. C) Alignment of the Pen-2 C-terminal domain across species including human, mouse, *Dictyostelium*, *P. patens* and *Arabidopsis*. The Pen-2 C-terminus is highly conserved across a number of species. Blue boxes indicate identical amino acids. Red box denotes a different amino acid in a conserved region.

The *Dictyostelium* and human Pen-2 proteins share a number of similarities in their structure. The orthologous Pen-2 proteins show similar size with the *Dictyostelium* protein containing 97 amino acids, and the human protein containing 101 amino acids. Additionally, both proteins contain similar sized and positioned transmembrane domains with a highly conserved C-terminal domain and DYSLF motif (Figure 3.3 A). Phylogenetic analysis demonstrates that the *Dictyostelium* protein more closely clusters to the animal and mammalian clade than the plant clade suggesting evolutionary conservation for this protein between animals and *Dictyostelium* (Figure 3.3 B). Finally, the C-terminus of Pen-2 is important for the protein to function and integrate into the  $\gamma$ -secretase complex (Mao et al., 2012). Here we show that the *Dictyostelium* Pen-2 C-terminus is highly conserved between *Dictyostelium*, humans, mouse and other organisms (Figure 3.3 C) including conserved amino acids within the important DYLSF motif (Mao et al., 2012) (Figure 3.3 A, C) (Appendix 3).

### 3.5 Localisation of the $\gamma$ -secretase complex components

In mammalian model organisms the  $\gamma$ -secretase complex localises to the endoplasmic reticulum (Area-Gomez et al., 2009). The complex forms sequentially, first Aph-1 and Nicastrin form a holocomplex, this complex is then joined by PsenA/B, and finally Pen-2 (Mao et al., 2012). Once fully formed the complex is shuttled between the plasma membrane, Golgi apparatus and ER. The vast majority (95%) of the complex is localised to the ER, whilst the remaining portion (5%) is localised to the Golgi Apparatus and plasma membrane (Smolarkiewicz et al., 2013).

In *Dictyostelium*, Presenilin has been found to localise to the endoplasmic reticulum (Ludtmann et al., 2014). This localisation is unaltered when catalytic activity is ablated, and is also preserved when the human Presenilin 1 protein is expressed in this organism (Ludtmann et al., 2014). The localisation of other components in *Dictyostelium* however is not yet known, as other studies have not yet investigated this.

### 3.5.1 Generation of overexpression constructs

To allow visualisation of  $\gamma$ -secretase complex components in *Dictyostelium*, overexpression constructs were generated for each component (Chapter II). Amplified genes were cloned into GFP-tagged vectors and expressed in *Dictyostelium* (Levi et al., 2000, Fischer et al., 2004) before visualisation and analysis of colocalisation.

#### 3.5.1.1 Generation of an Aph-1 overexpression construct

To determine subcellular localisation of Aph-1 an extrachromosomal overexpression construct was generated. The overexpression construct was generated through amplification of the Aph-1 open reading frame using a cDNA template. After amplification the product was cloned into the pTX-GFP expression vector (Levi et al., 2000) (Figure 3.4 A) and integration was confirmed by restriction digest (Figure 3.4 B). Vectors were sequenced to ensure they were mutation free and subsequently cloned into *Dictyostelium*. Transformants growing in the presence of neomycin were allowed to grow to confluency before visualisation to ensure fluorescent protein production. Localisation of GFP-Aph-1 appeared to be membrane bound and similar to the endoplasmic reticulum

localisation found in Presenilin studies in *Dictyostelium* (Ludtmann et al., 2014) (Figure 3.4 C).

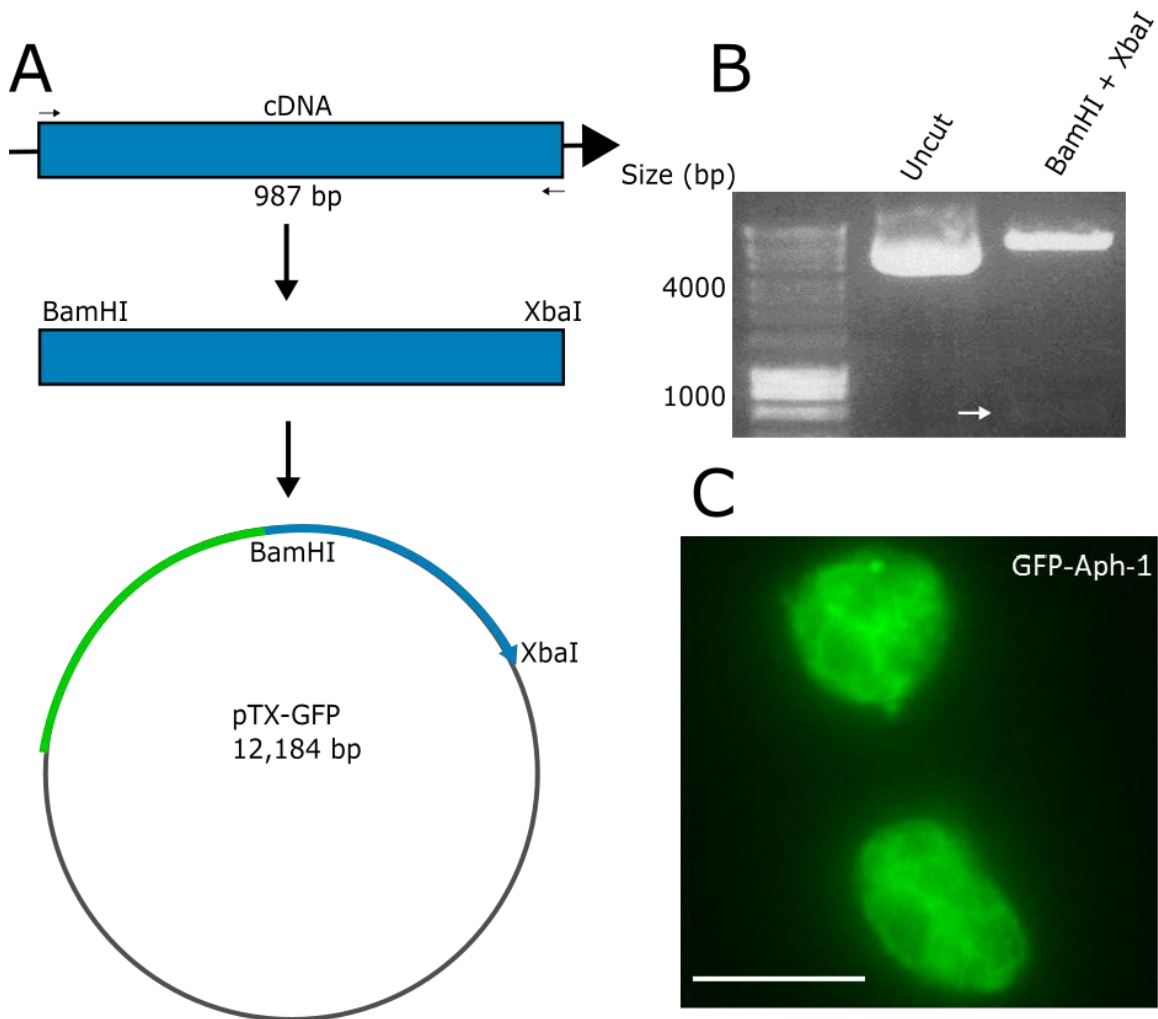


**Figure 3.4 Generation of an Aph-1 overexpression construct.** A) The Aph-1 open reading frame was amplified from cDNA using 5' and 3' primers containing cutsites for BamHI and XbaI. The generated product was cloned into the pTX-GFP containing an N-terminal GFP-tag. B) To confirm integration of the Aph-1 ORF restriction digest of the constructed vector was carried out using BamHI and XbaI. C) To confirm tagged protein production cells were visualised using a GFP-filter and 60x micoroscope objective. Scale bar = 10μm

### 3.5.1.2 Generation of a Nicastrin overexpression construct

To allow visualisation of Nicastrin in *Dictyostelium* an RFP-tagged overexpression construct was generated. The construct was generated by amplifying the Nicastrin open reading frame from cDNA before subsequent cloning into the C-terminal RFP vector 389-2 (a kind gift from Annette Muller-

Taubenberger) (Figure 3.5 A, B) and sequencing to ensure the construct was mutation free. After succesful cloning and transformation into *Dictyostelium* cells were visualised to confirm RFP tagged protein production. Visualisation of RFP-Nicastrin demonstrated membrane bound staining, potentially localising to the endoplasmic reticulum (Figure 3.5 C).

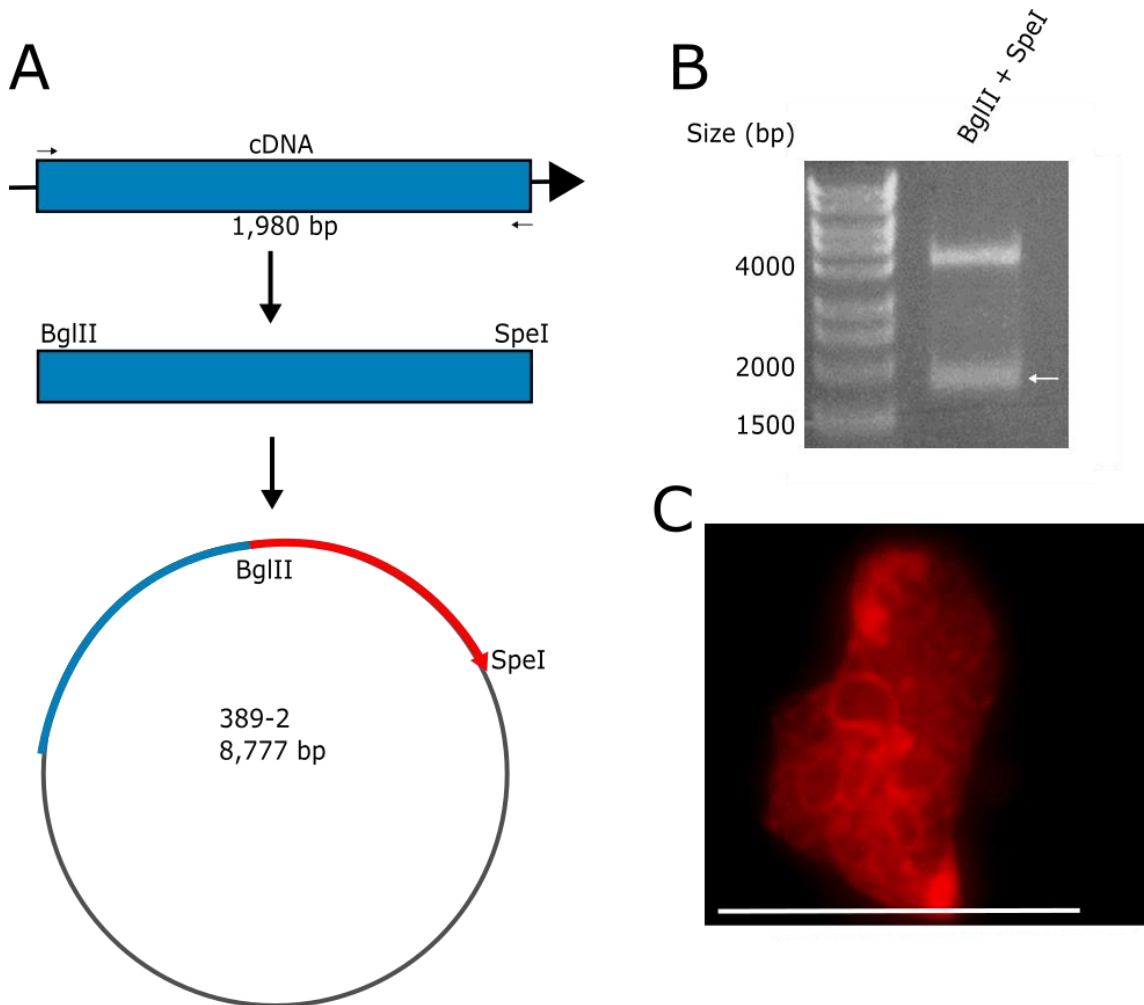


**Figure 3.5 Generation of a Nicastrin overexpression construct.** A) The Nicastrin open reading frame was amplified using 5' and 3' primers containing cutsites for BglII and SpeI. The generated product was cloned into the C-terminal RFP vector 389-2. B) Restriction digest of the constructed vector using BglII and SpeI showed successful integration of the Nicastrin open reading frame into the target vector. C) Visualisation of Ncstn-RFP cells showed the presence of fluorescently tagged protein. Scale bar = 10 $\mu$ m.

### 3.5.1.3 Generation of a Pen-2 overexpression construct

An RFP-Pen-2 construct was generated to allow visualisation of Pen-2 in *Dictyostelium*. The construct was generated by amplification of the Pen-2 open reading frame from cDNA before cloning into an N-terminal RFP vector, pTX-RFP (Figure 3.6 A) (Fischer et al., 2004). Following confirmation of cloning through restriction digest and sequencing the construct was transformed into *Dictyostelium* cells (Figure 3.6 B). Visualisation of RFP-Pen-2 transformants however did not show any specific protein localisation and the staining we observed was likely to be background staining (Figure 3.6 C). Subsequent western blot analysis of RFP-Pen-2 cells showed no fusion RFP-Pen-2 protein.

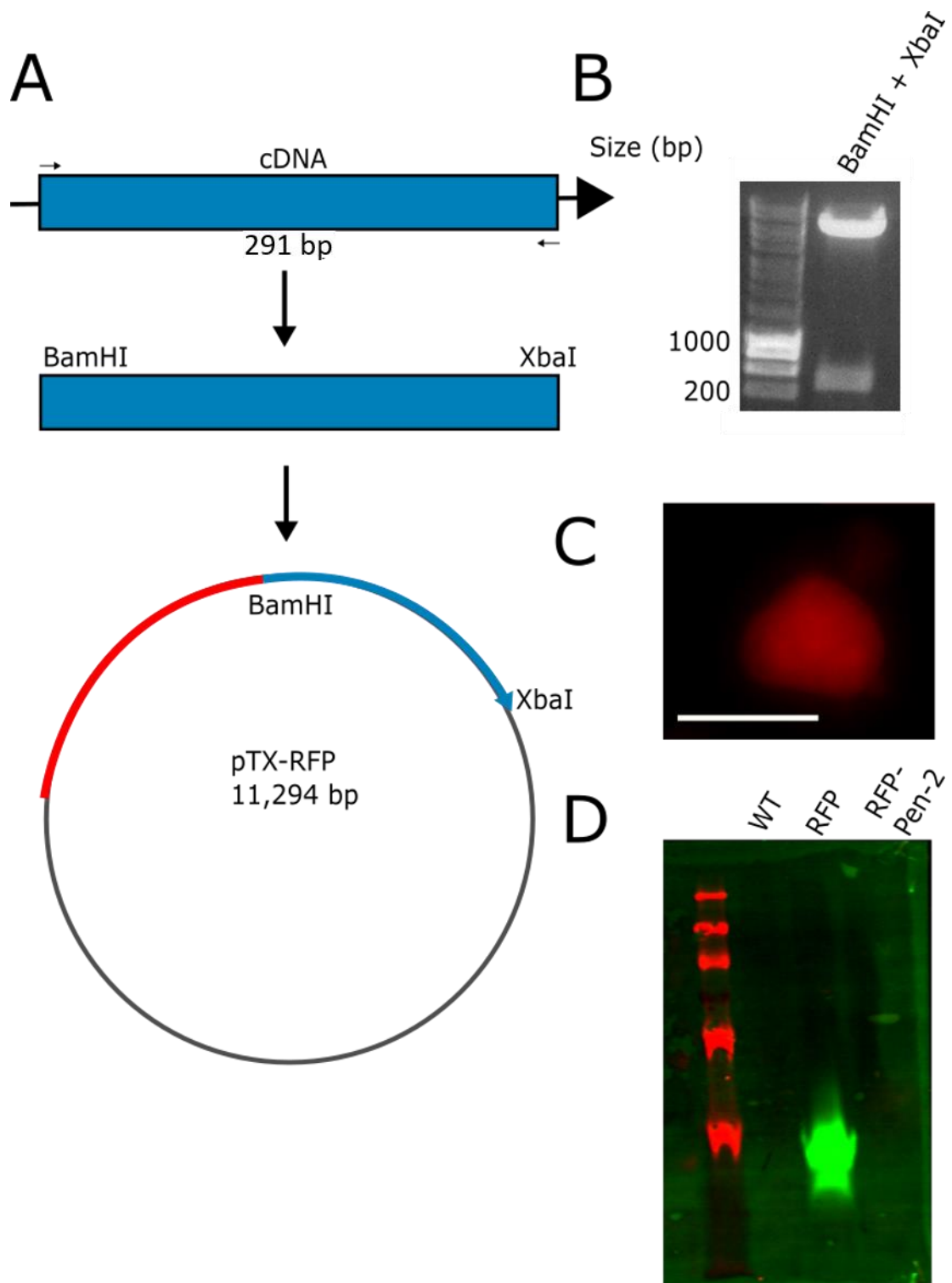


**Figure 3.6 Generation of an RFP-Pen-2 construct.** A) A Pen-2 overexpression construct was generated through the amplification of the Pen-2 open reading frame from a cDNA template with primers containing cutsites for the restriction enzymes BamHI and XbaI. Following amplification the product was ligated into the N-terminal RFP vector pTX-RFP. B) Restriction digest of the constructed vector with the enzymes BamHI and XbaI showed succesful cloning of the Pen-2 gene into the target vector. C) Visualisation of RFP-Pen-2 in cells showed no specific localisation of RFP-Pen-2 in wild-type *Dictyostelium* cells. D) Western blot analysis of RFP-Pen-2 cells for the presence of a fusion protein showed no RFP-tagged protein. Scale bar = 10µm.

### 3.5.2 Localisation of the $\gamma$ -secretase complex components in *Dictyostelium*

In mammalian cells the  $\gamma$ -secretase complex components have been shown to localise to the endoplasmic reticulum (Xia et al., 1998, Gu et al., 2003, Niimura et al., 2005). In *Dictyostelium*, Presenilin has also been found to localise to the ER (Ludtmann et al., 2014), however the localisation of the other cellular components is unknown.

In order to confirm whether the localisation observed upon overexpression of Aph-1 or Nicastrin (Figure 3.4 C, 3.5 C) is to the endoplasmic reticulum we carried out colocalisation studies using the endoplasmic reticulum protein calnexin (Muller-Taubenberger et al., 2001). Upon imaging and digitally overlaying cells overexpressing GFP-Aph-1 stained with  $\alpha$ -GFP and  $\alpha$ -calnexin antibodies we observed co-localisation between Aph-1 and Calnexin (Figure 3.7 A). However, due to the use of methanol in fixation the endoplasmic reticulum structure was not preserved. We sought to maintain the endoplasmic reticulum structure in these cells and next attempted to visualise live cells co-expressing GFP-Aph-1 and Nicastrin-RFP under a thin sheet of 1% agarose (Figure 3.7 B). In these experiments, co-localisation could once again be observed, and the endoplasmic reticulum was able to maintain its structure, however as the cells were still alive during the imaging process their movement altered the position of labelled structures.



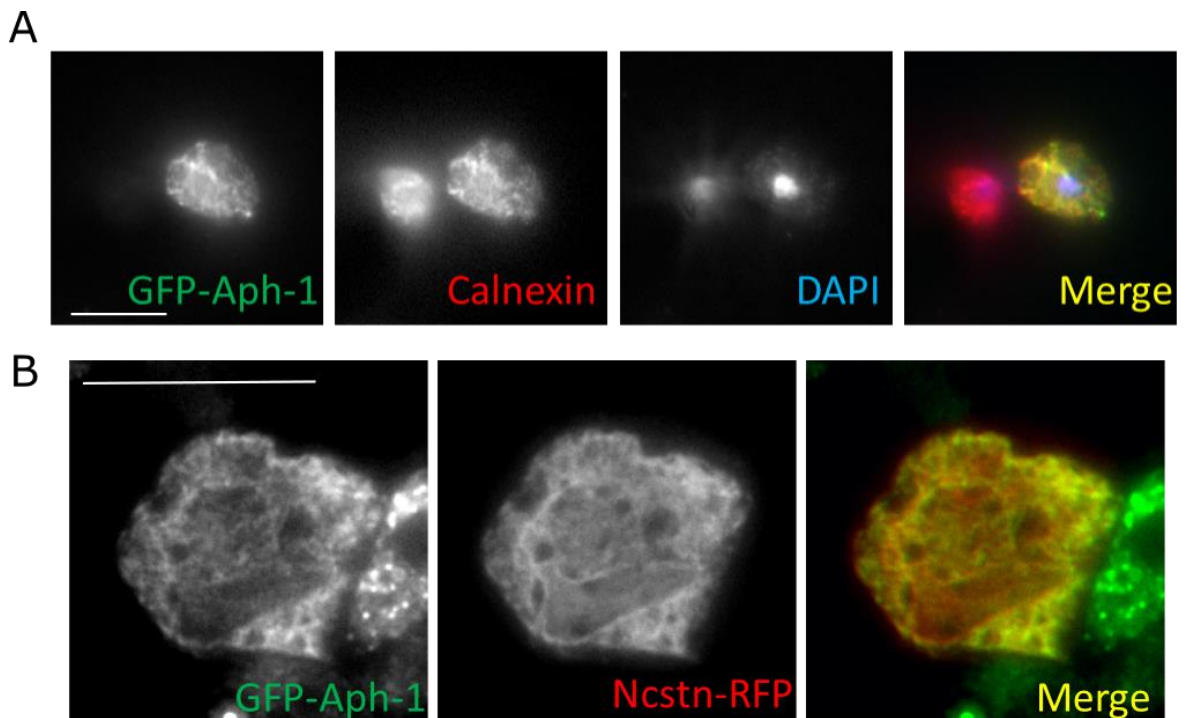


**Figure 3.7 Localisation of Aph-1 and Ncstn in *Dictyostelium*.** A) Immunofluorescence imaging of GFP-Aph-1 overexpressing cells stained with  $\alpha$ -GFP and  $\alpha$ -Calnexin antibodies. Cells show co-localisation between Aph-1 and Calnexin, however endoplasmic reticulum structure is disrupted due to fixation in methanol. B) Live cell imaging of cells overexpressing GFP-Aph-1 and Nicastrin-RFP. Co-localisation can be observed between Aph-1 and Nicastrin in these cells, however, as the cells were still alive during the imaging process the position of the internal structures was altered during imaging. Scale bar = 10 $\mu$ m.

To maintain the endoplasmic reticulum structure and ensure cells could not move during the imaging process we carried out immunofluorescence using -80°C methanol for fixation (Hagedorn et al., 2006). In these experiments we imaged cells overexpressing GFP-Aph-1, Nicastrin-RFP, and PsenB-GFP (Ludtmann et al., 2014). The antibodies used were  $\alpha$ -GFP to stain GFP-Aph-1 and PsenB-GFP,  $\alpha$ -RFP to stain Nicastrin and  $\alpha$ -calreticulin to stain the endoplasmic reticulum (Muller-Taubenberger et al., 2001). These experiments confirmed PsenB localises to the endoplasmic reticulum (Ludtmann et al., 2014), and further, showed for the first time that Aph-1 and Nicastrin also localise to the ER in *Dictyostelium* (Figure 3.8) indicating that the entire  $\gamma$ -secretase complex may localise to the ER in *Dictyostelium*. However, it is worth noting that mislocalisation

can be observed upon overexpression and these localisations must be confirmed using alternative methods.

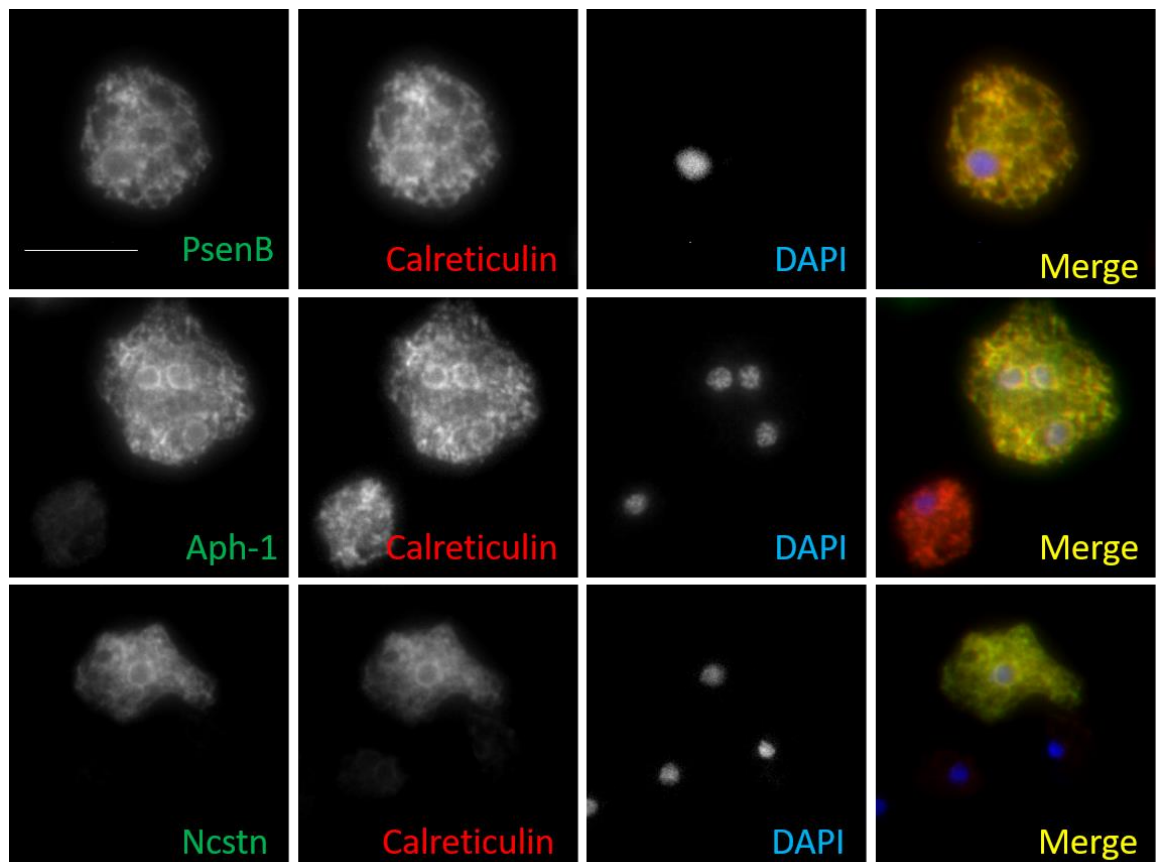


**Figure 3.8 Localisation of  $\gamma$ -secretase components, PsenB, Aph-1 and Ncstn in *Dictyostelium*.** In wild-type cells fixed in methanol, GFP tagged fusion proteins of PsenB, Aph-1, and Nicastrin co-localise with the endoplasmic reticulum marker calreticulin. Scale bar = 10 $\mu$ m.

### 3.6 Discussion

Understanding whether the *Dictyostelium*  $\gamma$ -secretase complex components share homology with their mammalian counterparts is important to determine whether the organism can be used to investigate these proteins. Whilst *Dictyostelium* has been used to investigate the  $\gamma$ -secretase complex (McMains et al., 2010, Ludtmann et al., 2014) there has been limited research done on the homology of these components between *Dictyostelium* and humans. Additionally, the localisation of the  $\gamma$ -secretase complex in *Dictyostelium* remains

uninvestigated, with only the Presenilin localisation known (Ludtmann et al., 2014).

In this chapter we analysed the homology between the *Dictyostelium*  $\gamma$ -secretase components Aph-1, Nicastrin and Pen-2 to their human counterparts to compare the conservation of protein size, structure and motifs and domains. We show here, that the *Dictyostelium* Aph-1 protein shares the motif GxxxGxxxG with mammalian and animal model organisms (Figure 3.1 C). This GxxxGxxxG motif has been suggested to be important for Aph-1 function within the  $\gamma$ -secretase complex as ablation of one of the glycine residues in *C. elegans* results in a Notch null phenotype, and non-integration of Aph-1 into the protein complex (Lee et al., 2004b). Further, whilst humans possess two Aph-1 proteins Aph-1 A and B (Lee et al., 2002), and mice possess three Aph-1 proteins Aph-1 A, B and C (Ma et al., 2005), *Dictyostelium* only possesses one Aph-1 isoform. The Aph-1 present in *Dictyostelium* shares higher homology to the human Aph-1 A, the primary Aph-1 protein in humans and mice during development (Ma et al., 2005), suggesting that this Aph-1 protein is likely to be the original Aph-1 isoform and the most evolutionarily conserved with the Aph-1 B isoform appearing later in the evolutionary timeline. The *Dictyostelium* and mammalian Nicastrin proteins share the conserved motif DYIGS (Figure 3.2 C). Whilst *Dictyostelium* does not have a completely conserved DYIGS motif, it does contain the conserved glycine residue shown to be important for the integration of Nicastrin into the  $\gamma$ -secretase complex, substrate recognition and subsequent processing (Lim et al., 2015, Dries et al., 2009), however this is controversial. Finally, the *Dictyostelium* Pen-2 protein contains a highly conserved C-terminal domain shown to be responsible for the stabilisation of the  $\gamma$ -secretase complex

(Prokop et al., 2005). The results shown, and data discussed here suggest that *Dictyostelium* can be used as a model organism to investigate the basic function of the  $\gamma$ -secretase complex due to the conservation of important motifs, domains, size and structure. Although phylogenetic trees are useful tools for evolutionary analysis of target genes or proteins several limitations do exist. These limitations include difficulties when genes may be altered through genetic recombination (Arenas and Posada, 2010) or horizontal gene transfer (Woese, 2002) giving anomalous branch positioning and therefore incorrect evolutionary analysis by showing unrelated organisms as descendants. Additionally, issues may arise due to long branch attraction artefacts where organisms undergoing rapid evolutionary changes appear related solely due to the large amount of change and not because they are related (Philippe et al., 2005). With these limitations in mind and the effects they may pose to the formation, and positioning of the phylogenetic tree it is important to view these as a literal scientific hypothesis upon which to base further research.

In mammals the localisation of the  $\gamma$ -secretase complex has been shown at the endoplasmic reticulum, Golgi apparatus and plasma membrane (Xia et al., 1998, Area-Gomez et al., 2009). However, in *Dictyostelium* only the localisation of Presenilin has been investigated and found at the endoplasmic reticulum (Ludtmann et al., 2014). In this chapter, we described for the first time to our knowledge the localisation of Aph-1 and Nicastrin to the endoplasmic reticulum in *Dictyostelium*, sharing localisation with *Dictyostelium* Presenilin and comparable localisation to the mammalian protein complex (Xia et al., 1998). It is important to note however that this endoplasmic reticulum localisation has been observed through the use of overexpression constructs. Overexpression of these

components may result in abnormal localisation as found in other studies (Gahlmann and Moerner, 2014), and therefore future studies may wish to use alternative methods to visualise protein localisation such as fluorescent tagged knock in proteins, or custom generated antibodies for immunofluorescence. Additionally, this chapter has detailed the efforts to generate a Pen-2 overexpression construct, however, this construct failed to produce full length RFP-Pen-2 fusion protein as observed through the absence of a fluorescent signal through microscopy and an absence of RFP-Pen-2 in western blot analysis. This was not pursued further due to time constraints, however causes behind the failure of expression may be due to disruption of signal/targetting peptides. C-terminal vectors may be pursued as these are less likely to interfere with protein localisation.

This chapter set out to determine whether *Dictyostelium* could provide a viable model organism for research of the  $\gamma$ -secretase complex. We have shown here, that the *Dictyostelium*  $\gamma$ -secretase complex components share important protein structure, motifs and domains with their human counterparts (Lee et al., 2004b, Lim et al., 2015, Prokop et al., 2005). We additionally demonstrate that the *Dictyostelium* Aph-1 and Nicastrin proteins localise to the endoplasmic reticulum with *Dictyostelium* Presenilin B (Ludtmann et al., 2014), sharing subcellular localisation with their human counterparts (Xia et al., 1998). These results suggest that *Dictyostelium* can be used as a model organism to investigate the function of the  $\gamma$ -secretase complex.

## Chapter IV

# Genetic manipulation of $\gamma$ -secretase components and characterisation of mutants

---

## 4.1 Introduction

As the  $\gamma$ -secretase complex is important for understanding both development and disease in mammalian model organisms, it is important to develop a thorough understanding of its function. However, in mammalian models, ablation of either single or multiple components of the complex is highly problematic due to embryonic lethality (De Strooper et al., 1999). Therefore, novel approaches are necessary to develop understanding of this complex. This chapter describes the genetic manipulation of the *aph-1* and *pen-2* genes in *Dictyostelium*. It further describes the effects of *aph-1* ablation on *Dictyostelium* development and compares these results to those previously published about *ncstn* and *psenA/B* ablation (Ludtmann et al., 2014, McMains et al., 2010). Finally, this chapter investigates the role of  $\gamma$ -secretase components on *Dictyostelium* growth in liquid media, and the localisation of these components in knock-out backgrounds for *aph-1* and *psenA/B*.

*Dictyostelium* development is a common method utilised to determine the effects of gene ablation on the organism (Ludtmann et al., 2014, McMains et al., 2010, Otto et al., 2016). Previous research has determined that the presenilin protein is required for this process to function normally in a manner not dependent upon the catalytic activity of the protein (McMains et al., 2010, Ludtmann et al., 2014). The roles for the other components however is controversial, *Ncstn* has been found to be both required, and dispensable for development over a 24 hour period (Ludtmann et al., 2014, McMains et al., 2010), whilst *Aph-1* has been found to be necessary (McMains et al., 2010).

Phagocytosis and macropinocytosis are both important processes by which *Dictyostelium* ingest extracellular nutrients for processes such as growth (Chubb et al., 2000, Muller-Taubenberger et al., 2001, Bloomfield et al., 2015). Presenilin has been shown to function in *Dictyostelium* phagocytosis as null mutants are unable to ingest yeast effectively when compared to wild-type cells, and therefore grow at a slower rate (McMains et al., 2010). This function is reliant upon catalytic activity of this protein, but is not reliant upon a fully formed  $\gamma$ -secretase complex as Aph-1 and Ncstn null cells are able to phagocytose normally (McMains et al., 2010). The effects of ablation of these components on growth in liquid media has not yet been investigated.

As the formation of the  $\gamma$ -secretase complex is sequential (Smolarkiewicz et al., 2013), we also set out to determine whether the localisation of these complex components are altered in null background lines. Thus far, to our knowledge, this has not been investigated in *Dictyostelium* or in mammalian models, however, it has been shown that presenilin localises to similar intracellular compartments as the mammalian orthologue in wild-type and PsenA/B null backgrounds (Ludtmann et al., 2014).

This chapter will report on successful deletion of part of the *Dictyostelium aph-1* to allow for analysis of the effects of *aph-1* ablation on *Dictyostelium* development, and will detail the efforts to delete part of the *Dictyostelium pen-2* gene. Additionally, this chapter will investigate the effects of  $\gamma$ -secretase ablation, through ablation of *aph-1*, *ncstn*, and *psenA/B* on *Dictyostelium* growth, and  $\gamma$ -secretase component localisation in the absence of Aph-1 and PsenA/B.



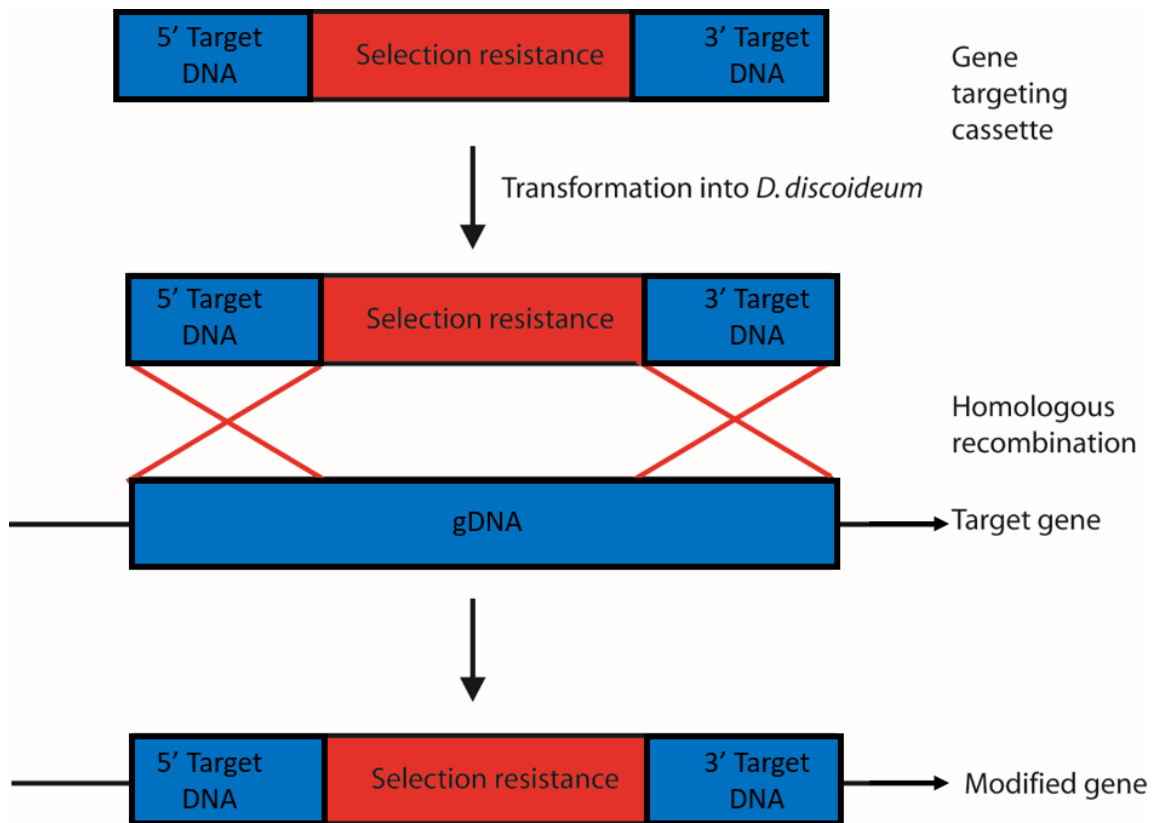


**Figure 4.1 Genetic modification through homologous recombination.** A gene targeting cassette is constructed with two arms of homology identical to the target gene flanking a resistance cassette. This is then transformed into *Dictyostelium* where homologous recombination occurs through a crossover of similar, or identical, nucleotides between two strands of DNA. The resultant modified gene now contains the desired substitution/deletion mutation.

## 4.2 Creating an *aph-1* knock-out mutant

The *Dictyostelium aph-1* gene was ablated through the homologous recombination of a knock-out cassette (Chapter 2.2.2.8) (Faix et al., 2004). The homologous recombination cassette was generated through the amplification of two arms of homology by PCR, a 5' fragment, and a 3' fragment matching the target gene, resulting in the deletion of 210 base pairs from the target gene (Figure 4.2 A, B). These fragments flank a blasticidin resistance marker that allows for selection of positive transformants (Figure 4.2 B). To confirm that the correct sequences were cloned into a knock-out vector (pLPBLP) (Faix et al., 2004) restriction digests were used to detect the presence of the 5' and 3' *aph-*

1 fragments and the entire homologous recombination cassette (Figure 4.2 C). The targeting cassette was also sequenced for further confirmation. Wild-type *Dictyostelium* Ax2 cells were transformed with the knock-out cassette digested with BamHI and KpnI, and plated in a 96-well plate containing blasticidin (10 $\mu$ g/mL) to allow for selection of positive transformants.

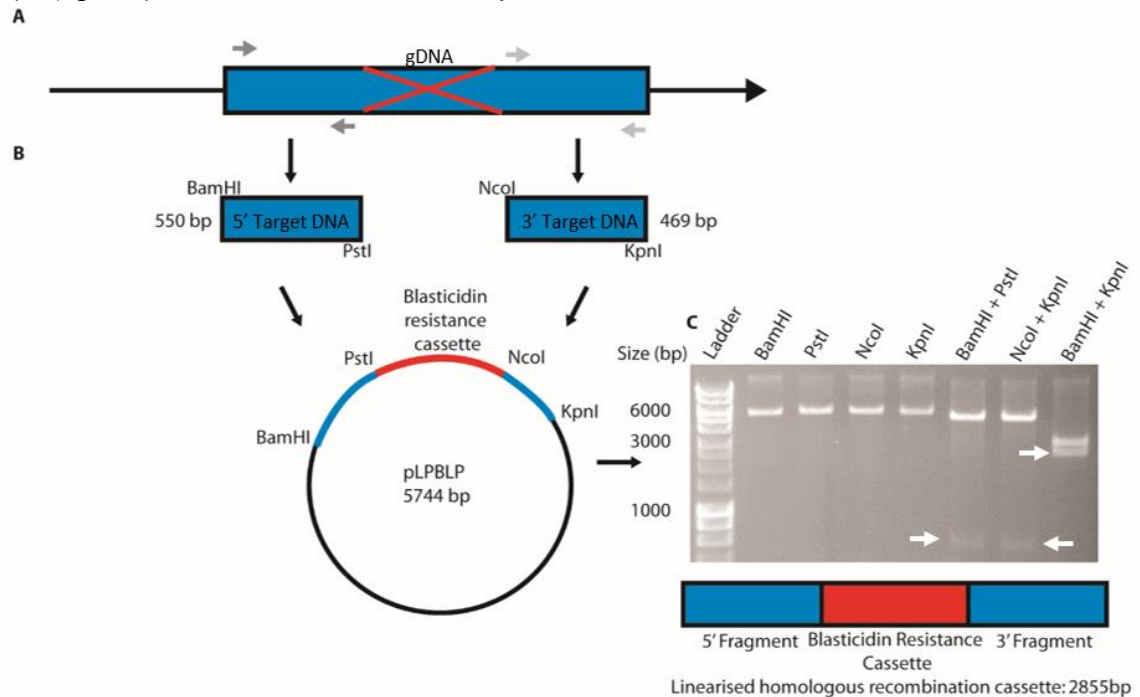


**Figure 4.2 Generation of an *aph-1* knockout cassette.** A) Fragments of *aph-1* genomic DNA were amplified by PCR using 5' and 3' primers containing cutsites for BamHI, PstI, NcoI, and KpnI. B) N-terminal (5') (550bp) and C-terminal (3') (469bp) fragments were cloned into the pLPBLP vector flanking a blasticidin resistance cassette. C) To confirm successful integration of 5' and 3' fragments, a series of restriction digests were used. Double digests of BamHI and PstI generated the correct 5' fragment, and NcoI and KpnI generated the correct 3' fragment, additionally a BamHI and KpnI digest generated a linearised homologous recombination cassette (2855bp) which would be used in electroporation. Single digests using BamHI, PstI, NcoI, and KpnI were used as controls to ensure adequate restriction digestion.

In order to identify strains that underwent homologous recombination of the knock-out cassette positive transformants growing in the presence of blasticidin were screened by PCR (Figure 4.3). In these experiments, three primer combinations were used genomic DNA (GC) control, vector DNA (VC) control and positive homologous recombination knock-outs (KO). The GC reaction primers were designed so that one primer annealed in the genomic DNA region outside the knock-out cassette and the other annealed within the genomic DNA

target region within the cassette generating a product for wild-type cells and all transformants. The VC reaction primers were designed so that one primer annealed within the genomic DNA region within the cassette and the other primer annealed to the blasticidin resistance gene, generating a product in cells successfully transformed with the knock-out cassette. The KO reaction used a primer from the GC reaction that is outside the targeting cassette and one primer within the blasticidin resistance cassette from the VC reaction, this product will only be present in cells that have undergone homologous integration. These three PCR reactions were used to screen both the 5' and 3' regions of the modified gene with N- or C-terminal specific primers. To identify positive *aph-1* cell lines, 234 blasticidin resistant colonies were screened. From these screens, three positive homologous knock-out strains were found showing homologous integration in both the 5' and 3' regions of the *aph-1* gene. Homologous integrants were serially diluted and plated onto SM Agar plates containing *R. planticola* to allow for isogenic cell line selection, these were then re-screened to allow for the selection of 3 independent isogenic homologous knock-out cell lines.

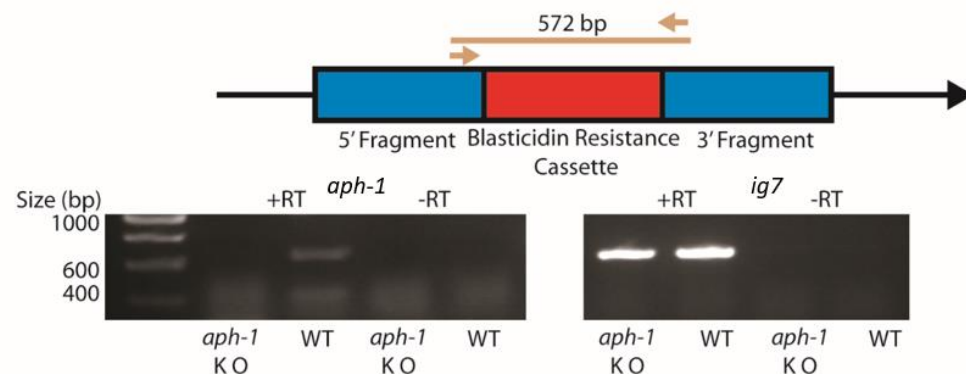
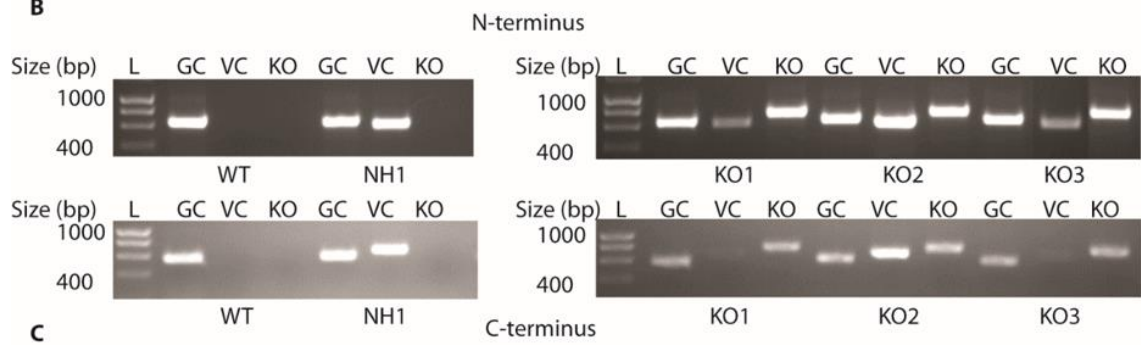
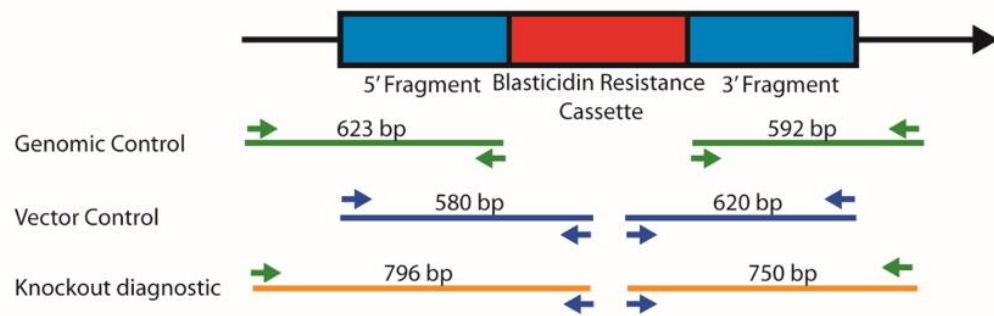


**Figure 4.3. PCR Screening for homologous recombinants of *aph-1*.** A) Genomic control, vector control and knock-out diagnostic primers were designed to screen successful transformants for homologous recombination. B) Gel electrophoresis of PCR products from genomic DNA show only genomic control bands in wild-type (WT), genomic control and vector control bands in non-homologous recombinants (NH1), and genomic control, vector control, and knock-out diagnostic bands in homologous recombinants (KO1, KO2, KO3) for both N-terminus and C-terminus. C) RT-PCR using primers flanking the blasticidin cassette shows Aph-1 expression in wild-type cells (472bp) but loss of expression in Aph-1 knock-out cell lines. Control bands show consistently expressed IG7 (559bp).

In order to confirm gene ablation in the identified *aph-1*<sup>-</sup> cell lines a reverse transcriptase PCR (RT-PCR) was used (Figure 4.3 C). In these experiments cDNA was synthesised from *aph-1*<sup>-</sup> mutant cells and also from wild-type cells. The primers used in this PCR were designed to anneal to the genomic DNA

flanking the blasticidin resistance cassette. Using this approach, PCR analysis from cDNA from wild-type cells provided a 472 base pair band, this indicated transcription of *aph-1* mRNA, which was absent in the *aph-1* knock-out line. As a control for presence of successfully synthesised DNA, primers amplifying a 559 base pair region of the mitochondrial large subunit rRNA (lg7) (Vinet et al., 2014) was used in the RT-PCR. To confirm that these products were generated from the cDNA templates, negative controls without reverse transcriptase were also used in the PCR.

#### 4.3 Creating a *pen-2* knock-out mutant

In order to generate a *pen-2* knock-out mutant, a knockout cassette was created. This cassette consisted of two regions of the *pen-2* gene amplified through PCR. The N-terminal (5') region of the cassette was amplified from genomic DNA upstream of *pen-2* and the C-terminal (3') region incorporated the entire second intron of *pen-2* and genomic DNA downstream of the gene. The knockout cassette therefore resulted in a deletion of 372 base pairs from *pen-2* including upstream genomic DNA, intron 1 and part of exon 1. These 5' and 3' fragments were cloned into pLPBLP flanking a blasticidin resistance cassette and a series of restriction digests were carried out to confirm successful cloning (Figure 4.4) (Faix et al., 2004), the knock-out vector was then sequenced to confirm sequence identity. Wild-type *Dictyostelium* cells were then transformed with the entire linearised homologous recombination cassette and plated into 96 well plates to allow for selection using blasticidin (10µg/mL) and subsequent growth of positive transformants.

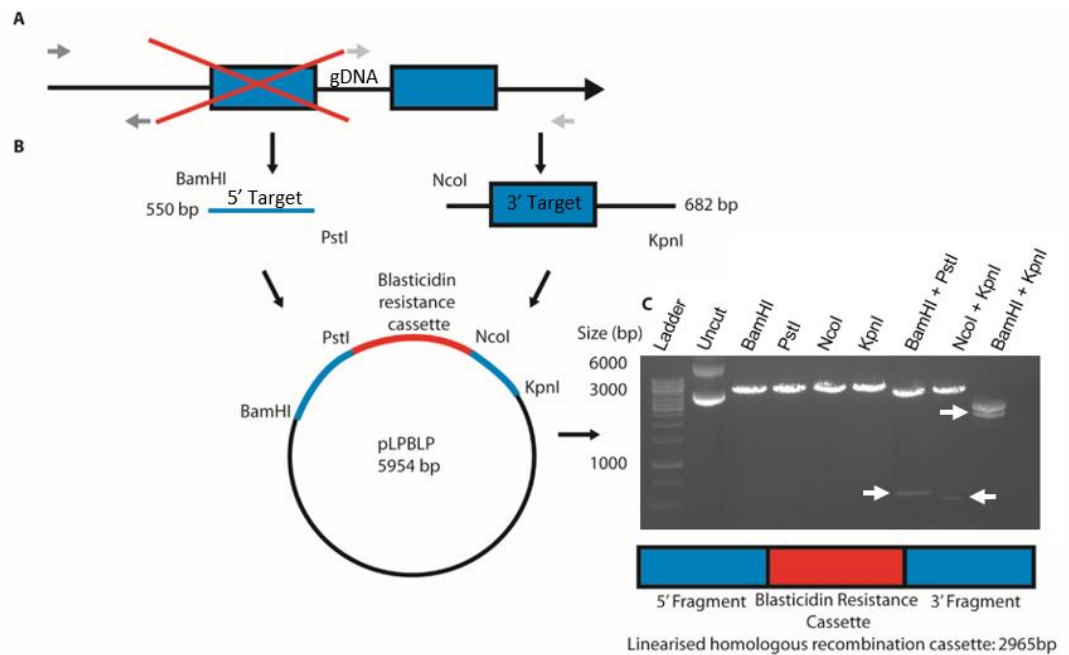


**Figure 4.4 Vector generation for a *pen-2* knockout cassette.** A) The knock-out vector consists of a 5' and 3' fragment of *pen-2* genomic DNA. These fragments were amplified by PCR using primers containing cutsites for BamHI, PstI, NcoI, and KpnI. B) N-terminal (550bp) and C-terminal (682bp) fragments were cloned into the pLPBLP vector flanking a blasticidin resistance cassette. C) To confirm successful integration of 5' and 3' fragments, a series of restriction digests were used. Double digests of BamHI and PstI generated the correct 5' fragment, and NcoI and KpnI generated the correct 3' fragment, additionally a BamHI and KpnI digest generated a linearised homologous recombination cassette (2965bp) which would be used in electroporation. Single digests using BamHI, PstI, NcoI, and KpnI were used as controls to ensure adequate restriction digestion.

To determine whether homologous recombinants were generated, *pen-2* transformants grown in the presence of blasticidin were screened by PCR. In these experiments a similar screening approach to that of *aph-1* was used with primers combinations for the *pen-2* knockout vector. In short there were three reactions, a genomic control (GC), a vector control (VC) and a knock-out diagnostic band (KO). Each combination of primers will give a different product with the genomic control band expected in all cell lines, the vector control band expected solely in those cells transformed with a knock-out cassette, and the KO band only in those cells that have undergone homologous recombination. In total 276 different *pen-2* colonies were screened with no homologous recombinants found.

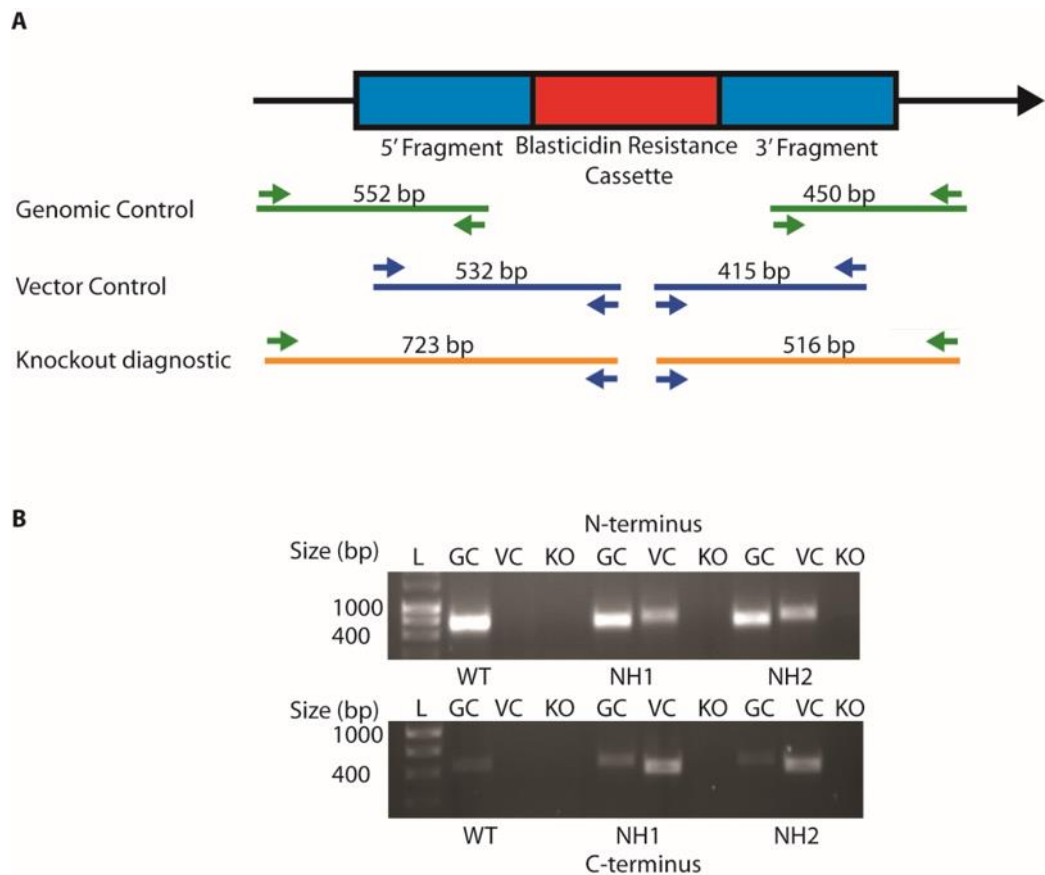


**Figure 4.5. PCR Screening for homologous recombinants of *pen-2*.** A) Genomic control, vector control and knock-out diagnostic primers were designed to screen successful transformants for homologous recombination. B) Gel electrophoresis of PCR products from genomic DNA show only genomic control bands in wild-type (WT), genomic control and vector control bands in non-homologous recombinants (NH1, NH2), for both N-terminus and C-terminus.

To aid in ablating *pen-2* in *Dictyostelium*, a secondary *pen-2* knockout construct was generated (Figure 4.6). This knockout construct incorporated more of the *pen-2* open reading frame than previously, resulting in ablation of only 5 base pairs from exon 2 of the *pen-2* gene. The 5' and 3' arms of homology were cloned into a pLPBLP knockout vector and cloning was confirmed through restriction digest and sequencing (Figure 4.6 C). The resultant construct was transformed into *Dictyostelium* cells, and positive transformants were screened by PCR to identify homologous recombinants (Figure 4.6 D). In total 232 different *pen-2* colonies were screened using this vector resulting in a total 508 colonies

screened with no homologous recombinants found. Unfortunately, the small size of the *pen-2* gene makes it difficult to generate significantly different knockout cassettes and therefore further attempts to ablate this gene were abandoned.

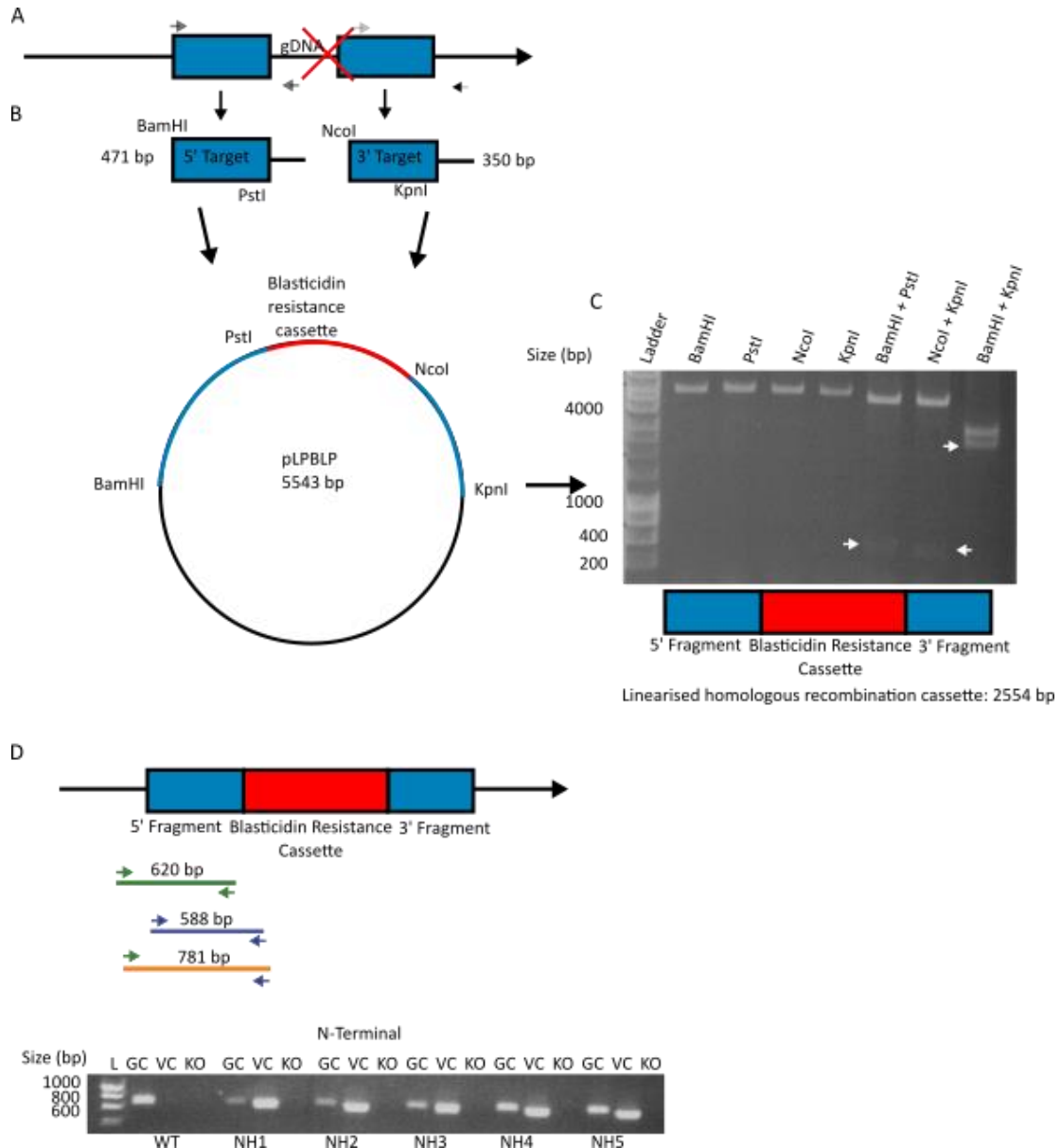


**Figure 4.6 Vector generation of second *pen-2* construct and PCR screening for homologous recombinants.** A) The knockout construct for Pen-2 was generated through PCR amplification of 5' and 3' arms of homology from genomic DNA. B) The 5' (471 bp) and 3' (350 bp) arms of homology were cloned into the target pLPBLP vector flanking a blastidicin resistance cassette gene. C) To confirm succesful integration of arms of homology into the target vector restriction digests were performed using the enzymes BamHI, PstI, NcoI and KpnI. Double digests confirmed the presence of both the 3' and 5' arms of homology, and a BamHI + KpnI digest generated the correct linearised knockout cassette. D) Genomic control, vector control and knock-out diagnostic primers were designed to screen succesful transformants for homologous recombination. Gel electrophoresis of resultant PCR products from genomic DNA results in only genomic control bands in wild-type cells (WT) and genomic control and vector control bands in non-homologous recombinants (NH 1 – 5) for the N-terminus.



#### 4.4 Development of *aph-1*<sup>-</sup> and *nicastrin*<sup>-</sup> mutants

When *Dictyostelium* cells are starved of nutrients they begin to aggregate and form fruiting bodies over a 24 hour period. Previous research in *Dictyostelium* has indicated that the  $\gamma$ -secretase/Presenilin proteins contribute towards this process, however whether the entire protein complex is involved or only the presenilin proteins is controversial (McMains et al., 2010, Ludtmann et al., 2014). In this experiment wild-type cells were allowed to develop under three different developmental conditions, (1) on phosphate buffer soaked filter pads, (2) on 1% agar plates containing KK2 phosphate buffer, or (3) nitrocellulose filters placed on 1% agar plates with phosphate buffer. Under all three of these conditions wild-type cells developed into fruiting bodies consisting of a basal disk, stalk and spore head (Figure 4.4 A, B, C).

In order to investigate the effects of *aph-1* ablation and *nicastrin* ablation (previously generated (Ludtmann et al., 2014)) on development *aph-1*<sup>-</sup> and *nicastrin*<sup>-</sup> cell development was analysed. When *aph-1*<sup>-</sup> mutants developed over 24 hours we see different developmental phenotypes depending on the substrate used. When developed on nitrocellulose filters placed upon phosphate buffer soaked filter pads *aph-1*<sup>-</sup> cells generated wild-type morphology fruiting bodies (Figure 4.4 A). However, when developed on a substrate containing 1% agar, or a nitrocellulose membrane placed on top of a 1% agar plate these cells failed to form morphologically normal fruiting bodies, and development was arrested at the mound stage at 24 hours (Figure 4.4 B, C). Upon ablation of *nicastrin*, cells develop fully formed fruiting bodies on nitrocellulose filters over 24 hours (Figure 4.4 A), however, when developed on agar plates these cells failed to form fruiting bodies within 24 hours. The data here concurs with, and confirms, previously

published data on the development of  $\gamma$ -secretase component null mutants, including *presenilin*, *nicastrin* and *aph-1* (Ludtmann et al., 2014, McMains et al., 2010). Additionally, the shared block in development when incubated on agar observed across these mutants indicates an important role for the  $\gamma$ -secretase complex in *Dictyostelium* development. However, it is worth noting the different phenotypes observed upon developing these cells under different substrates, and the reasons underlying this warrant further research and study to determine the cause.

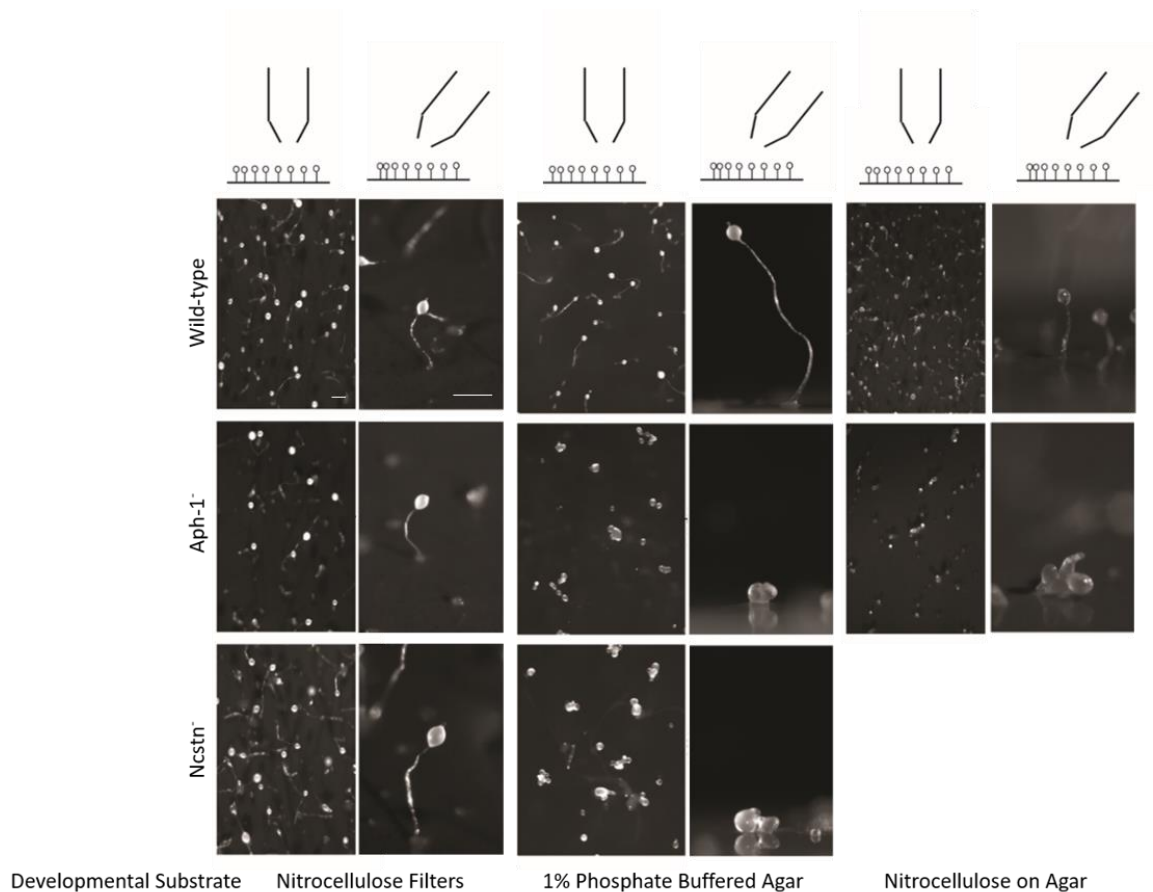


**Figure 4.7 Effects of *aph-1* and *nicastrin* ablation on *Dictyostelium* development.** Wild-type, *aph-1*<sup>-</sup>, and *nicastrin*<sup>-</sup> cells were developed on different developmental substrates over 24 hours. Cells were developed on nitrocellulose filters placed on phosphate buffer soaked filter pads. Under these conditions wild-type, *aph-1*<sup>-</sup>, and *nicastrin*<sup>-</sup> cell lines all developed into wild-type comparable fruiting bodies. When developed on 1% Agar containing phosphate buffer plates. Under these conditions wild-type cells developed into fruiting bodies over a 24 hour period, however *aph-1*<sup>-</sup>, and *nicastrin*<sup>-</sup> cells lines failed to develop in 24 hours and halted development at the mound stage. When developed on nitrocellulose membranes placed on 1% agar containing phosphate buffer plates. Under these conditions wild-type cells differentiate into mature fruiting bodies at 24 hours, but *aph-1*<sup>-</sup> cells exhibit similar developmental defects to those seen on 1% agar phosphate buffer plates and halt development at the mound stage. Scale bar denotes 0.5mm.

#### 4.5 Growth rates of $\gamma$ -secretase deficient *Dictyostelium* mutants

Research investigating the roles of the  $\gamma$ -secretase complex in mammalian model organisms has implicated the complex in endocytosis (Tamboli et al., 2008, Zhang et al., 2006). These studies have investigated macropinocytosis in cells lacking the protein complex, and show decreased rates of nutrient uptake upon ablation of presenilin (Tamboli et al., 2008, Zhang et al., 2006). Although these studies do not investigate growth rate, cells lacking the ability to macropinocytose nutrients efficiently could be expected to show a decreased growth rate, as these cells will be unable to take up sufficient nutrients compared to wild-type cells (Upadhyay and Shaw, 2008, Munn and Riezman, 1994, Otomo et al., 2008). An earlier study suggested that in *Dictyostelium*, the presenilin proteins function in phagocytosis, and phagocytic dependent growth in a  $\gamma$ -secretase complex independent, but presenilin only catalytically dependent manner (McMains et al., 2010), however the effects of  $\gamma$ -secretase component ablation on macropinocytosis has not yet been investigated.

In order to determine whether macropinocytosis in *Dictyostelium* is altered by  $\gamma$ -secretase ablation, a simple growth assay was utilised. This growth assay monitored cell count in liquid medium, and cell density was calculated relative to wild-type cells (Figure 4.7). In these growth assays wild-type cells exhibit a lag phase, exponential phase, and plateau phase of growth. In these experiments cell number at day 7 was normalised to 100% to eliminate biological variance in cell number from experiment to experiment. Upon ablation of either *aph-1* or *ncstn* cells grew comparably to control, with no significant difference in cell number ( $p=0.29$  and  $p=0.23$  respectively). Upon ablation of *psenA/B* however,

cells reached a 60% growth of wild-type cells indicating a role for this protein in *Dictyostelium* growth ( $p=0.0001$ ) (Figure 4.7 A).

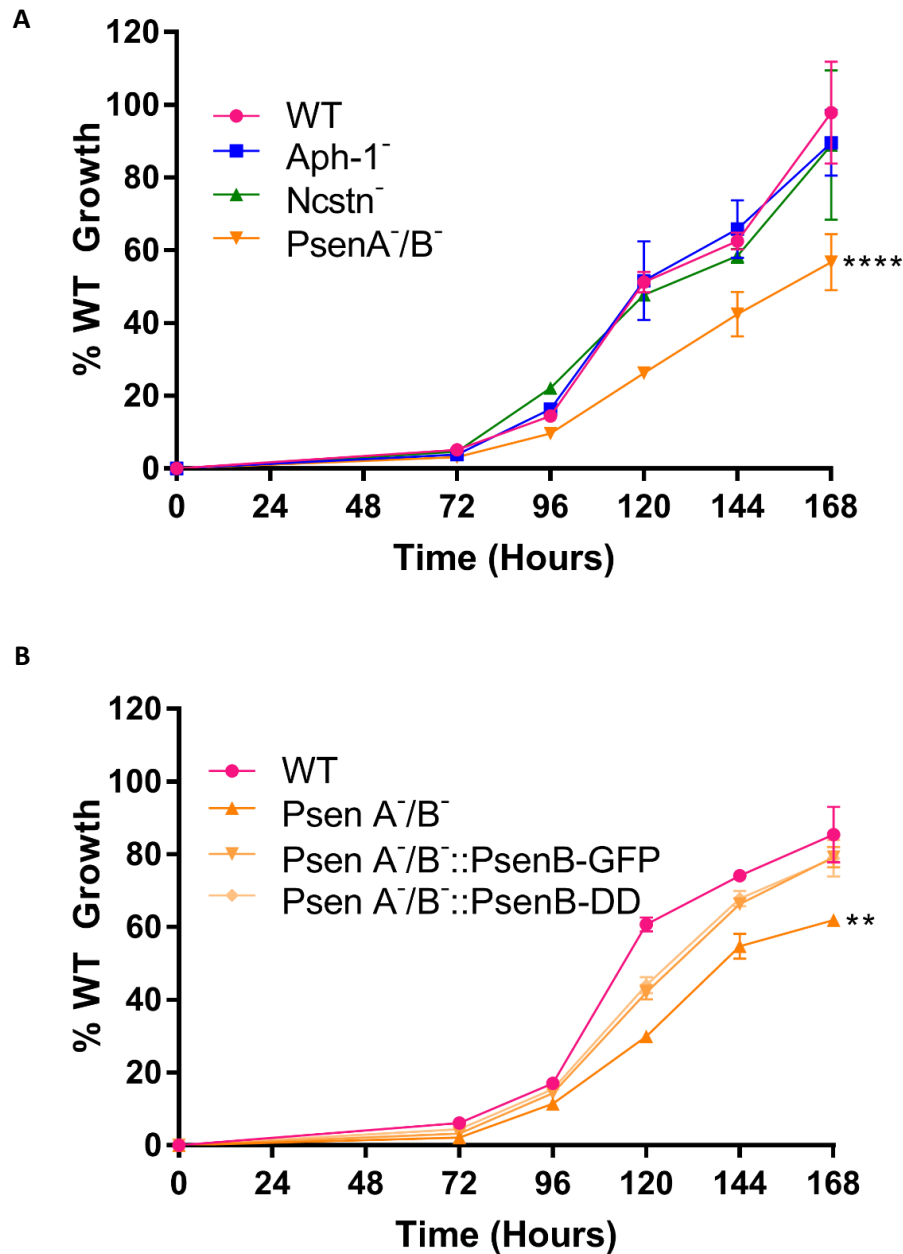


**Figure 4.8 Growth rates of  $\gamma$ -secretase null *Dictyostelium* in liquid media.** A) Under normal growth conditions in liquid media wild-type cells exhibit a typical lag, exponential and plateau phase. Aph-1<sup>-</sup> ( $P=0.29$ ) and Ncstn<sup>-</sup> ( $P=0.23$ ) cells exhibit no significant growth defects under these conditions. PsenA<sup>-</sup>/B<sup>-</sup> cells however, exhibit a 40% decrease in growth compared to wild-type cells ( $P=0.0001$ ). B) Further analysis of PsenA<sup>-</sup>/B<sup>-</sup> growth showed that expression of a catalytic, or non-catalytic PsenB rescue plasmid in PsenA<sup>-</sup>/B<sup>-</sup> cells restores growth levels to those of wild-type, rescuing the defects observed upon presenilin ablation (PsenA<sup>-</sup>/B<sup>-</sup>  $P=0.0007$ ; PsenA<sup>-</sup>/B<sup>-</sup>::PsenB-GFP  $P=0.80$ ; PsenA<sup>-</sup>/B<sup>-</sup>::PsenB-DD  $P=0.78$ ).

We next set out to determine whether the observed growth defect in liquid medium was dependent upon the catalytic activity of the  $\gamma$ -secretase complex (Figure 4.7 B). Upon expression of catalytically active PsenB-GFP (Ludtmann et al., 2014) growth was restored to wild-type levels ( $p=0.80$ ), rescuing the effects of presenilin ablation. Additionally, when expressing a catalytically inactive version of PsenB with mutated aspartate residues at positions 348, and 395 (Ludtmann et al., 2014) growth rates are once again restored to those of wild-type levels ( $p=0.78$ ). These data suggest that in *Dictyostelium* the presenilin component of the  $\gamma$ -secretase complex has a function in growth in liquid media independent of the  $\gamma$ -secretase complex, and that this role is not dependent upon catalytic activity.

#### 4.6 $\gamma$ -secretase localisation in null mutants

As the formation of the  $\gamma$ -secretase complex is sequential in mammalian models (De Strooper et al., 2012, Strooper, 2003, Mao et al., 2012), Aph-1 and Nicastrin first form an initial complex before being joined by Psen1 and Pen-2 (Smolarkiewicz et al., 2013), we set out to determine whether the complex exhibits aberrant localisation upon component ablation. Utilising previously described overexpression constructs (Chapter III), we were able to visualise the localisation of fluorescently tagged Aph-1, Ncstn and PsenB in backgrounds lacking functional Aph-1 and PsenA/B.

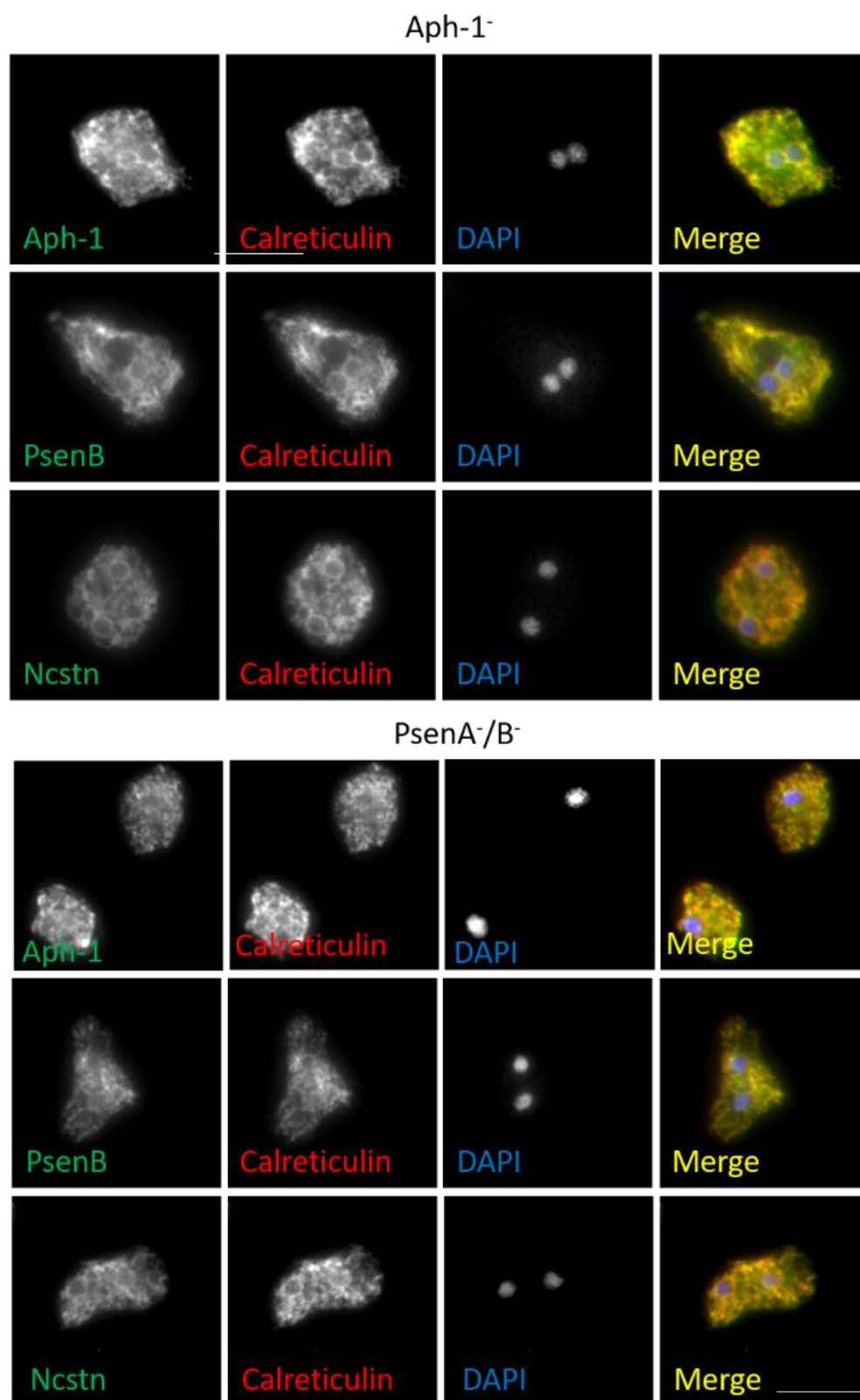


**Figure 4.9**  
**Localisation of  $\gamma$ -secretase components in  $\gamma$ -secretase null mutants.** In cells lacking Aph-1 or PsenA/B the localisation of the  $\gamma$ -secretase components Aph-1, PsenB and Ncstn is unaltered. Components are still localised to the endoplasmic reticulum as in wild-type counterparts (chapter III). Scale bar = 10  $\mu$ m.

As shown in previous chapters, the  $\gamma$ -secretase complex localises to the endoplasmic reticulum in wild-type cells. This localisation corresponds with observations in mammalian model organisms (Smolarkiewicz et al., 2013, Xia et al., 1998). Upon ablation of Aph-1, one of the first two components to begin formation of the complex, localisation is unaltered (Figure 4.8). Furthermore, Aph-1, PsenB, and Ncstn are still found to be localised to the ER. Similarly, upon ablation of PsenB, the localisation of these components remains at the ER and is therefore unaltered.

## 4.7 Discussion

Understanding the basic function of the components of the  $\gamma$ -secretase complex is important in order to understand the physiological role of this protein complex. *Dictyostelium* provides a useful model organism for this purpose as it is a haploid organism gene ablation does not require ablation of two copies of each gene compared to mammalian model organisms. Additionally, in this model organism there is no embryonic lethality upon  $\gamma$ -secretase ablation as there is in mammalian organisms (Otto et al., 2016, Ludtmann et al., 2014, McMains et al., 2010, De Strooper et al., 2012). *Dictyostelium* has also been used to determine catalytic and non-catalytic presenilin functions, as well as showing evolutionary conservation between *Dictyostelium* and man (Ludtmann et al., 2014, McMains et al., 2010).

In this chapter we described the ablation of *aph-1* in *Dictyostelium* by generating a null cell line with a 17% deletion of the central region of the encoding gene through homologous recombination. We confirmed loss of *aph-1* expression through RT-PCR after deletion. Additionally, we attempted to ablate



*Dictyostelium pen-2*, but were unsuccessful. The small coding region of *pen-2* renders it difficult to delete as a small, low specificity targeting region reduces the likelihood of homologous crossover, and therefore we have not continued to investigate this protein. Alternatives to gene ablation may be utilised in the future such as RNAi (Martens et al., 2002). Finally, we have investigated the effects of  $\gamma$ -secretase ablation using cell lines lacking *aph-1*, *ncstn*, and *psenA/B* in development, growth and component localisation to determine whether these functions are complex dependent or independent.

The role of the  $\gamma$ -secretase complex in *Dictyostelium* development remains to be fully explored. Previous studies in this model organism have demonstrated a common role for PsenA/B in *Dictyostelium* development (Ludtmann et al., 2014, McMains et al., 2010), however differing results have been found for cell lines lacking Ncstn (McMains et al., 2010, Ludtmann et al., 2014). In this chapter we have shown that *Dictyostelium* cell lines lacking *aph-1* and *ncstn* develop differently depending on the substrate they are incubated upon. When these cell lines are developed on nitrocellulose filters they form wild-type morphology fruiting bodies (Ludtmann et al., 2014), however, when these cell lines are incubated upon phosphatate buffered agar plates they show a similar developmental phenotype to PsenA/B null cell lines halting development at the mound or first finger stage (McMains et al., 2010). These data confirm the findings of both earlier studies and suggests a function for the entire  $\gamma$ -secretase complex in *Dictyostelium* dependent upon external factors such as developmental substrate.

The  $\gamma$ -secretase complex/Presenilin proteins have been implicated in uptake through macropinocytosis and phagocytosis in mammalian model organisms and *Dictyostelium* (Cataldo et al., 2000, Tamboli et al., 2008, Jutras et al., 2005, McMains et al., 2010). Previous research using *Dictyostelium* has indicated an important role for presenilin in nutrient uptake through phagocytosis dependent upon catalytic activity (McMains et al., 2010), here we show that in addition to this role in phagocytosis the presenilin proteins also have a function related to fluid phase nutrient uptake and that this function is not dependent upon the catalytic activity of the protein. We demonstrate here that Presenilin B, but not Aph-1 or Ncstn, also function in nutrient uptake in liquid media and that this function is not dependent upon catalytic activity. This data suggests a potential, previously unknown, role of presenilin in the mediation of fluid-phase uptake by this protein in *Dictyostelium*. The role of presenilin in fluid-phase nutrient uptake has been investigated in mammalian model organisms (Tamboli et al., 2008, Zhang et al., 2006, Cataldo et al., 2000). These studies show that in mouse embryonic fibroblasts, ablation of presenilin or usage of chemical  $\gamma$ -secretase inhibitors, but not Alzheimer's disease causing mutations, results in impaired lipoprotein particle uptake, and subsequent decreased protein clearance from the endocytic pathway (Tamboli et al., 2008, Zhang et al., 2006). Additionally, in mammalian organisms it has been found that ablation of Presenilin results abnormalities in the endocytic pathway which precede the deposition of neurotoxic A $\beta$ 42 plaques and Alzheimer's disease progression (Cataldo et al., 2000). This is the first time, to our knowledge, that Presenilin has been implicated in *Dictyostelium* fluid phase nutrient uptake. Whilst the roles for endocytosis differ between mammalian neurons, where the function of endocytosis is not to engulf

nutrients, but rather lipoprotein particles and neurotransmitters (Cosker and Segal, 2014), and *Dictyostelium* where the function is nutrient uptake for growth, the abnormalities observed here in fluid-phase uptake upon Presenilin ablation are conserved across these two species suggesting an ancestral role for this protein in this role.

Previously in this thesis we have shown that the localisation of  $\gamma$ -secretase components in *Dictyostelium* is conserved between mammalian model systems and *Dictyostelium*, and that the components Aph-1, Ncstn and PsenB localise to the endoplasmic reticulum. The localisation of the  $\gamma$ -secretase components in the absence of other constituents, however, has not been investigated before. Utilising immunoprecipitation researchers have demonstrated that the formation of the  $\gamma$ -secretase complex is sequential in mammalian model organisms (Mao et al., 2012), where Aph-1 and Ncstn first form an initial holocomplex, before being joined by Presenilin and finally Pen-2 (Mao et al., 2012). Our study shows that upon ablation of Aph-1 or PsenA/B, localisation of the other complex components, Aph-1, Ncstn and PsenB, are unaltered in *Dictyostelium*. With regards to these data it is possible that Aph-1 and Ncstn have unaltered localisation in null backgrounds as these components form the initial scaffold of the  $\gamma$ -secretase complex (Smolarkiewicz et al., 2013) and therefore will localise to their appropriate cellular compartments regardless of the presence of other components. In contrast, in mammalian models Psen1, requires an Aph-1/Ncstn complex to form before it is able to join the  $\gamma$ -secretase complex and therefore unaltered localisation may be due to a distinct mechanism of component localisation to that shown in mammalian models, erroneous localisation due to protein overexpression, or aberrant protein localisation due to GFP-tagging

proteins (Gahlmann and Moerner, 2014). Whilst our study does demonstrate that the protein localisation is not altered when compared to mammalian model organisms an alternative approach utilising knock-in tagged proteins may allow for greater insight into protein localisation in *Dictyostelium* in the presence or absence of other complex components.

In this chapter we have examined *Dictyostelium* development, growth and  $\gamma$ -secretase component localisation in cell lines lacking  $\gamma$ -secretase components. We show that in the absence of Aph-1 and Ncstn, *Dictyostelium* development is dependent upon developmental substrate. Additionally we show that the ablation of Presenilin B decreases *Dictyostelium* growth in liquid media, demonstrating a conserved role for this protein in fluid-phase uptake previously suggested in mammalian organisms (Fukumori et al., 2006, Tamboli et al., 2008, Zhang et al., 2006). Finally we demonstrate that in *Dictyostelium* upon ablation of Aph-1, or PsenB localisation of  $\gamma$ -secretase components is unaltered and these proteins continue to localise to the ER, however, this work utilised overexpression constructs which may present their own difficulties (Gahlmann and Moerner, 2014), and so alternative methods may be more beneficial such as knock-in approaches (Hanks et al., 1995).

## Chapter V

# The Role of the *Dictyostelium* $\gamma$ -Secretase Complex in Macropinocytosis and Autophagy

---

## 5.1 Introduction

The central function of the  $\gamma$ -secretase complex has been thought to be through its proteolytic cleavage of target substrates (De Strooper, 2003, De Strooper et al., 1998, Zhang et al., 2000, Zhao et al., 2010). In this role the catalytic component of the complex, Presenilin, is required to cleave a wide variety of substrates including Alzheimer's disease related amyloid precursor protein (De Strooper et al., 1998), and developmental protein Notch (Zhao et al., 2010). Alongside these proteolytic functions several non-proteolytic roles have also been suggested, relying on a scaffolding function of the complex (Khandelwal et al., 2007, Otto et al., 2016, Ludtmann et al., 2014, Dobrowolski et al., 2012, Murayama et al., 1998, Zhang et al., 1998). Within this subset of roles, a number of studies have investigated the role of the  $\gamma$ -secretase complex/Presenilin in mammalian endocytosis and autophagy (Esselens et al., 2004, Lee et al., 2015, Lee et al., 2010, Neely et al., 2011, Cataldo et al., 2000, Tamboli et al., 2008, Zhang et al., 2006), however it is not known whether these processes rely on the entire  $\gamma$ -secretase complex, presenilin proteins alone, or whether proteolytic activity also plays a role.

Other roles for the  $\gamma$ -secretase complex have also been suggested. In mammalian model organisms,  $\gamma$ -secretase /Presenilin has been found to be a crucial component for efficient protein clearance from the endocytic recycling compartment (Zhang et al., 2006), and for normal endocytic uptake of lipoprotein particles (Tamboli et al., 2008). Utilising Chinese hamster ovary cells it was shown that treatment with the  $\gamma$ -secretase inhibitor DAPT retained 2 – 3 times the amount of fluorescently labelled transferrin for a greater measurement of time

when compared to wild-type cells, this was also found with cells lacking the Presenilin proteins and cells with ablated catalytic activity (Zhang et al., 2006). Additionally, analysis with FITC-Dextran, a late endosomal marker, showed no significant co-localisation between labelled transferrin and FITC-Dextran in cells lacking Presenilin/ $\gamma$ -secretase activity. Through the use of mouse embryonic fibroblasts, and mouse neurons, with ablated Presenilin proteins, or transgenic expression of AD causing mutated Presenilin, researchers have demonstrated that loss of the  $\gamma$ -secretase complex results in diminished uptake of lipoproteins through a mistargeting of proteins responsible for endocytic regulation of the LDL receptor causing elevated levels of apolipoprotein E in these cells (Tamboli et al., 2008). These mammalian studies establish a link between endocytosis and the  $\gamma$ -secretase complex, but unfortunately are not able to distinguish between roles dependent upon the complex as a whole, and roles dependent upon only the Presenilin proteins.

The role of the  $\gamma$ -secretase complex/Presenilin in autophagy has also been investigated in mammalian model organisms (Lee et al., 2015, Lee et al., 2010, Neely et al., 2011, Wolfe et al., 2013). Studies exploring this function of  $\gamma$ -secretase have implicated insufficient lysosomal acidification as a key factor in autophagic disruption in these model organisms. Upon ablation of presenilin, Presenilin null mouse blastocysts demonstrate elevated lysosomal pH as a result of dysfunctional v-ATPase subunit localisation, a phenotype shared in cells expressing AD causing Presenilin mutations (Lee et al., 2010). Additionally, cells lacking Presenilin exhibit an accumulation of autophagosomes, indicative of autophagy disruption, that is not present upon halting  $\gamma$ -secretase proteolytic

activity through the use of complex specific inhibitors (Neely et al., 2011). These results are consistent when examined in fibroblasts from AD patients with AD causing  $\gamma$ -secretase complex mutations (Wolfe et al., 2013). The proposed mechanism for this defect in lysosomal acidification is aberrant calcium homeostasis as a result of presenilin ablation, a function shown to be  $\gamma$ -secretase independent (Sarasija and Norman, 2015), however restoration of intracellular calcium concentration to wild-type levels did not rescue the defects observed in autophagy upon Presenilin ablation (Lee et al., 2015). These studies demonstrate an important role for the  $\gamma$ -secretase complex/ Presenilin in maintaining autophagy/lysosomal acidification in mammalian model organisms, but once again do not shed light upon whether this function is due to the entire complex, presenilin alone, or proteolytic activity.

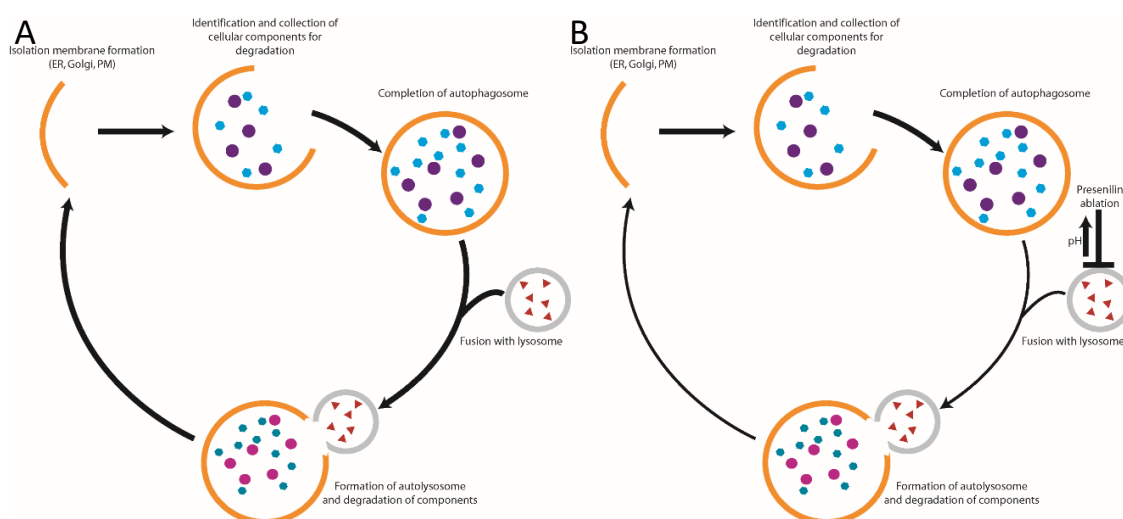


**Figure 5.1 The Effects of Presenilin Ablation on Autophagy.** A) In wild-type cells autophagy progresses as follows: Formation of isolation membrane, collection of cellular components for degradation, fusion of autophagosome with lysosome, subsequent degradation of cellular material. B) In the absence of Presenilin the pH in the lysosome is elevated, therefore decreasing the degradation of material contained within the autophagosome causing a decrease in the rate of autophagy and resulting in an accumulation of autophagosomes.



*Dictyostelium* has been established as a model organism for the investigation of endocytosis and autophagy, often resulting in translation to mammalian model systems (Annesley et al., 2011, Chubb et al., 2000, Commisso et al., 2013, King et al., 2013). *Dictyostelium* mutants lacking autophagy related proteins demonstrate differing developmental defects dependent upon developmental substrate as observed in mutants lacking Aph-1 and Ncstn (Chapter 4.4). Additionally, *Dictyostelium* has been used to demonstrate a non-catalytic role of Presenilin in *Dictyostelium* development, with conserved function when expressing the human Presenilin 1 protein (Ludtmann et al., 2014), and has shown a Presenilin function in *Dictyostelium* phagocytosis in a catalytic dependent manner (McMains et al., 2010) providing a useful model organism for investigating the effects of  $\gamma$ -secretase ablation in endocytosis and autophagy.

This chapter will report on the use of *Dictyostelium* to investigate the role of the  $\gamma$ -secretase complex in *Dictyostelium* endocytosis, specifically macropinocytosis, and *Dictyostelium* autophagy. Use of this model organism will allow for differentiation between roles dependent upon the entire protein complex or Presenilin only functions, as well as roles dependent upon catalytic activity. This approach will allow the exploration of evolutionarily conserved function by expressing human presenilin proteins in *psenA<sup>-</sup>/B<sup>-</sup>* cells.

## 5.2 Macropinocytosis in $\gamma$ -secretase Component Null Mutants

As endocytic uptake is inhibited upon presenilin ablation in mammalian organisms (Tamboli et al., 2008) we set out to determine whether the dominant form of fluid phase uptake in *Dictyostelium* - macropinocytosis, is also inhibited upon presenilin/ $\gamma$ -secretase ablation. Utilising the fluorescently labelled dextran,

TRITC-Dextran, we can measure fluid phase nutrient uptake, and therefore quantify uptake corresponding to macropinocytosis in *Dictyostelium* cells (Hacker et al., 1997).

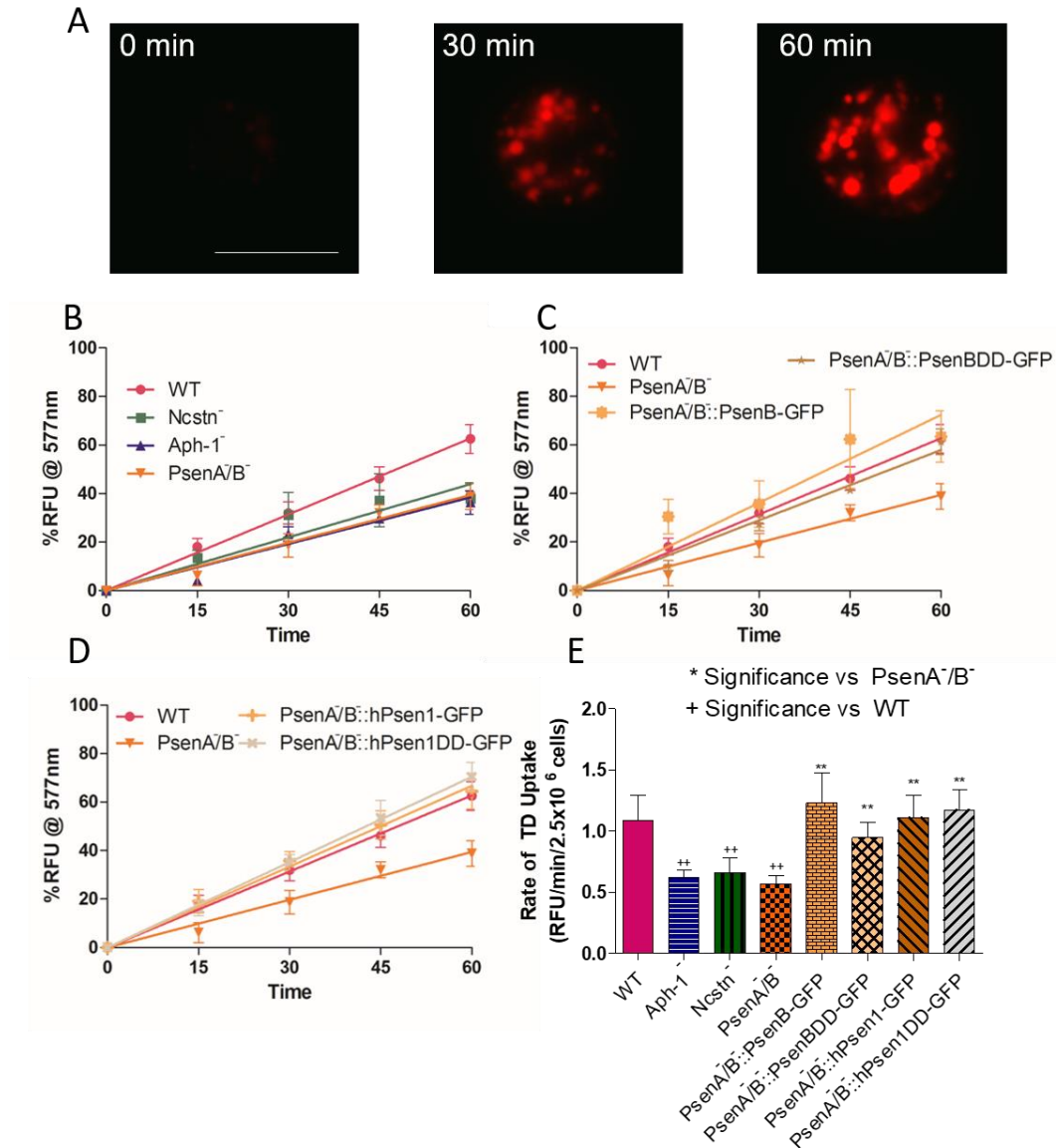


**Figure 5.2 Macropinocytosis in *Dictyostelium*  $\gamma$ -secretase mutants.** A) Representative images of TRITC-Dextran uptake in *Dictyostelium* cells over 60 minutes. B) TRITC-Dextran uptake in wild-type, *ncstn*<sup>-</sup>, *aph-1*<sup>-</sup>, and *psenA/B*<sup>-</sup> *Dictyostelium* cells. Normalised against wild-type cells *Dictyostelium*  $\gamma$ -secretase mutants show a decrease in TRITC-Dextran uptake through macropinocytosis. C) TRITC-Dextran uptake in wild-type, *psenA/B*<sup>-</sup>, and *Dictyostelium* catalytically active and inactive rescues show restoration of TRITC-Dextran uptake regardless of Presenilin catalytic activity compared to *psenA/B*<sup>-</sup> cells. D) TRITC-Dextran uptake in wild-type, *psenA/B*<sup>-</sup>, and human catalytically active and inactive rescues show restoration of TRITC-Dextran uptake regardless of Presenilin catalytic activity compared to *psenA/B*<sup>-</sup> cells. E) Rates of TRITC-Dextran uptake comparing wild-type,  $\gamma$ -secretase null mutants, and *Dictyostelium* and human Presenilin rescue mutants.

Using the first 60 minutes of macropinocytosis when uptake of TRITC-Dextran is linear (Figure 5.2 B) the rate of fluid phase uptake can be calculated. In this experiment, wild-type cells showed a rate of  $1 \pm 0.25$  RFU/min/ $2.5 \times 10^6$  cells whilst cells lacking Aph-1 (Figure 5.2 C), Ncstn and Presenilin showed decreased rates of  $0.6 \pm 0.05$ ,  $0.65 \pm 0.15$ ,  $0.5 \pm 0.05$  RFU/min/ $2.5 \times 10^6$  cells respectively. These data indicate that the entire  $\gamma$ -secretase complex functions to ensure normal macropinocytosis in *Dictyostelium*, and not only the Presenilin proteins.

As Presenilins show both catalytic and non-catalytic functions we next sought to determine whether macropinocytosis is dependent upon  $\gamma$ -secretase proteolytic activity. Expression of a catalytically active PsenB-GFP in *psenA/B* cells restored macropinocytosis to wild-type levels ( $1.26 \pm 0.4$  RFU/min/ $2.5 \times 10^6$  cells) (Figure 5.2 B, C), as did expression of the catalytically inactive PsenBDD-GFP lacking residues D348 and D394 catalytic ( $0.98 \pm 0.12$  RFU/min/ $2.5 \times 10^6$  cells) indicating that this role is not dependent upon proteolytic activity. Further, expression of a human Presenilin 1 protein also rescued macropinocytosis defects due to Presenilin ablation, once again in the presence or absence of catalytic activity ( $1.1 \pm 0.3$ , and  $1.2 \pm 0.2$  RFU/min/ $2.5 \times 10^6$  cells respectively).

### 5.3 The Effects of pH on $\gamma$ -secretase Mutant Development

Since in mammalian models,  $\gamma$ -secretase/presenilin ablation gives rise to increased lysosomal pH we set out to determine whether vesicle acidification in *Dictyostelium* is also perturbed upon  $\gamma$ -secretase/presenilin ablation. One approach to identifying acidification defects in *Dictyostelium* was illustrated in the study of the vesicle acidification mutant *hgr5* (Davies et al., 1996). These cells fail to form terminal developmental structures under neutral pH but exhibit an

increased sensitivity to developmental pH and are further delayed when developed in the presence of weak bases (Davies et al., 1996). Additionally, the role of acidification in development was confirmed by development in acidic conditions where the developmental defects observed at neutral pH are rescued (Davies et al., 1996). In order to determine whether *Dictyostelium*  $\gamma$ -secretase mutants exhibit vesicular acidification defects  $\gamma$ -secretase null cell lines were developed under a variety of pH conditions. In these experiments, *aph-1*<sup>-</sup>, *ncstn*<sup>-</sup> and *psenA*<sup>-</sup>/*B*<sup>-</sup> cells were developed at pH 7, pH 8 and pH 9 on nitrocellulose membranes. Here, wild-type cells formed mature fruiting bodies consisting of a basal disk, stalk and spore head under all conditions (Figure 5.3 A). In contrast, *aph-1*<sup>-</sup> and *ncstn*<sup>-</sup> cells formed fruiting bodies at pH 7 as shown previously (Figure 5.3 B), but failed to develop beyond the first finger stage at pH 8 and pH 9 (Figure 5.3 B). *psenA*<sup>-</sup>/*B*<sup>-</sup> cells failed to develop fruiting bodies at pH 7 as shown previously (Ludtmann et al., 2014) and were halted at the earlier mound stage at the more basic pH 9 (Figure 5.3 A). These data indicate  $\gamma$ -secretase component null mutants possess a sensitivity to basic pH suggesting a vesicle acidification defect.

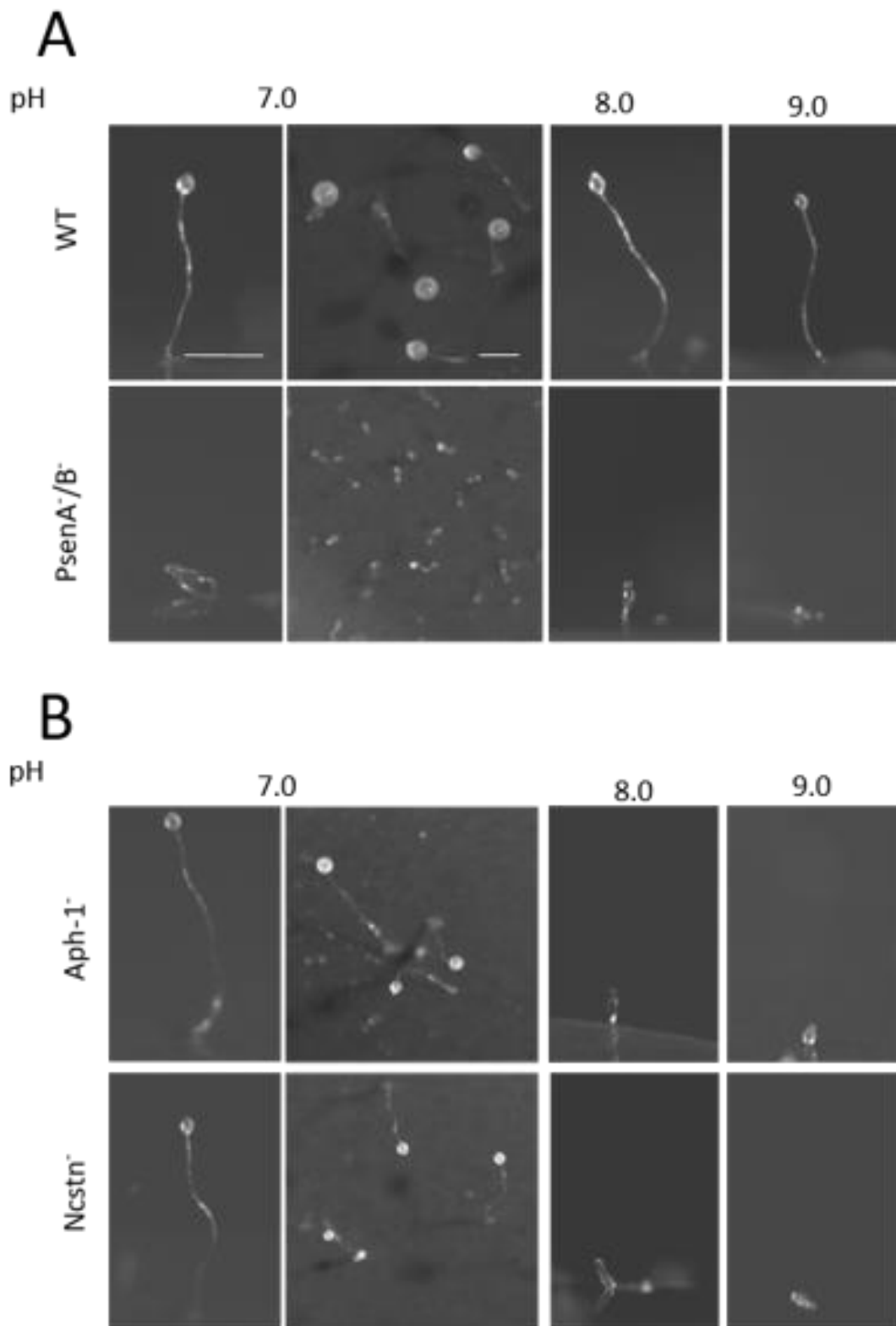


**Figure 5.3 Development of *Dictyostelium*  $\gamma$ -secretase null mutants under basic pH.** A) Under basic conditions wild-type cells develop normal morphology fruiting bodies. *psenA<sup>-</sup>/B<sup>-</sup>* cells fail to develop at pH 7 and are further inhibited at pH 8 and pH 9. B) *aph-1<sup>-</sup>* and *ncstn<sup>-</sup>* cells develop normal morphology fruiting bodies at pH 7, but fail to develop at pH 8 and pH 9 indicating increased sensitivity to pH.

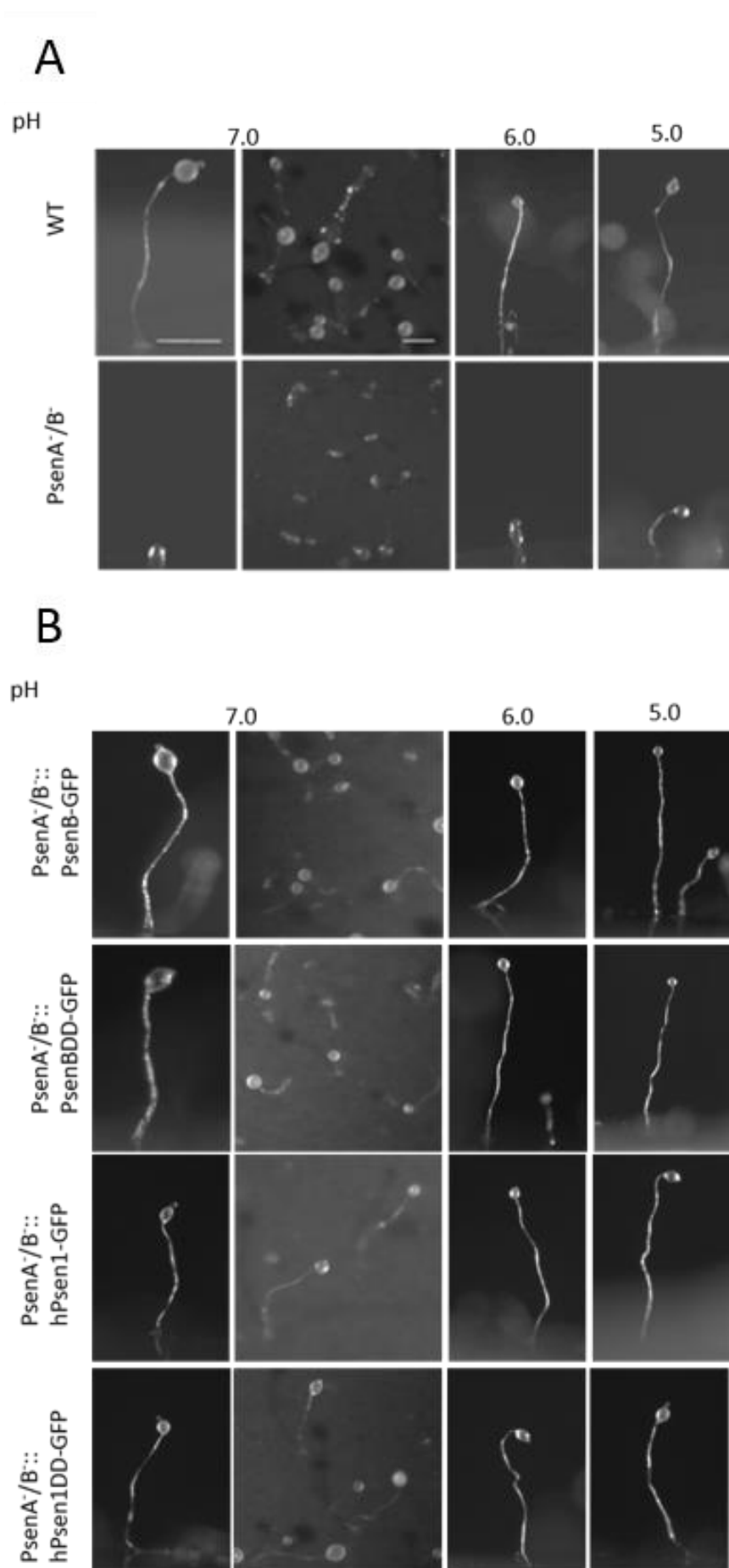


**Figure 5.4**  
**Development of**  
***Dictyostelium***  **$\gamma$ -**  
**secretase null**  
**mutants under**  
**acidic pH.** A) Under acidic conditions wild-type cells form normal morphology fruiting bodies. *psenA<sup>-</sup>/B<sup>-</sup>* cells are partially rescued at pH 5, forming smaller sized fruiting bodies consisting of a basal disk, stalk and spore head. B) Presenilin rescue mutants are able to develop at pH 7 and under acidic pH conditions regardless of catalytic or non-catalytic activity, replicating wild-type cells.

As *PsenA*<sup>-</sup>/*B*<sup>-</sup> mutants fail to develop at neutral pH when compared to wild-type and *Aph-1*<sup>-</sup>, *Ncstn*<sup>-</sup> cells we next set out to examine whether this developmental defect can be rescued under acidic pH conditions. In these experiments, *psenA*<sup>-</sup>/*B*<sup>-</sup> cells were developed under acidic pH conditions at pH 6, and pH 5 alongside wild-type cells. Under these conditions, wild-type cells formed mature fruiting bodies at both acidic pHs (Figure 5.4 A) whilst *psenA*<sup>-</sup>/*B*<sup>-</sup> cells formed morphologically normal, but smaller in size, fruiting bodies at pH 5 (Figure 5.4 A) indicating a partial rescue. These results suggested that the developmental defect observed in *PsenA*<sup>-</sup>/*B*<sup>-</sup> cells is partially due to a pH imbalance within these cells. Importantly, Presenilin mutants rescued by catalytically active or inactive *Dictyostelium* Presenilin B, or human Presenilin 1 constructs were unaffected by pH conditions and developed morphologically normal fruiting bodies (Figure 5.4 B). These results suggest that vesicle acidification in *Dictyostelium* is not reliant upon the catalytic activity of the  $\gamma$ -secretase complex, but rather a non-catalytic scaffolding function that has been conserved through evolution.

#### 5.4 The Effects of $\gamma$ -secretase Ablation on Autophagy and Protein Ubiquitination

As autophagy is required for development in *Dictyostelium* (Otto et al., 2004), we sought to determine whether autophagy is also disrupted in cells lacking functional Presenilin/ $\gamma$ -secretase, and to establish whether this role is carried out by Presenilin alone or by the entire protein complex. *Dictyostelium* cells defective in autophagy show large aggregates of the autophagy protein marker GFP-Atg8 (Calvo-Garrido and Escalante, 2010, Otto et al., 2004, King et al., 2011). Measurement of GFP-Atg8 positive aggregates in *Dictyostelium* was achieved by expressing GFP-Atg8 in wild-type cells, cells lacking *PsenA* and

PsenB, and cells lacking Aph-1 were visualised under agarose to stimulate autophagy (King et al., 2011). In these experiments, wild-type cells show a majority (79%) of small diameter autophagosomes (below 0.4 $\mu$ m) with very few structures (1.4%) above 0.8 $\mu$ m (Figure 5.5 A, C) indicating normally functioning autophagy. Upon ablation of *aph-1* cells showed a significant decrease ( $p<0.01$ ) of autophagosomes below 0.4 $\mu$ m (26%) and a significant increase ( $p<0.05$ ) in large diameter autophagosomes (17%) (Figure 5.5 A, C). Similarly, cells lacking Presenilin showed a significant decrease ( $p<0.05$ ) in small autophagosomes (38%) and a significant increase in large (greater than 0.8 $\mu$ m) GFP-Atg8 positive structures ( $p<0.001$ , 18%) (Figure 5.5 B, C). These data suggest that loss of the  $\gamma$ -secretase complex causes autophagic dysfunction.



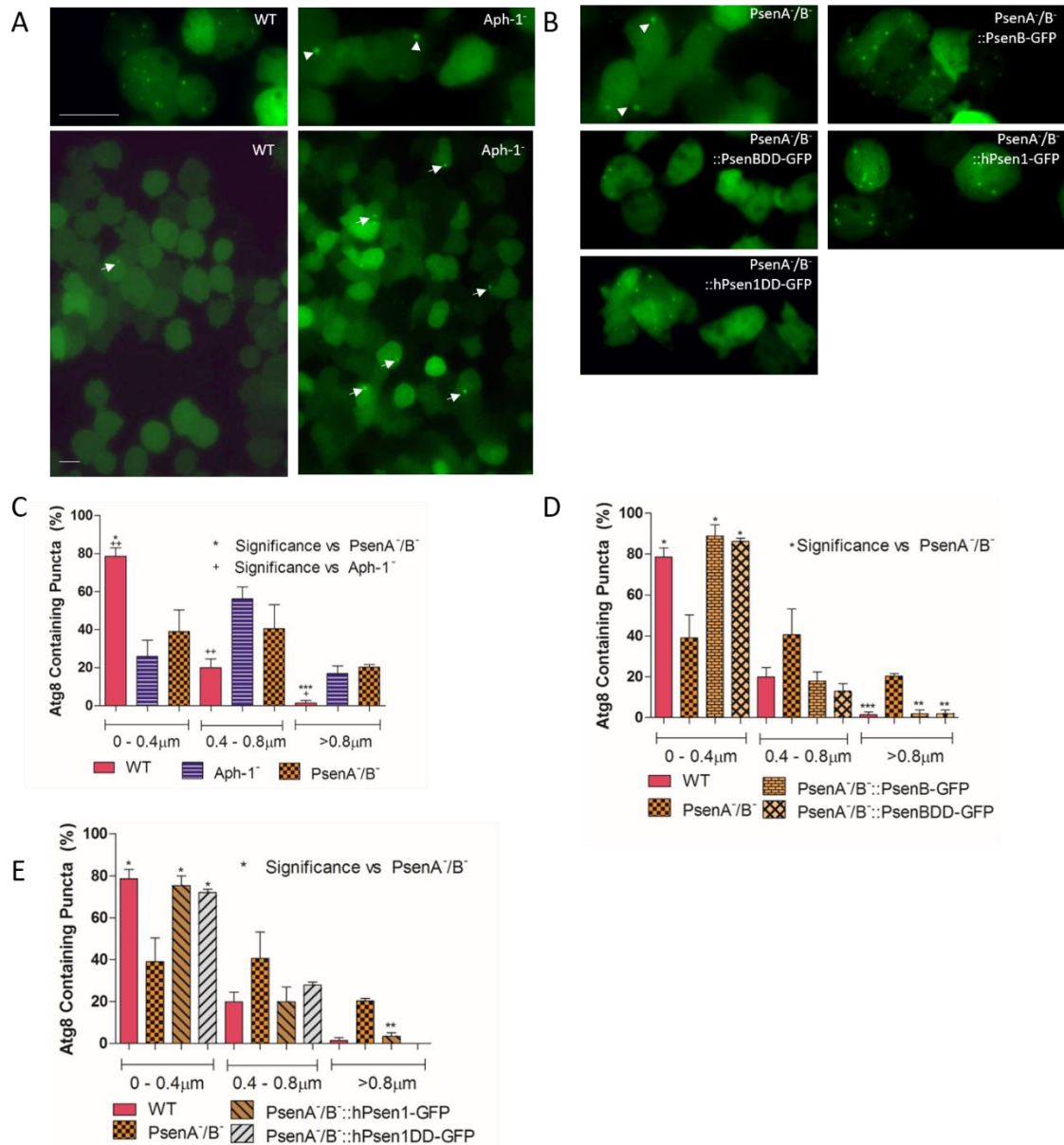


**Figure 5.5 Localisation and size measurement of GFP-Atg8 positive vesicles in *Dictyostelium*.** A) Wild-type cells expressing GFP-Atg8 show several GFP positive puncta per cell. A proportion of *aph-1*<sup>-</sup> cells show a distinct, single, large GFP-positive punctum (white arrow heads). B) *psenA/B*<sup>-</sup> cells also exhibit a single, large, GFP positive puncta in a portion of cells. Presenilin rescue constructs expressed in *psenA/B*<sup>-</sup> cells show a restoration of the wild-type GFP-Atg8 localisation, restoring localisation to several small puncta per cell. C) Quantification of GFP-Atg8 puncta show that wild-type cells exhibit a majority of small GFP-positive puncta with very few medium or large sized puncta. *Aph-1*<sup>-</sup> and *PsenA/B*<sup>-</sup> cells exhibit a significant decrease in small GFP positive puncta and a significant increase in large (>0.8 μm) puncta. D) Expression of catalytically active or inactive *Dictyostelium* PsenB rescues GFP-Atg8 puncta defects observed in *psenA/B*<sup>-</sup> cells. E) Expression of a catalytically active or inactive human Psen1 restores GFP-Atg8 puncta defects observed upon presenilin ablation in *Dictyostelium*.

To determine whether the role of the  $\gamma$ -secretase complex in autophagy is dependent upon catalytic activity GFP-Atg8 was co-expressed in cells expressing

*Dictyostelium* catalytically active or inactive Presenilin B, and in cells expressing human catalytically active or inactive Presenilin 1. In all cases, restoration of Presenilin rescued the autophagic defects observed in *psenA<sup>-</sup>/B<sup>-</sup>* cells (Figure 5.5 B, D, E). These results confirm that this function of the  $\gamma$ -secretase complex is not reliant upon catalytic activity, but rather a scaffolding function, and is conserved with the human Presenilin protein.

A typical response to autophagic dysfunction is the accumulation of high molecular weight ubiquitinated protein (Calvo-Garrido and Escalante, 2010). Large GFP-Atg8 positive aggregates show co-localisation with ubiquitin, and increased high molecular weight ubiquitin in western blot (Calvo-Garrido and Escalante, 2010). To investigate this effect in relation to loss of  $\gamma$ -secretase components, cells expressing GFP-Atg8 were fixed in -80°C methanol and stained for GFP and ubiquitin. In these experiments, wild-type cells exhibited GFP-positive puncta and generalised ubiquitin staining with no co-localisation (Figure 5.6 A). Following Aph-1 or PsenA/B ablation a portion of cells exhibited a single GFP-positive punctum that was also positive for ubiquitin which was not observed in wild-type cells. When Presenilin constructs were expressed in *psenA<sup>-</sup>*

/B<sup>-</sup> cells GFP-Atg8 no longer co-localised with ubiquitin, and the majority of GFP-positive puncta were <0.4μm regardless of catalytic activity.

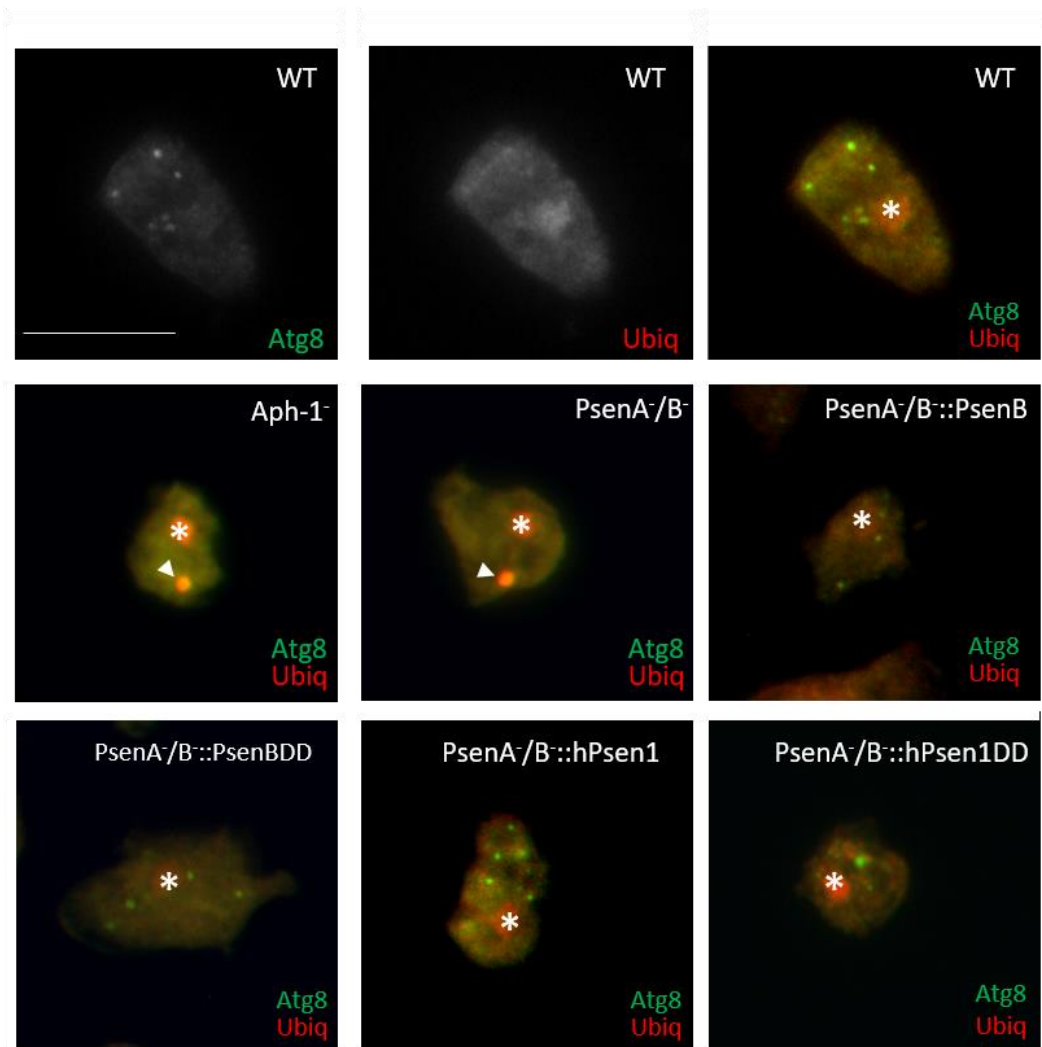


**Figure 5.6 High molecular weight ubiquitin aggregation and localisation in *Dictyostelium*  $\gamma$ -secretase mutants.** A) Wild-type cells fixed and stained for GFP and ubiquitin exhibit typical small GFP-Atg8 positive puncta and non-specific ubiquitin staining. *Aph-1*<sup>-</sup> and *psenA*<sup>-</sup>/*B*<sup>-</sup> cells exhibit co-localisation between GFP-Atg8 and ubiquitin not observed in wild-type cells (White arrow heads). Upon expression of PsenB or Psen1 GFP-Atg8 localisation was rescued, no longer co-localising with ubiquitin. Scale bar = 10μm.

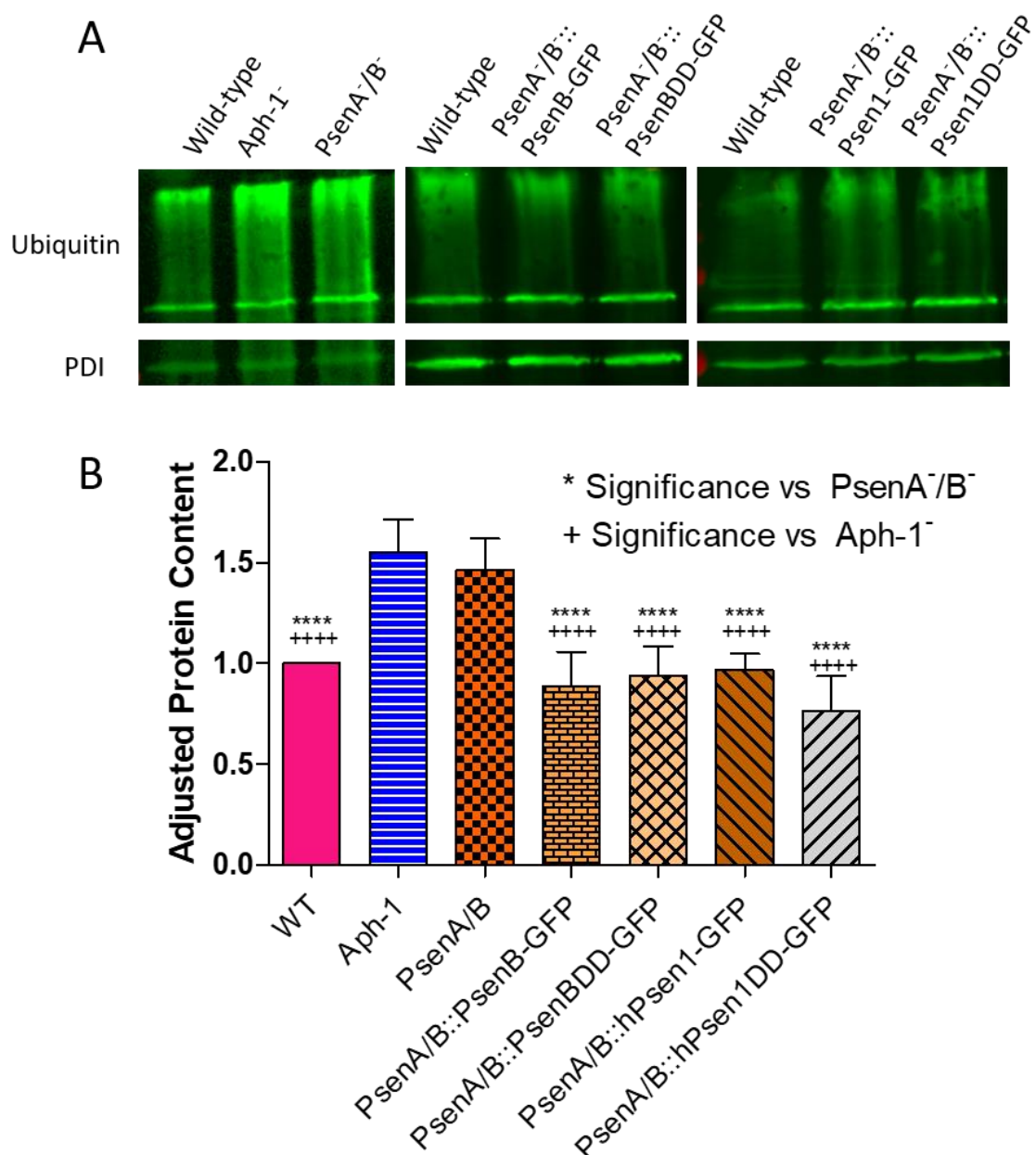


**Figure 5.7 Quantification of high molecular weight ubiquitin in *Dictyostelium*  $\gamma$ -secretase mutants.** A) Western blot analysis demonstrates an increased level of high molecular weight ubiquitin in cells lacking *aph-1* and *psenA/B* which is not observed upon expression of catalytically active or inactive *Dictyostelium* PsenB or human Psen1. B) Quantification of high molecular weight ubiquitin shows a significant increase in cells lacking Aph-1 and PsenA/B, this is restored upon expression of catalytically active or inactive PsenB or Psen1.

Quantification of high molecular weight ubiquitin can be determined through western blot. These assays usually utilise cells expressing GFP-Atg8 (Calvo-Garrido and Escalante, 2010, Xiong et al., 2015), however it is not known whether

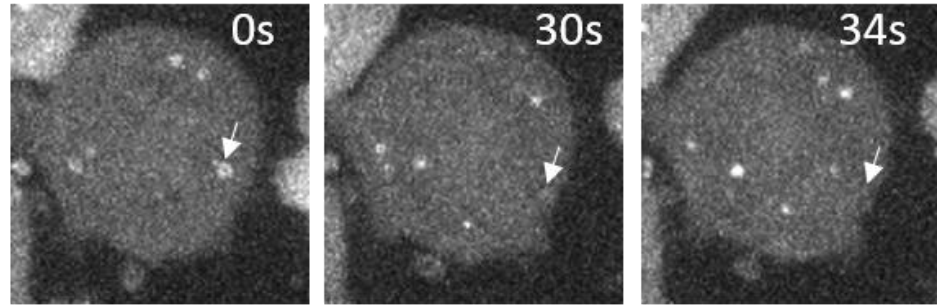
the presence of GFP-Atg8 affects the presence of ubiquitinated protein. In order to ensure that expression of GFP-Atg8 did not affect these experiments we utilised wild-type cells and base null strains *psenA/B*, and *aph-1* for analysis. In this assay, high molecular weight ubiquitin was quantified and normalised to wild-type levels using the loading control endoplasmic reticulum protein PDI (Figure 5.7 A, B) (Muller-Taubenberger et al., 2001). Ablation of Aph-1 resulted in increased high molecular weight ubiquitin, increasing levels to  $155 \pm 12\%$  ( $p = 0.0002$ ) of wild-type cells (Figure 5.7 A, B), ablation of PsenA/B also resulted in an increase of  $146 \pm 10\%$  ( $p = 0.0001$ ) compared to wild-type cells suggesting a dysfunction in protein degradation in these mutants (Figure 5.7 A, B). Restoration of *Dictyostelium* or human Psen (catalytically active or inactive) reversed the observed increase in high molecular weight ubiquitin.

## 5.5 $\gamma$ -secretase Ablation Causes Vesicle Acidification Defects

Degradation of intracellular components by autophagy is reliant upon lysosomal activity (Luzio et al., 2000). We therefore investigated the acidification of autophagosomes in cells lacking  $\gamma$ -secretase components. The fluorescence of GFP-Atg8 is quenched when exposed to acidic conditions (such as those found in lysosomes) (Figure 5.8 A) and so we analysed the GFP quenching time in wild-type cells and cells lacking Aph-1 and PsenA/B to indirectly measure lysosomal pH. In these experiments, wild-type cells exhibited an average GFP quenching time of  $35.3 \pm 6.8$  seconds (Figure 5.8 B). Loss of Aph-1 significantly increased quenching time to  $49.8 \pm 6.8$  seconds ( $p < 0.0001$ ), and loss of PsenA/B also significantly increased quenching time to  $46.4 \pm 9.7$  seconds ( $p < 0.0001$ ) indicating a dysfunction in lysosomal acidification in these mutants. Expression of *Dictyostelium* catalytically active PsenB rescued this acidification defect

(32.2±4.7 seconds) as did expression of a catalytically inactive PsenB (31.5±6.5 seconds). Similarly, expression of the catalytically active or inactive human Psen1 proteins also rescued acidification (32.8±6.4 seconds and 28.8±5.6 seconds respectively). Therefore, we suggest that these acidification defects are reliant upon the  $\gamma$ -secretase complex, through a non-catalytic role, that is conserved from *Dictyostelium* to man.

A



B

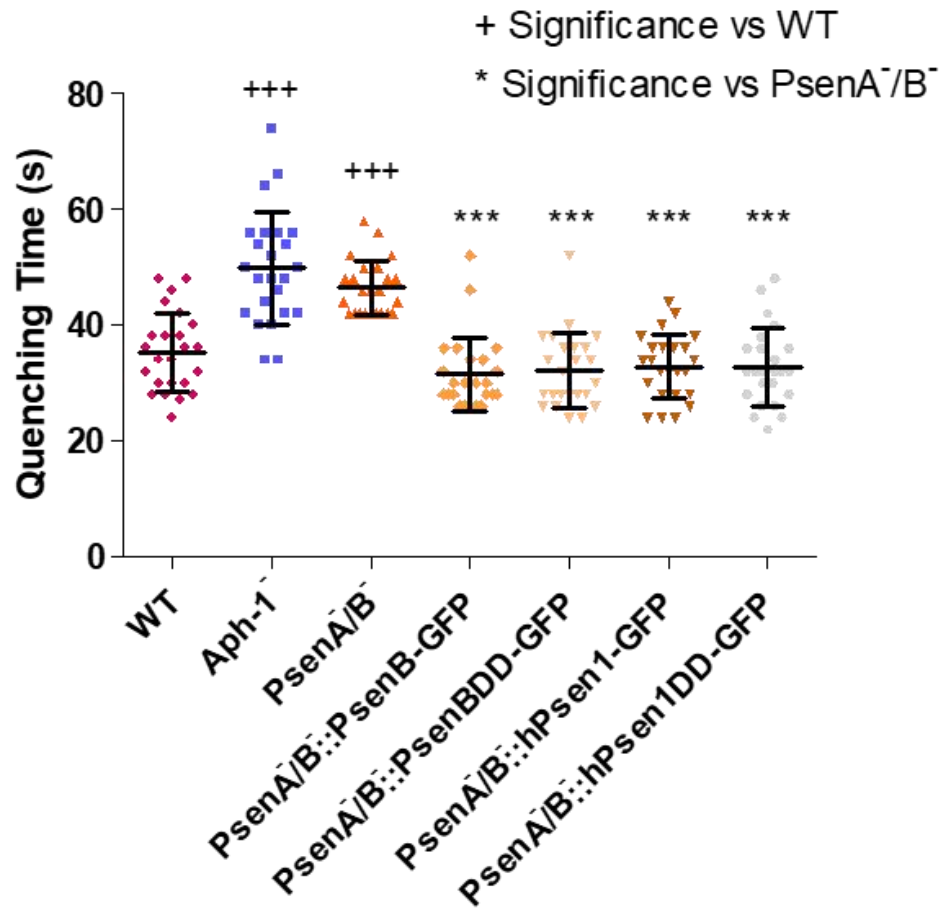


**Figure 5.8 Acidification of autophagosomes in *Dictyostelium*  $\gamma$ -secretase null mutants.** A) Representative images of GFP-Atg8 quenching in *Dictyostelium* wild-type cells. B) Quantification of GFP-Atg8 quenching shows a significant increase upon ablation of Aph-1 or PsenA/B. Restoration of Presenilin activity restores GFP quenching to wild-type levels rescuing acidification defects observed upon presenilin ablation. Catalytically inactive Presenilin proteins are also able to restore acidification to wild-type levels.

An alternative process reliant upon lysosomal acidification for normal function is phagocytosis (King et al., 2013). Since presenilin has been previously implicated in *Dictyostelium* phagocytosis we sought to determine whether this was also due

to acidification defects (McMains et al., 2010). To investigate this, a set of experiments were conducted by Dr. Jason King (University of Sheffield) to measure the acidification of phagosomes by measuring the proteolysis of beads coated with the self-quenching dye (DQ-BSA) which fluoresces upon proteolysis. This assay showed wild-type proteolytic activity measured at  $1 \pm 0.3$  a.u and ablation of Aph-1 or PsenA/B resulted in a significant reduction in proteolytic activity to  $0.41 \pm 0.07$  a.u ( $p=0.05$ ) and  $0.42 \pm 0.22$  a.u ( $p=0.03$ ) respective to wild-type cells (Appendix 4). Expression of catalytically active or inactive *Dictyostelium* PsenB restored proteolysis to  $0.79 \pm 0.24$  a.u ( $p=0.1$ ) and  $1.29 \pm 0.5$  a.u ( $p=0.36$ ) compared to wild-type cells, and expression of a human active or inactive Psen1 restored degradation rate to  $0.99 \pm 0.22$  a.u ( $p=1.00$ ) and  $1.21 \pm 0.16$  a.u ( $p=0.35$ ). These data suggest that in *Dictyostelium* lysosomal activity depends upon the entire  $\gamma$ -secretase complex and functions through a non-catalytic mechanism that is conserved with the human Presenilin proteins.

## 5.6 Discussion

In this chapter, we have shown that the *Dictyostelium*  $\gamma$ -secretase complex plays an important role in *Dictyostelium* macropinocytosis, and phagocytosis through reduced vesicle acidification leading to defects in autophagy. We suggest that the most likely mechanism responsible for these defects is dysfunctional lysosomal acidification. Recent studies in mammalian organisms have investigated the roles of  $\gamma$ -secretase in vesicular trafficking and implicate dysfunction of these processes in the pathology and progression of Alzheimer's disease (Cataldo et al., 2000, Fukumori et al., 2006, Tamboli et al., 2008, Zhang et al., 2006, Esselens et al., 2004, Lee et al., 2015, Lee et al., 2010, Neely et al., 2011, Wolfe et al., 2013). These studies typically indicate that presenilin is the



protein component responsible for aberrant intracellular degeneration, and do not determine whether the entire complex is also involved (Esselens et al., 2004, Lee et al., 2015, Neely et al., 2011, Zhang et al., 2006). Here, we employed the social amoeba *Dictyostelium* as a model organism to investigate these processes and determine if presenilin alone or the entire  $\gamma$ -secretase complex is necessary for optimal vesicle acidification. We show that in *Dictyostelium* the entire  $\gamma$ -secretase, and not only presenilin, is necessary to enable normal macropinocytosis and autophagy, additionally we demonstrate that these processes are not reliant upon the catalytic activity of the complex where the role is conserved between the *Dictyostelium* Presenilin B and the human Presenilin 1 proteins.

We show that upon ablation of  $\gamma$ -secretase components macropinocytosis, the main mechanism used by laboratory strain *Dictyostelium* to ingest nutrients (Bloomfield et al., 2015), is dysfunctional. *Dictyostelium* has been used to investigate the mechanisms behind macropinocytosis leading to discoveries including the role of RasS (Chubb et al., 2000), PI3-kinases (Hoeller et al., 2013), WASH (Buckley et al., 2016) and Neurofibromin (Bloomfield et al., 2015) in macropinocytosis, that have been replicated in mammalian organisms (Gopaldass et al., 2012, Sasaki et al., 2007, Buckley et al., 2016). Our data now suggests, for the first time, that a functional and complete  $\gamma$ -secretase complex is required for macropinocytosis in *Dictyostelium* in a structural role. In mammalian studies it has been unclear thus far whether presenilin alone or an entire  $\gamma$ -secretase complex functions in macropinocytosis (Zhang et al., 2006) that may contribute to Alzheimer's disease progression (Cataldo et al., 2000). Mammalian studies utilising Psen null mutants, or  $\gamma$ -secretase inhibitors, are unable to

determine whether the processes investigated are due to the absence of presenilin as a complex-independent protein or due to the absence of  $\gamma$ -secretase as a protein complex (Zhang et al., 2006). Here, we demonstrate, that the entire  $\gamma$ -complex and not only presenilin functions to mediate macropinocytosis, and further show conservation of this function between catalytically active or inactive *Dictyostelium* Presenilin and human Presenilin proteins.

After internalisation, extracellular material is moved through the endocytic pathway before fusion with lysosomes causes vesicular material degradation (Gruenberg and Maxfield, 1995, Luzio et al., 2000). *Dictyostelium* mutants that are unable to properly acidify intracellular vesicles have been shown to be pH sensitive when undergoing development (Davies et al., 1996). As mammalian cells lacking presenilin proteins show defects in acidification (Lee et al., 2015, Lee et al., 2010, Wolfe et al., 2013) we sought to determine whether these proteins also function in acidification in *Dictyostelium*. Here, we have demonstrated that *Dictyostelium*  $\gamma$ -secretase mutants exhibit sensitivity to pH when undergoing development, suggesting defective vesicular acidification. Additionally, we show that defects arising from presenilin ablation are rescued through expression of non-catalytic *Dictyostelium* and human presenilin proteins. Our data indicate that normal *Dictyostelium* vesicular acidification is dependent upon a complete  $\gamma$ -secretase complex, and not only the presenilin proteins, in a non-catalytic manner that has been conserved between *Dictyostelium* and man which has not been shown previously.

Autophagy, the process by which cells degrade intracellular material, is another cellular process dependent upon lysosomal degradation (Mizushima et al., 2002).

*Dictyostelium* as a model organism has been widely used to investigate autophagy and its role in multicellular development (Calvo-Garrido and Escalante, 2010, King et al., 2013, King et al., 2011, Otto et al., 2004, Xiong et al., 2015). Additionally, autophagic dysfunction has been implicated in Alzheimer's disease where Presenilin is suggested to function in a complex independent role to maintain lysosomal pH, and that this disruption leads to increased build-up of neurotoxic peptides in patient neurons (Ghavami et al., 2014, Lee et al., 2015, Lee et al., 2010, Neely et al., 2011, Wolfe et al., 2013). In mammalian studies, cells lacking Psen1 exhibit aggregation of the autophagosome marker apg12 and the neuronal protein telencephalin (Esselens et al., 2004). These aggregates are likely to be due to deficiencies in the ubiquitin proteasomal system, and are suppressed through the expression of FAD-linked presenilin mutants suggesting it is not dependent upon catalytic activity (Esselens et al., 2004). However, whether this defect is dependent upon the presenilin proteins as a component of the  $\gamma$ -secretase complex, or solely the presenilin proteins is not understood. Here, we show that cells lacking  $\gamma$ -secretase components share hallmark characteristics with autophagy dysfunctional mutants, including aberrant GFP-Atg8 localisation, co-localisation of GFP-Atg8 and ubiquitin aggregates and increased high molecular weight ubiquitin (Calvo-Garrido and Escalante, 2010, Otto et al., 2004, Xiong et al., 2015). We further demonstrate that these deficiencies in autophagy are not dependent solely upon the presenilin proteins and can be rescued through non-catalytic *Dictyostelium* or human presenilin expression demonstrating a scaffolding role for the entire  $\gamma$ -secretase complex in *Dictyostelium* autophagy conserved between *Dictyostelium* and man.

As autophagy and macropinocytosis are both reliant upon normal lysosomal acidification to function we indirectly investigated lysosomal pH by monitoring autophagy in  $\gamma$ -secretase mutants. Upon ablation of  $\gamma$ -secretase components *Dictyostelium* cells show typical acidification defects with longer GFP acidification times compared to wild-type cells (King et al., 2013). These data correlate with those found in mammalian cells where non-functional  $\gamma$ -secretase/Presenilin results in decreased lysosomal pH, and subsequent dysfunctional protein clearance from cells (Lee et al., 2015, Lee et al., 2010, Neely et al., 2011). However, whether these functions are reliant upon the entire protein complex, or solely the Presenilin proteins is not fully understood, nor is the role of catalytic/structural activity (Neely et al., 2011, Lee et al., 2015). This thesis adds to the current pool of knowledge by showing that this process relies upon the entire  $\gamma$ -secretase complex and not only the Presenilin proteins. Further, we confirm that this function does not rely upon the catalytic activity of the protein complex as suggested in mammalian cells (Lee et al., 2015) and show conservation between the human and *Dictyostelium* Presenilin proteins. Additionally, we confirm these defects utilising phagocytosis assays (kindly carried out by Dr. Jason King) and directly measure proteolysis and acidification.

In this chapter, we demonstrate that the *Dictyostelium*  $\gamma$ -secretase complex is a key component in *Dictyostelium* macropinocytosis and autophagy, and that this process may be disrupted due to dysfunctional lysosomal pH mediation. Further, we show that these defects are dependent upon having a complete  $\gamma$ -secretase complex as single component null lines share the same defects, and that this function is not dependent upon catalytic activity. Finally, we show that these roles

are shared between the *Dictyostelium* and human proteins indicating a conservation of function across these two evolutionarily distinct species.

## Chapter VI

### Discussion

---

Alzheimer's disease poses a significant healthcare cost and burden, with affected individuals expected to increase as the ageing population grows (Anders et al., 2015). The  $\gamma$ -secretase complex has been associated with Alzheimer's disease progression and has been thoroughly investigated in its proteolytic function (De Strooper, 2003, De Strooper et al., 1998, Dries et al., 2009, Luo et al., 2003), however evidence suggests a non-catalytic structural function for this complex that may also contribute towards Alzheimer's disease progression and pathology (Murayama et al., 1998). conserved throughout evolution (Otto et al., 2016, Kang et al., 1999, Ludtmann et al., 2014, Khandelwal et al., 2007). This study set out to confirm previous controversial  $\gamma$ -secretase research utilising *Dictyostelium*, and to determine the role of the components that make up this protein complex. This study led to the discovery of roles for the *Dictyostelium*  $\gamma$ -secretase complex in endocytosis, and autophagy as shown in mammalian model systems (Tamboli et al., 2008, Zhang et al., 2006, Lee et al., 2015, Lee et al., 2010, Neely et al., 2011). Additionally, this study set out to investigate whether the function of the  $\gamma$ -secretase complex in this role is as an entire unit, or only the presenilin components as previously suggested and the role of catalytic function in these processes (Lee et al., 2015).

## 6.1 Confirming Previous Research in *Dictyostelium*

Whilst *Dictyostelium* has been used to investigate the  $\gamma$ -secretase complex previously (McMains et al., 2010, Ludtmann et al., 2014), little is known about the homology between *aph-1*, *ncstn* and *pen-2* between *Dictyostelium* and humans. Here we have demonstrated that the *Dictyostelium*  $\gamma$ -secretase components share important motifs and domains across evolution (Chapter III).

*Dictyostelium* Aph-1 shares a common number of transmembrane domains, and important motifs between humans and *Dictyostelium* including the GxxxGxxxG utilised for integrating and stabilising Aph-1 into the  $\gamma$ -secretase complex (Lee et al., 2004b). Ncstn also shares an essential stabilising/substrate sensing DYIGS motif between several species (Lim et al., 2015), and Pen-2 contains a strongly conserved C-terminal sequence (Chapter III).

Localisation of the  $\gamma$ -secretase complex in *Dictyostelium* was not investigated prior to this study, although Presenilin was shown to co-localise with calnexin at the endoplasmic reticulum (Ludtmann et al., 2014). Here, we confirmed Psen localisation to the endoplasmic reticulum, and further showed a similar localisation where Aph-1 and Ncstn colocalise with the ER marker calreticulin (Chapter III). The localisation of three out of four components to the ER in *Dictyostelium* strongly suggests that this protein complex is localised to the ER in this model system is consistent with that in mammals (Fassler et al., 2011). However, this localisation utilised overexpression constructs presenting a host of difficulties in interpretation (Gahlmann and Moerner, 2014), and therefore future studies may utilise knock-in approaches to allow for visualisation and localisation.

Previous research utilising *Dictyostelium* to investigate the  $\gamma$ -secretase complex has been controversial. Studies have suggested that the Presenilin, Aph-1 and Ncstn components of the  $\gamma$ -secretase complex function in *Dictyostelium* development (McMains et al., 2010), or that only the Presenilin proteins play a role in a non-catalytic manner (Ludtmann et al., 2014). In this study, we confirmed that *Dictyostelium* development in the absence of  $\gamma$ -secretase components is dependent upon the developmental substrate utilised (Chapter IV). *psenA/B*



cells demonstrate dysfunctional development under all conditions (McMains et al., 2010, Ludtmann et al., 2014), but *aph-1*<sup>-</sup> and *ncstr*<sup>-</sup> cells develop fully formed fruiting bodies on nitrocellulose filters as previously suggested (Ludtmann et al., 2014), and fail to develop fruiting bodies on 1% KK2 agar plates as demonstrated previously (McMains et al., 2010). This thesis confirms both of the previous studies observed developmental phenotypes.

## 6.2 The Role of *Dictyostelium* $\gamma$ -secretase in Vesicular Trafficking

*Dictyostelium* has been utilised to investigate a large body of work relating to vesicular trafficking including endocytosis (Bloomfield et al., 2015, Chubb et al., 2000, Hacker et al., 1997) and autophagy (Calvo-Garrido and Escalante, 2010, King et al., 2013, King et al., 2011, Otto et al., 2004, Xiong et al., 2015). In this thesis we utilised *aph-1*<sup>-</sup> cells (Chapter IV), *ncstr*<sup>-</sup>, and *psenA/B*<sup>-</sup> cells (Ludtmann et al., 2014) to investigate whether the  $\gamma$ -secretase complex functioned in *Dictyostelium* vesicle trafficking.

This thesis has shown that in *Dictyostelium* the entire  $\gamma$ -secretase complex plays a role in macropinocytosis and is required for normal function. Ablation of any of the components results in decreased overall macropinocytosis and a decreased rate of macropinocytosis (Chapter V). Additionally, we have established that this role is not dependent upon the catalytic activity of the protein complex, as catalytically inactive Presenilin rescue constructs can restore macropinocytosis to wild-type levels. Finally, we show a conservation of function between *Dictyostelium* and human through expression of a human Presenilin in *Dictyostelium*, once again restoring macropinocytosis function regardless of catalytic activity.

In *Dictyostelium* research, autophagy mutants exhibit different developmental phenotypes dependent upon substrate (Otto et al., 2004). As we demonstrated the same phenotypes in cells lacking  $\gamma$ -secretase components (Chapter III) we sought to determine whether these mutants also exhibit autophagy defects. Utilizing the autophagosome marker GFP-Atg8 we have demonstrated for the first time that the *Dictyostelium*  $\gamma$ -secretase complex exhibits characteristic autophagy defects including increased GFP-Atg8 vesicle size, and increased levels of high molecular weight ubiquitin (Chapter V). These results show that in *Dictyostelium* the  $\gamma$ -secretase complex functions to mediate autophagy, although it remains unknown if this occurs through a direct or indirect manner. Additionally, this process is not reliant upon the catalytic activity of the complex, and is evolutionarily conserved between humans and *Dictyostelium* as shown through the use of human Presenilin protein constructs.

The processes of macropinocytosis and autophagy both converge at the point of lysosomal acidification (Hu et al., 2015). Through the use of GFP-quenching assays we have indirectly shown that lysosomal acidification in *Dictyostelium*  $\gamma$ -secretase null mutants is dysfunctional (Chapter V). Additionally, we have confirmed this role more directly using phagocytic proteolysis assays utilizing DQ-BSA (Appendix 4, Dr. Jason King). Cells lacking a functional  $\gamma$ -secretase exhibit decreased acidification, and proteolysis, defects that are observed in mammalian models for Alzheimer's disease (Lee et al., 2015, Lee et al., 2010). Additionally, we confirm that the process of vesicle acidification is not reliant upon catalytic activity, however, in *Dictyostelium* the process is reliant upon the whole  $\gamma$ -

secretase complex being present, and not only the presenilin proteins as observed in mammalian cells (Lee et al., 2015).

In this thesis, we have successfully shown that the *Dictyostelium*  $\gamma$ -secretase complex is required for normally functioning macropinocytosis and autophagy. This dysfunction may be due to defects in acidification of lysosomes which therefore affects the processes of autophagy, macropinocytosis and phagocytosis downstream, further studies may wish to investigate this dysfunction directly. Whilst in mammalian studies it has been suggested that this acidification defect is due to dysfunctional calcium homeostasis, however, upon restoration of calcium levels cells still exhibited basic lysosomal pH (Lee et al., 2015). Future studies may wish to investigate whether the localisation and function of the v-ATPase pump is altered upon  $\gamma$ -secretase ablation (Lee et al., 2010). Additionally, this thesis has not been able to investigate the function of Pen-2 as a component of the  $\gamma$ -secretase complex. This thesis supports a role for the  $\gamma$ -secretase complex in dysfunctional vesicle acidification as suggested in mammalian studies (Lee et al., 2015, Lee et al., 2010), but expands findings to show that the entire complex functions in this process and not only the Presenilin proteins. Dysfunction in the endocytic pathway is believed to precede Alzheimer's disease pathology and progression (Cataldo et al., 2000), and this process may provide alternative therapeutic pathways for the treatment, and prevention of Alzheimer's disease.

## References

---

- ALLEN, H. B. 2016. Alzheimer's Disease: Assessing the Role of Spirochetes, Biofilms, the Immune System, and Amyloid-beta with Regard to Potential Treatment and Prevention. *J Alzheimers Dis*, 53, 1271-6.
- ALTSCHUL, S. F., GISH, W., MILLER, W., MYERS, E. W. & LIPMAN, D. J. 1990. Basic local alignment search tool. *J Mol Biol*, 215, 403-10.
- ALVES, G. S., OERTEL KNOCH, V., KNOCH, C., CARVALHO, A. F., PANTEL, J., ENGELHARDT, E. & LAKS, J. 2015. Integrating retrogenesis theory to Alzheimer's disease pathology: insight from DTI-TBSS investigation of the white matter microstructural integrity. *Biomed Res Int*, 2015, 291658.
- ANDERS, L., MERTINS, P., LAMMICH, S., MURGIA, M., HARTMANN, D., SAFTIG, P., HAASS, C. & ULLRICH, A. 2006. Furin-, ADAM 10-, and gamma-secretase-mediated cleavage of a receptor tyrosine phosphatase and regulation of beta-catenin's transcriptional activity. *Mol Cell Biol*, 26, 3917-34.
- ANDERS, W. & PRINCE, M. 2010. World Alzheimer Report 2010. <http://www.alz.co.uk>: Alzheimer's Disease International.
- ANDERS, W., PRINCE, M., GUERCHET, M., ALI, G., WU, Y. & PRINA, M. 2015. World Alzheimer Report 2015. <http://www.alz.co.uk>: Alzheimer's Disease International.
- ANDROUTSELLIS-THEOTOKIS, A., LEKER, R. R., SOLDNER, F., HOEPPNER, D. J., RAVIN, R., POSER, S. W., RUEGER, M. A., BAE, S. K., KITTAPPA, R. & MCKAY, R. D. 2006. Notch signalling regulates stem cell numbers in vitro and in vivo. *Nature*, 442, 823-6.
- ANNESLEY, S. J., BAGO, R., BOSNAR, M. H., FILIC, V., MARINOVIC, M., WEBER, I., MEHTA, A. & FISHER, P. R. 2011. Dictyostelium discoideum nucleoside diphosphate kinase C plays a negative regulatory role in phagocytosis, macropinocytosis and exocytosis. *PLoS One*, 6, e26024.
- ARAKI, Y., MIYAGI, N., KATO, N., YOSHIDA, T., WADA, S., NISHIMURA, M., KOMANO, H., YAMAMOTO, T., DE STROOPER, B., YAMAMOTO, K. & SUZUKI, T. 2004. Coordinated metabolism of Abeta and amyloid beta-protein precursor regulates FE65-dependent gene transactivation. *J Biol Chem*, 279, 24343-54.
- AREA-GOMEZ, E., DE GROOF, A. J., BOLDOGH, I., BIRD, T. D., GIBSON, G. E., KOEHLER, C. M., YU, W. H., DUFF, K. E., YAFFE, M. P., PON, L. A. & SCHON, E. A. 2009. Presenilins are enriched in endoplasmic reticulum membranes associated with mitochondria. *Am J Pathol*, 175, 1810-6.
- ARENAS, M. & POSADA, D. 2010. The effect of recombination on the reconstruction of ancestral sequences. *Genetics*, 184, 1133-9.
- BARTUS, R. T., DEAN, R. L., 3RD, BEER, B. & LIPPA, A. S. 1982. The cholinergic hypothesis of geriatric memory dysfunction. *Science*, 217, 408-14.
- BEEL, A. J. & SANDERS, C. R. 2008. Substrate specificity of gamma-secretase and other intramembrane proteases. *Cell Mol Life Sci*, 65, 1311-34.
- BEGLEY, J. G., DUAN, W., CHAN, S., DUFF, K. & MATTSON, M. P. 1999. Altered calcium homeostasis and mitochondrial dysfunction in cortical synaptic compartments of presenilin-1 mutant mice. *J Neurochem*, 72, 1030-9.
- BERCHTOLD, N. C. & COTMAN, C. W. 1998. Evolution in the conceptualization of dementia and Alzheimer's disease: Greco-Roman period to the 1960s. *Neurobiol Aging*, 19, 173-89.
- BLOOMFIELD, G., TRAYNOR, D., SANDER, S. P., VELTMAN, D. M., PACHEBAT, J. A. & KAY, R. R. 2015. Neurofibromin controls macropinocytosis and phagocytosis in Dictyostelium. *Elife*, 4.
- BOECKELER, K. & WILLIAMS, R. S. B. 2001. Dictyostelium as a Biomedical Model. eLS. John Wiley & Sons, Ltd.
- BOLOS, V., GREGO-BESSA, J. & DE LA POMPA, J. L. 2007. Notch signaling in development and cancer. *Endocr Rev*, 28, 339-63.

- BONDY, S. C. 2016. Low levels of aluminum can lead to behavioral and morphological changes associated with Alzheimer's disease and age-related neurodegeneration. *Neurotoxicology*, 52, 222-9.
- BORCHELT, D. R., RATOVITSKI, T., VAN LARE, J., LEE, M. K., GONZALES, V., JENKINS, N. A., COPELAND, N. G., PRICE, D. L. & SISODIA, S. S. 1997. Accelerated amyloid deposition in the brains of transgenic mice coexpressing mutant presenilin 1 and amyloid precursor proteins. *Neuron*, 19, 939-45.
- BORCHELT, D. R., THINAKARAN, G., ECKMAN, C. B., LEE, M. K., DAVENPORT, F., RATOVITSKY, T., PRADA, C. M., KIM, G., SEEKINS, S., YAGER, D., SLUNT, H. H., WANG, R., SEEGER, M., LEVEY, A. I., GANDY, S. E., COPELAND, N. G., JENKINS, N. A., PRICE, D. L., YOUNKIN, S. G. & SISODIA, S. S. 1996. Familial Alzheimer's disease-linked presenilin 1 variants elevate A $\beta$ 1-42/1-40 ratio in vitro and in vivo. *Neuron*, 17, 1005-13.
- BUCKLEY, C. M., GOPALDASS, N., BOSMANI, C., JOHNSTON, S. A., SOLDATI, T., INSALL, R. H. & KING, J. S. 2016. WASH drives early recycling from macropinosomes and phagosomes to maintain surface phagocytic receptors. *Proc Natl Acad Sci U S A*, 113, E5906-E5915.
- CALVO-GARRIDO, J. & ESCALANTE, R. 2010. Autophagy dysfunction and ubiquitin-positive protein aggregates in Dictyostelium cells lacking Vmp1. *Autophagy*, 6, 100-9.
- CASTEL, D., MOURIKIS, P., BARTELS, S. J., BRINKMAN, A. B., TAJBAKHS, S. & STUNNENBERG, H. G. 2013. Dynamic binding of RBPJ is determined by Notch signaling status. *Genes Dev*, 27, 1059-71.
- CATALDO, A. M., PETERHOFF, C. M., TRONCOSO, J. C., GOMEZ-ISLA, T., HYMAN, B. T. & NIXON, R. A. 2000. Endocytic pathway abnormalities precede amyloid  $\beta$  deposition in sporadic Alzheimer's disease and Down syndrome: differential effects of APOE genotype and presenilin mutations. *Am J Pathol*, 157, 277-86.
- CHANG, P., ORABI, B., DERANIEH, R. M., DHAM, M., HOELLER, O., SHIMSHONI, J. A., YAGEN, B., BIALER, M., GREENBERG, M. L., WALKER, M. C. & WILLIAMS, R. S. 2012. The antiepileptic drug valproic acid and other medium-chain fatty acids acutely reduce phosphoinositide levels independently of inositol in Dictyostelium. *Dis Model Mech*, 5, 115-24.
- CHAVEZ-GUTIERREZ, L., TOLIA, A., MAES, E., LI, T., WONG, P. C. & DE STROOPER, B. 2008. Glu(332) in the Nicastrin ectodomain is essential for gamma-secretase complex maturation but not for its activity. *J Biol Chem*, 283, 20096-105.
- CHEN, A. C., GUO, L. Y., OSTASZEWSKI, B. L., SELKOE, D. J. & LAVOIE, M. J. 2010. Aph-1 associates directly with full-length and C-terminal fragments of gamma-secretase substrates. *J Biol Chem*, 285, 11378-91.
- CHUBB, J. R., WILKINS, A., THOMAS, G. M. & INSALL, R. H. 2000. The Dictyostelium Ras protein is required for macropinocytosis, phagocytosis and the control of cell movement. *J Cell Sci*, 113 ( Pt 4), 709-19.
- CITRON, M., OLTERSDORF, T., HAASS, C., MCCONLOGUE, L., HUNG, A. Y., SEUBERT, P., VIGO-PELFREY, C., LIEBERBURG, I. & SELKOE, D. J. 1992. Mutation of the beta-amyloid precursor protein in familial Alzheimer's disease increases beta-protein production. *Nature*, 360, 672-4.
- COMMISSO, C., DAVIDSON, S. M., SOYDANER-AZELOGLU, R. G., PARKER, S. J., KAMPHORST, J. J., HACKETT, S., GRABOCKA, E., NOFAL, M., DREBIN, J. A., THOMPSON, C. B., RABINOWITZ, J. D., METALLO, C. M., VANDER HEIDEN, M. G. & BAR-SAGI, D. 2013. Macropinocytosis of protein is an amino acid supply route in Ras-transformed cells. *Nature*, 497, 633-7.
- COSKER, K. E. & SEGAL, R. A. 2014. Neuronal signaling through endocytosis. *Cold Spring Harb Perspect Biol*, 6.
- CUADRADO-TEJEDOR, M. & GARCIA-OSTA, A. 2014. Current animal models of Alzheimer's disease: challenges in translational research. *Front Neurol*, 5, 182.

- DAVIES, L., FARRAR, N. A., SATRE, M., DOTTIN, R. P. & GROSS, J. D. 1996. Vacuolar H(+)-ATPase and weak base action in Dictyostelium. *Mol Microbiol*, 22, 119-26.
- DAVIES, P. & MALONEY, A. J. 1976. Selective loss of central cholinergic neurons in Alzheimer's disease. *Lancet*, 2, 1403.
- DE STROOPER, B. 2003. Aph-1, Pen-2, and Nicastrin with Presenilin generate an active gamma-Secretase complex. *Neuron*, 38, 9-12.
- DE STROOPER, B., ANNAERT, W., CUPERS, P., SAFTIG, P., CRAESSAERTS, K., MUMM, J. S., SCHROETER, E. H., SCHRIJVERS, V., WOLFE, M. S., RAY, W. J., GOATE, A. & KOPAN, R. 1999. A presenilin-1-dependent gamma-secretase-like protease mediates release of Notch intracellular domain. *Nature*, 398, 518-22.
- DE STROOPER, B., IWATSUBO, T. & WOLFE, M. S. 2012. Presenilins and gamma-secretase: structure, function, and role in Alzheimer Disease. *Cold Spring Harb Perspect Med*, 2, a006304.
- DE STROOPER, B., SAFTIG, P., CRAESSAERTS, K., VANDERSTICHELE, H., GUHDE, G., ANNAERT, W., VON FIGURA, K. & VAN LEUVEN, F. 1998. Deficiency of presenilin-1 inhibits the normal cleavage of amyloid precursor protein. *Nature*, 391, 387-90.
- DOBROWOLSKI, R., VICK, P., PLOPER, D., GUMPER, I., SNITKIN, H., SABATINI, D. D. & DE ROBERTIS, E. M. 2012. Presenilin deficiency or lysosomal inhibition enhances Wnt signaling through relocalization of GSK3 to the late-endosomal compartment. *Cell Rep*, 2, 1316-28.
- DRIES, D. R., SHAH, S., HAN, Y. H., YU, C., YU, S., SHEARMAN, M. S. & YU, G. 2009. Glu-333 of nicastrin directly participates in gamma-secretase activity. *J Biol Chem*, 284, 29714-24.
- DUPUIS, M. J. 1988. [Multiple neurologic manifestations of Borrelia burgdorferi infection]. *Rev Neurol (Paris)*, 144, 765-75.
- EICHINGER, L., PACHEBAT, J. A., GLOCKNER, G., RAJANDREAM, M. A., SUCGANG, R., BERRIMAN, M., SONG, J., OLSEN, R., SZAFRANSKI, K., XU, Q., TUNGGAL, B., KUMMERFELD, S., MADERA, M., KONFORTOV, B. A., RIVERO, F., BANKIER, A. T., LEHMANN, R., HAMLIN, N., DAVIES, R., GAUDET, P., FEY, P., PILCHER, K., CHEN, G., SAUNDERS, D., SODERGREN, E., DAVIS, P., KERHORNOU, A., NIE, X., HALL, N., ANJARD, C., HEMPHILL, L., BASON, N., FARBROTHER, P., DESANY, B., JUST, E., MORIO, T., ROST, R., CHURCHER, C., COOPER, J., HAYDOCK, S., VAN DRIESSCHE, N., CRONIN, A., GOODHEAD, I., MUZNY, D., MOURIER, T., PAIN, A., LU, M., HARPER, D., LINDSAY, R., HAUSER, H., JAMES, K., QUILES, M., MADAN BABU, M., SAITO, T., BUCHRIESER, C., WARDROPER, A., FELDER, M., THANGAVELU, M., JOHNSON, D., KNIGHTS, A., LOULSEGED, H., MUNGALL, K., OLIVER, K., PRICE, C., QUAIL, M. A., URUSHIHARA, H., HERNANDEZ, J., RABBINOWITSCH, E., STEFFEN, D., SANDERS, M., MA, J., KOHARA, Y., SHARP, S., SIMMONDS, M., SPIEGLER, S., TIVEY, A., SUGANO, S., WHITE, B., WALKER, D., WOODWARD, J., WINCKLER, T., TANAKA, Y., SHAULSKY, G., SCHLEICHER, M., WEINSTOCK, G., ROSENTHAL, A., COX, E. C., CHISHOLM, R. L., GIBBS, R., LOOMIS, W. F., PLATZER, M., KAY, R. R., WILLIAMS, J., DEAR, P. H., NOEGEL, A. A., BARRELL, B. & KUSPA, A. 2005. The genome of the social amoeba Dictyostelium discoideum. *Nature*, 435, 43-57.
- ESSELENS, C., OORSCHOT, V., BAERT, V., RAEMAEEKERS, T., SPITTAELS, K., SERNEELS, L., ZHENG, H., SAFTIG, P., DE STROOPER, B., KLUMPERMAN, J. & ANNAERT, W. 2004. Presenilin 1 mediates the turnover of telencephalin in hippocampal neurons via an autophagic degradative pathway. *J Cell Biol*, 166, 1041-54.
- EXLEY, C. 2007. Aluminium, tau and Alzheimer's disease. *J Alzheimers Dis*, 12, 313-5; author reply 317-8.
- FAIX, J., KREPPEL, L., SHAULSKY, G., SCHLEICHER, M. & KIMMEL, A. R. 2004. A rapid and efficient method to generate multiple gene disruptions in Dictyostelium discoideum using a single selectable marker and the Cre-loxP system. *Nucleic Acids Res*, 32, e143.

- FASSLER, M., LI, X. & KAETHER, C. 2011. Polar transmembrane-based amino acids in presenilin 1 are involved in endoplasmic reticulum localization, Pen2 protein binding, and gamma-secretase complex stabilization. *J Biol Chem*, 286, 38390-6.
- FELLER, J., SCHNEIDER, A., SCHUSTER-GOSSLER, K. & GOSSLER, A. 2008. Noncyclic Notch activity in the presomitic mesoderm demonstrates uncoupling of somite compartmentalization and boundary formation. *Genes Dev*, 22, 2166-71.
- FISCHER, M., HAASE, I., SIMMETH, E., GERISCH, G. & MULLER-TAUBENBERGER, A. 2004. A brilliant monomeric red fluorescent protein to visualize cytoskeleton dynamics in Dictyostelium. *FEBS Lett*, 577, 227-32.
- FIUZA, U. M. & ARIAS, A. M. 2007. Cell and molecular biology of Notch. *J Endocrinol*, 194, 459-74.
- FRANCIONE, L. M., ANNESLEY, S. J., CARILLA-LATORRE, S., ESCALANTE, R. & FISHER, P. R. 2011. The Dictyostelium model for mitochondrial disease. *Semin Cell Dev Biol*, 22, 120-30.
- FRANCIS, P. T., PALMER, A. M., SNAPE, M. & WILCOCK, G. K. 1999. The cholinergic hypothesis of Alzheimer's disease: a review of progress. *J Neurol Neurosurg Psychiatry*, 66, 137-47.
- FUKUMORI, A., OKOCHI, M., TAGAMI, S., JIANG, J., ITOH, N., NAKAYAMA, T., YANAGIDA, K., ISHIZUKA-KATSURA, Y., MORIHARA, T., KAMINO, K., TANAKA, T., KUDO, T., TANII, H., IKUTA, A., HAASS, C. & TAKEDA, M. 2006. Presenilin-dependent gamma-secretase on plasma membrane and endosomes is functionally distinct. *Biochemistry*, 45, 4907-14.
- GAHLMANN, A. & MOERNER, W. E. 2014. Exploring bacterial cell biology with single-molecule tracking and super-resolution imaging. *Nat Rev Microbiol*, 12, 9-22.
- GAUDET, P., PILCHER, K. E., FEY, P. & CHISHOLM, R. L. 2007. Transformation of Dictyostelium discoideum with plasmid DNA. *Nat Protoc*, 2, 1317-24.
- GHAVAMI, S., SHOJAEI, S., YEGANEH, B., ANDE, S. R., JANGAMREDDY, J. R., MEHRPOUR, M., CHRISTOFFERSSON, J., CHAABANE, W., MOGHADAM, A. R., KASHANI, H. H., HASHEMI, M., OWJI, A. A. & LOS, M. J. 2014. Autophagy and apoptosis dysfunction in neurodegenerative disorders. *Prog Neurobiol*, 112, 24-49.
- GOPALDASS, N., PATEL, D., KRATZKE, R., DIECKMANN, R., HAUSHERR, S., HAGEDORN, M., MONROY, R., KRUGER, J., NEUHAUS, E. M., HOFFMANN, E., HILLE, K., KUZNETSOV, S. A. & SOLDATI, T. 2012. Dynamin A, Myosin IB and Abp1 couple phagosome maturation to F-actin binding. *Traffic*, 13, 120-30.
- GOUJON, M., MCWILLIAM, H., LI, W., VALENTIN, F., SQUIZZATO, S., PAERN, J. & LOPEZ, R. 2010. A new bioinformatics analysis tools framework at EMBL-EBI. *Nucleic Acids Res*, 38, W695-9.
- GOUTTE, C., TSUNOZAKI, M., HALE, V. A. & PRIESS, J. R. 2002. APH-1 is a multipass membrane protein essential for the Notch signaling pathway in Caenorhabditis elegans embryos. *Proc Natl Acad Sci U S A*, 99, 775-9.
- GREGORY, G. C. & HALLIDAY, G. M. 2005. What is the dominant Abeta species in human brain tissue? A review. *Neurotox Res*, 7, 29-41.
- GRUENBERG, J. & MAXFIELD, F. R. 1995. Membrane transport in the endocytic pathway. *Curr Opin Cell Biol*, 7, 552-63.
- GU, Y., CHEN, F., SANJO, N., KAWARAI, T., HASEGAWA, H., DUTHIE, M., LI, W., RUAN, X., LUTHRA, A., MOUNT, H. T., TANDON, A., FRASER, P. E. & ST GEORGE-HYSLOP, P. 2003. APH-1 interacts with mature and immature forms of presenilins and nicastrin and may play a role in maturation of presenilin.nicastrin complexes. *J Biol Chem*, 278, 7374-80.
- HAAPASALO, A. & KOVACS, D. M. 2011. The many substrates of presenilin/gamma-secretase. *J Alzheimers Dis*, 25, 3-28.
- HAASS, C. & SELKOE, D. J. 1993. Cellular processing of beta-amyloid precursor protein and the genesis of amyloid beta-peptide. *Cell*, 75, 1039-42.



- HACKER, U., ALBRECHT, R. & MANIAK, M. 1997. Fluid-phase uptake by macropinocytosis in Dictyostelium. *J Cell Sci*, 110 ( Pt 2), 105-12.
- HAGEDORN, M., NEUHAUS, E. M. & SOLDATI, T. 2006. Optimized fixation and immunofluorescence staining methods for Dictyostelium cells. *Methods Mol Biol*, 346, 327-38.
- HANKS, M., WURST, W., ANSON-CARTWRIGHT, L., AUERBACH, A. B. & JOYNER, A. L. 1995. Rescue of the En-1 mutant phenotype by replacement of En-1 with En-2. *Science*, 269, 679-82.
- HOELLER, O., BOLOURANI, P., CLARK, J., STEPHENS, L. R., HAWKINS, P. T., WEINER, O. D., WEEKS, G. & KAY, R. R. 2013. Two distinct functions for PI3-kinases in macropinocytosis. *J Cell Sci*, 126, 4296-307.
- HOLMES, O., PATURI, S., SELKOE D, J. & WOLFE, M. S. 2014. Pen-2 is essential for  $\gamma$ -secretase complex stability and trafficking but partially dispensable for endoproteolysis. *Biochemistry*.
- HOOPER, C., KILLICK, R. & LOVESTONE, S. 2008. The GSK3 hypothesis of Alzheimer's disease. *J Neurochem*, 104, 1433-9.
- HU, S., BEGUM, A. N., JONES, M. R., OH, M. S., BEECH, W. K., BEECH, B. H., YANG, F., CHEN, P., UBEDA, O. J., KIM, P. C., DAVIES, P., MA, Q., COLE, G. M. & FRAUTSCHY, S. A. 2009. GSK3 inhibitors show benefits in an Alzheimer's disease (AD) model of neurodegeneration but adverse effects in control animals. *Neurobiol Dis*, 33, 193-206.
- HU, Y. B., DAMMER, E. B., REN, R. J. & WANG, G. 2015. The endosomal-lysosomal system: from acidification and cargo sorting to neurodegeneration. *Transl Neurodegener*, 4, 18.
- IJIMA, K., LIU, H. P., CHIANG, A. S., HEARN, S. A., KONSOLAKI, M. & ZHONG, Y. 2004. Dissecting the pathological effects of human Abeta40 and Abeta42 in Drosophila: a potential model for Alzheimer's disease. *Proc Natl Acad Sci U S A*, 101, 6623-8.
- IKEUCHI, T. & SISODIA, S. S. 2003. The Notch ligands, Delta1 and Jagged2, are substrates for presenilin-dependent "gamma-secretase" cleavage. *J Biol Chem*, 278, 7751-4.
- ITTNER, L. M. & GOTZ, J. 2011. Amyloid-beta and tau--a toxic pas de deux in Alzheimer's disease. *Nat Rev Neurosci*, 12, 65-72.
- JANG, W. & GOMER, R. H. 2011. Initial cell type choice in Dictyostelium. *Eukaryot Cell*, 10, 150-5.
- JUTRAS, I., LAPLANTE, A., BOULAIS, J., BRUNET, S., THINAKARAN, G. & DESJARDINS, M. 2005. Gamma-secretase is a functional component of phagosomes. *J Biol Chem*, 280, 36310-7.
- KANDIMALLA, R., VALLAMKONDU, J., CORGIAT, E. B. & GILL, K. D. 2016. Understanding Aspects of Aluminum Exposure in Alzheimer's Disease Development. *Brain Pathol*, 26, 139-54.
- KANG, D. E., SORIANO, S., FROSCH, M. P., COLLINS, T., NARUSE, S., SISODIA, S. S., LEIBOWITZ, G., LEVINE, F. & KOO, E. H. 1999. Presenilin 1 facilitates the constitutive turnover of beta-catenin: differential activity of Alzheimer's disease-linked PS1 mutants in the beta-catenin-signaling pathway. *J Neurosci*, 19, 4229-37.
- KASTENHOLZ, B., GARFIN, D. E., HORST, J. & NAGEL, K. A. 2009. Plant metal chaperones: a novel perspective in dementia therapy. *Amyloid*, 16, 81-3.
- KELLER, J. N., GUO, Q., HOLTSBERG, F. W., BRUCE-KELLER, A. J. & MATTSON, M. P. 1998. Increased sensitivity to mitochondrial toxin-induced apoptosis in neural cells expressing mutant presenilin-1 is linked to perturbed calcium homeostasis and enhanced oxyradical production. *J Neurosci*, 18, 4439-50.
- KHANDELWAL, A., CHANDU, D., ROE, C. M., KOPAN, R. & QUATRANO, R. S. 2007. Moonlighting activity of presenilin in plants is independent of gamma-secretase and evolutionarily conserved. *Proc Natl Acad Sci U S A*, 104, 13337-42.

- KING, J. S., GUEHO, A., HAGEDORN, M., GOPALDASS, N., LEUBA, F., SOLDATI, T. & INSALL, R. H. 2013. WASH is required for lysosomal recycling and efficient autophagic and phagocytic digestion. *Mol Biol Cell*, 24, 2714-26.
- KING, J. S., TEO, R., RYVES, J., REDDY, J. V., PETERS, O., ORABI, B., HOELLER, O., WILLIAMS, R. S. & HARWOOD, A. J. 2009. The mood stabiliser lithium suppresses PIP3 signalling in Dictyostelium and human cells. *Dis Model Mech*, 2, 306-12.
- KING, J. S., VELTMAN, D. M. & INSALL, R. H. 2011. The induction of autophagy by mechanical stress. *Autophagy*, 7, 1490-9.
- KROGH, A., LARSSON, B., VON HEIJNE, G. & SONNHAMMER, E. L. 2001. Predicting transmembrane protein topology with a hidden Markov model: application to complete genomes. *J Mol Biol*, 305, 567-80.
- KUMAR, S., NEI, M., DUDLEY, J. & TAMURA, K. 2008. MEGA: a biologist-centric software for evolutionary analysis of DNA and protein sequences. *Brief Bioinform*, 9, 299-306.
- LEE, H. G., CASADESUS, G., ZHU, X., TAKEDA, A., PERRY, G. & SMITH, M. A. 2004a. Challenging the amyloid cascade hypothesis: senile plaques and amyloid-beta as protective adaptations to Alzheimer disease. *Ann N Y Acad Sci*, 1019, 1-4.
- LEE, J. H., MCBRAYER, M. K., WOLFE, D. M., HASLETT, L. J., KUMAR, A., SATO, Y., LIE, P. P., MOHAN, P., COFFEY, E. E., KOMPPELLA, U., MITCHELL, C. H., LLOYD-EVANS, E. & NIXON, R. A. 2015. Presenilin 1 Maintains Lysosomal Ca(2+) Homeostasis via TRPML1 by Regulating vATPase-Mediated Lysosome Acidification. *Cell Rep*, 12, 1430-44.
- LEE, J. H., YU, W. H., KUMAR, A., LEE, S., MOHAN, P. S., PETERHOFF, C. M., WOLFE, D. M., MARTINEZ-VICENTE, M., MASSEY, A. C., SOVAK, G., UCHIYAMA, Y., WESTAWAY, D., CUERVO, A. M. & NIXON, R. A. 2010. Lysosomal proteolysis and autophagy require presenilin 1 and are disrupted by Alzheimer-related PS1 mutations. *Cell*, 141, 1146-58.
- LEE, S. F., SHAH, S., LI, H., YU, C., HAN, W. & YU, G. 2002. Mammalian APH-1 interacts with presenilin and nicastrin and is required for intramembrane proteolysis of amyloid-beta precursor protein and Notch. *J Biol Chem*, 277, 45013-9.
- LEE, S. F., SHAH, S., YU, C., WIGLEY, W. C., LI, H., LIM, M., PEDERSEN, K., HAN, W., THOMAS, P., LUNDKVIST, J., HAO, Y. H. & YU, G. 2004b. A conserved GXXXG motif in APH-1 is critical for assembly and activity of the gamma-secretase complex. *J Biol Chem*, 279, 4144-52.
- LEE, S. H., SHARMA, M., SUDHOF, T. C. & SHEN, J. 2014. Synaptic function of nicastrin in hippocampal neurons. *Proc Natl Acad Sci U S A*, 111, 8973-8.
- LEVI, S., POLYAKOV, M. & EGELHOFF, T. T. 2000. Green fluorescent protein and epitope tag fusion vectors for Dictyostelium discoideum. *Plasmid*, 44, 231-8.
- LEVITAN, D. & GREENWALD, I. 1995. Facilitation of lin-12-mediated signalling by sel-12, a Caenorhabditis elegans S182 Alzheimer's disease gene. *Nature*, 377, 351-4.
- LEVY-LAHAD, E., WIJSMAN, E. M., NEMENS, E., ANDERSON, L., GODDARD, K. A., WEBER, J. L., BIRD, T. D. & SCHELLENBERG, G. D. 1995. A familial Alzheimer's disease locus on chromosome 1. *Science*, 269, 970-3.
- LIDSKY, T. I. 2014. Is the Aluminum Hypothesis dead? *J Occup Environ Med*, 56, S73-9.
- LIM, A., MOUSSAVI NIK, S. H., EBRAHIMIE, E. & LARDELLI, M. 2015. Analysis of nicastrin gene phylogeny and expression in zebrafish. *Dev Genes Evol*, 225, 171-8.
- LINGGI, B., CHENG, Q. C., RAO, A. R. & CARPENTER, G. 2006. The ErbB-4 s80 intracellular domain is a constitutively active tyrosine kinase. *Oncogene*, 25, 160-3.
- LUDTMANN, M. H., OTTO, G. P., SCHILDE, C., CHEN, Z. H., ALLAN, C. Y., BRACE, S., BEESLEY, P. W., KIMMEL, A. R., FISHER, P., KILLICK, R. & WILLIAMS, R. S. 2014. An ancestral non-proteolytic role for presenilin proteins in multicellular development of the social amoeba Dictyostelium discoideum. *J Cell Sci*, 127.
- LUO, W. J., WANG, H., LI, H., KIM, B. S., SHAH, S., LEE, H. J., THINAKARAN, G., KIM, T. W., YU, G. & XU, H. 2003. PEN-2 and APH-1 coordinately regulate proteolytic processing of presenilin 1. *J Biol Chem*, 278, 7850-4.

- LUZIO, J. P., ROUS, B. A., BRIGHT, N. A., PRYOR, P. R., MULLOCK, B. M. & PIPER, R. C. 2000. Lysosome-endosome fusion and lysosome biogenesis. *J Cell Sci*, 113 ( Pt 9), 1515-24.
- MA, G., LI, T., PRICE, D. L. & WONG, P. C. 2005. A $\beta$ 1 is the principal mammalian A $\beta$ 1 isoform present in gamma-secretase complexes during embryonic development. *J Neurosci*, 25, 192-8.
- MACDONALD, A. B. 1986. Borrelia in the brains of patients dying with dementia. *JAMA*, 256, 2195-6.
- MACDONALD, A. B. 2006. Spirochetal cyst forms in neurodegenerative disorders,...hiding in plain sight. *Med Hypotheses*, 67, 819-32.
- MACWILLIAMS, H. K. & BONNER, J. T. 1979. The prestalk-prespore pattern in cellular slime molds. *Differentiation*, 14, 1-22.
- MAJDAN, M., LACHANCE, C., GLOSTER, A., ALOYZ, R., ZEINDLER, C., BAMJI, S., BHAKAR, A., BELLIVEAU, D., FAWCETT, J., MILLER, F. D. & BARKER, P. A. 1997. Transgenic mice expressing the intracellular domain of the p75 neurotrophin receptor undergo neuronal apoptosis. *J Neurosci*, 17, 6988-98.
- MAO, G., CUI, M. Z., LI, T., JIN, Y. & XU, X. 2012. Pen-2 is dispensable for endoproteolysis of presenilin 1, and nicastrin-A $\beta$  subcomplex is important for both gamma-secretase assembly and substrate recruitment. *J Neurochem*, 123, 837-44.
- MARAMBAUD, P., SHIOI, J., SERBAN, G., GEORGAKOPOULOS, A., SARNER, S., NAGY, V., BAKI, L., WEN, P., EFTHIMIOPOULOS, S., SHAO, Z., WISNIEWSKI, T. & ROBAKIS, N. K. 2002. A presenilin-1/gamma-secretase cleavage releases the E-cadherin intracellular domain and regulates disassembly of adherens junctions. *EMBO J*, 21, 1948-56.
- MARTENS, H., NOVOTNY, J., OBERSTRASS, J., STECK, T. L., POSTLETHWAIT, P. & NELLEN, W. 2002. RNAi in Dictyostelium: the role of RNA-directed RNA polymerases and double-stranded RNase. *Mol Biol Cell*, 13, 445-53.
- MARTORANA, A., ESPOSITO, Z. & KOCH, G. 2010. Beyond the cholinergic hypothesis: do current drugs work in Alzheimer's disease? *CNS Neurosci Ther*, 16, 235-45.
- MATEO, I., INFANTE, J., LLORCA, J., RODRIGUEZ, E., BERCIANO, J. & COMBARROS, O. 2006. Association between glycogen synthase kinase-3 $\beta$  genetic polymorphism and late-onset Alzheimer's disease. *Dement Geriatr Cogn Disord*, 21, 228-32.
- MCMAINS, V. C., LIAO, X. H. & KIMMEL, A. R. 2008. Oscillatory signaling and network responses during the development of Dictyostelium discoideum. *Ageing Res Rev*, 7, 234-48.
- MCMAINS, V. C., MYRE, M., KREPPEL, L. & KIMMEL, A. R. 2010. Dictyostelium possesses highly diverged presenilin/gamma-secretase that regulates growth and cell-fate specification and can accurately process human APP: a system for functional studies of the presenilin/gamma-secretase complex. *Dis Model Mech*, 3, 581-94.
- MECKLER, X., ROSEMAN, J., DAS, P., CHENG, H., PEI, S., KEAT, M., KASSARIAN, B., GOLDE, T. E., PARENT, A. T. & THINAKARAN, G. 2010. Reduced Alzheimer's disease ss-amyloid deposition in transgenic mice expressing S-palmitoylation-deficient A $\beta$ 1 and nicastrin. *J Neurosci*, 30, 16160-9.
- MENZIES, F. M., FLEMING, A. & RUBINSZTEIN, D. C. 2015. Compromised autophagy and neurodegenerative diseases. *Nat Rev Neurosci*, 16, 345-57.
- MIKLOSSY, J. 1993. Alzheimer's disease--a spirochetosis? *Neuroreport*, 4, 1069.
- MIKLOSSY, J. 2011. Alzheimer's disease - a neurospirochetosis. Analysis of the evidence following Koch's and Hill's criteria. *J Neuroinflammation*, 8, 90.
- MIZUSHIMA, N., OHSUMI, Y. & YOSHIMORI, T. 2002. Autophagosome formation in mammalian cells. *Cell Struct Funct*, 27, 421-9.
- MULLER-TAUBENBERGER, A., LUPAS, A. N., LI, H., ECKE, M., SIMMETH, E. & GERISCH, G. 2001. Calreticulin and calnexin in the endoplasmic reticulum are important for phagocytosis. *EMBO J*, 20, 6772-82.

- MUNN, A. L. & RIEZMAN, H. 1994. Endocytosis is required for the growth of vacuolar H(+)-ATPase-defective yeast: identification of six new END genes. *J Cell Biol*, 127, 373-86.
- MURAYAMA, M., TANAKA, S., PALACINO, J., MURAYAMA, O., HONDA, T., SUN, X., YASUTAKE, K., NIHONMATSU, N., WOLOZIN, B. & TAKASHIMA, A. 1998. Direct association of presenilin-1 with beta-catenin. *FEBS Lett*, 433, 73-7.
- NEELY, K. M., GREEN, K. N. & LAFERLA, F. M. 2011. Presenilin is necessary for efficient proteolysis through the autophagy-lysosome system in a gamma-secretase-independent manner. *J Neurosci*, 31, 2781-91.
- NELLEN, W., SILAN, C. & FIRTEL, R. A. 1984. DNA-mediated transformation in Dictyostelium discoideum: regulated expression of an actin gene fusion. *Mol Cell Biol*, 4, 2890-8.
- NI, C. Y., MURPHY, M. P., GOLDE, T. E. & CARPENTER, G. 2001. gamma-Secretase cleavage and nuclear localization of ErbB-4 receptor tyrosine kinase. *Science*, 294, 2179-81.
- NIIMURA, M., ISOO, N., TAKASUGI, N., TSURUOKA, M., UI-TEI, K., SAIGO, K., MOROHASHI, Y., TOMITA, T. & IWATSUBO, T. 2005. Aph-1 contributes to the stabilization and trafficking of the gamma-secretase complex through mechanisms involving intermolecular and intramolecular interactions. *J Biol Chem*, 280, 12967-75.
- NUNAN, J. & SMALL, D. H. 2000. Regulation of APP cleavage by alpha-, beta- and gamma-secretases. *FEBS Lett*, 483, 6-10.
- NYABI, O., BENTAHIR, M., HORRE, K., HERREMAN, A., GOTTARDI-LITTELL, N., VAN BROECKHOVEN, C., MERCHERS, P., SPITTAELS, K., ANNAERT, W. & DE STROOPER, B. 2003. Presenilins mutated at Asp-257 or Asp-385 restore Pen-2 expression and Nicastrin glycosylation but remain catalytically inactive in the absence of wild type Presenilin. *J Biol Chem*, 278, 43430-6.
- OKAMOTO, I., KAWANO, Y., MURAKAMI, D., SASAYAMA, T., ARAKI, N., MIKI, T., WONG, A. J. & SAYA, H. 2001. Proteolytic release of CD44 intracellular domain and its role in the CD44 signaling pathway. *J Cell Biol*, 155, 755-62.
- OTOMO, A., KUNITA, R., SUZUKI-UTSUNOMIYA, K., MIZUMURA, H., ONOE, K., OSUGA, H., HADANO, S. & IKEDA, J. E. 2008. ALS2/alsin deficiency in neurons leads to mild defects in macropinocytosis and axonal growth. *Biochem Biophys Res Commun*, 370, 87-92.
- OTTO, G. P., SHARMA, D. & WILLIAMS, R. S. 2016. Non-Catalytic Roles of Presenilin Throughout Evolution. *J Alzheimers Dis*, 52, 1177-87.
- OTTO, G. P., WU, M. Y., KAZGAN, N., ANDERSON, O. R. & KESSIN, R. H. 2004. Dictyostelium macroautophagy mutants vary in the severity of their developmental defects. *J Biol Chem*, 279, 15621-9.
- PARKS, A. L. & CURTIS, D. 2007. Presenilin diversifies its portfolio. *Trends Genet*, 23, 140-50.
- PASQUIER, C., PROMPONAS, V. J., PALAIOS, G. A., HAMODRAKAS, J. S. & HAMODRAKAS, S. J. 1999. A novel method for predicting transmembrane segments in proteins based on a statistical analysis of the SwissProt database: the PRED-TMR algorithm. *Protein Eng*, 12, 381-5.
- PERRY, E. K., TOMLINSON, B. E., BLESSED, G., BERGMANN, K., GIBSON, P. H. & PERRY, R. H. 1978. Correlation of cholinergic abnormalities with senile plaques and mental test scores in senile dementia. *Br Med J*, 2, 1457-9.
- PHILIPPE, H., ZHOU, Y., BRINKMANN, H., RODRIGUE, N. & DELSUC, F. 2005. Heterotachy and long-branch attraction in phylogenetics. *BMC Evol Biol*, 5, 50.
- PHINNEY, A. L., CALHOUN, M. E., WOLFER, D. P., LIPP, H. P., ZHENG, H. & JUCKER, M. 1999. No hippocampal neuron or synaptic bouton loss in learning-impaired aged beta-amyloid precursor protein-null mice. *Neuroscience*, 90, 1207-16.
- PRILLER, C., BAUER, T., MITTEREGGER, G., KREBS, B., KRETZSCHMAR, H. A. & HERMS, J. 2006. Synapse formation and function is modulated by the amyloid precursor protein. *J Neurosci*, 26, 7212-21.

- PRINCE, M., KNAPP, M., GUERCHET, M., MCCRONE, P., PRINA, M., COMAS-HERRERA, A., WITTENBERG, R., ADELAJA, B., HU, B., KING, D., REHILL, A. & SALIMKUMAR, D. 2014. Dementia UK Update. [alzheimers.org.uk/dementiauk](http://alzheimers.org.uk/dementiauk): Alzheimer's Society.
- PROKOP, S., HAASS, C. & STEINER, H. 2005. Length and overall sequence of the PEN-2 C-terminal domain determines its function in the stabilization of presenilin fragments. *J Neurochem*, 94, 57-62.
- RAPER, K. B. 1935. Dictyostelium discoideum, a new species of slime mold from decaying forest leaves. *J. Agr. Res*, 50, 135-147.
- REBECK, G. W., REITER, J. S., STRICKLAND, D. K. & HYMAN, B. T. 1993. Apolipoprotein E in sporadic Alzheimer's disease: allelic variation and receptor interactions. *Neuron*, 11, 575-80.
- REISBERG, B., FRANSSEN, E. H., HASAN, S. M., MONTEIRO, I., BOKSAY, I., SOUREN, L. E., KENOWSKY, S., AUER, S. R., ELAHI, S. & KLUGER, A. 1999a. Retrogenesis: clinical, physiologic, and pathologic mechanisms in brain aging, Alzheimer's and other dementing processes. *Eur Arch Psychiatry Clin Neurosci*, 249 Suppl 3, 28-36.
- REISBERG, B., KENOWSKY, S., FRANSSEN, E. H., AUER, S. R. & SOUREN, L. E. 1999b. Towards a science of Alzheimer's disease management: a model based upon current knowledge of retrogenesis. *Int Psychogeriatr*, 11, 7-23.
- RIVIERE, G. R., RIVIERE, K. H. & SMITH, K. S. 2002. Molecular and immunological evidence of oral Treponema in the human brain and their association with Alzheimer's disease. *Oral Microbiol Immunol*, 17, 113-8.
- RODELLA, L. F., RICCI, F., BORSANI, E., STACCHIOTTI, A., FOGLIO, E., FAVERO, G., REZZANI, R., MARIANI, C. & BIANCHI, R. 2008. Aluminium exposure induces Alzheimer's disease-like histopathological alterations in mouse brain. *Histol Histopathol*, 23, 433-9.
- SANTIBANEZ, M., BOLUMAR, F. & GARCIA, A. M. 2007. Occupational risk factors in Alzheimer's disease: a review assessing the quality of published epidemiological studies. *Occup Environ Med*, 64, 723-32.
- SARASIJA, S. & NORMAN, K. R. 2015. A gamma-Secretase Independent Role for Presenilin in Calcium Homeostasis Impacts Mitochondrial Function and Morphology in Caenorhabditis elegans. *Genetics*, 201, 1453-66.
- SASAKI, A. T., JANETOPOULOS, C., LEE, S., CHAREST, P. G., TAKEDA, K., SUNDHEIMER, L. W., MEILI, R., DEVREOTES, P. N. & FIRTEL, R. A. 2007. G protein-independent Ras/PI3K/F-actin circuit regulates basic cell motility. *J Cell Biol*, 178, 185-91.
- SATTLER, N., MONROY, R. & SOLDATI, T. 2013. Quantitative analysis of phagocytosis and phagosome maturation. *Methods Mol Biol*, 983, 383-402.
- SAUNDERS, A. M., STRITTMATTER, W. J., SCHMECHEL, D., GEORGE-HYSLOP, P. H., PERICAK-VANCE, M. A., JOO, S. H., ROSI, B. L., GUSELLA, J. F., CRAPPER-MACLACHLAN, D. R., ALBERTS, M. J. & ET AL. 1993. Association of apolipoprotein E allele epsilon 4 with late-onset familial and sporadic Alzheimer's disease. *Neurology*, 43, 1467-72.
- SCHAEFFER, S., LE DOZE, F., DE LA SAYETTE, V., BERTRAN, F. & VIADER, F. 1994. [Dementia in Lyme disease]. *Presse Med*, 23, 861.
- SCHEUNER, D., ECKMAN, C., JENSEN, M., SONG, X., CITRON, M., SUZUKI, N., BIRD, T. D., HARDY, J., HUTTON, M., KUKULL, W., LARSON, E., LEVY-LAHAD, E., VIITANEN, M., PESKIND, E., POORKAJ, P., SCHELLENBERG, G., TANZI, R., WASCO, W., LANNFELT, L., SELKOE, D. & YOUNKIN, S. 1996. Secreted amyloid beta-protein similar to that in the senile plaques of Alzheimer's disease is increased in vivo by the presenilin 1 and 2 and APP mutations linked to familial Alzheimer's disease. *Nat Med*, 2, 864-70.
- SCHINDELIN, J., ARGANDA-CARRERAS, I., FRISE, E., KAYNIG, V., LONGAIR, M., PIETZSCH, T., PREIBISCH, S., RUEDEN, C., SAALFELD, S., SCHMID, B., TINEVEZ, J. Y., WHITE, D. J., HARTENSTEIN, V., ELICEIRI, K., TOMANCAK, P. & CARDONA, A. 2012. Fiji: an open-source platform for biological-image analysis. *Nat Methods*, 9, 676-82.

- SCHON, E. A. & AREA-GOMEZ, E. 2010. Is Alzheimer's disease a disorder of mitochondria-associated membranes? *J Alzheimers Dis*, 20 Suppl 2, S281-92.
- SCHROETER, E. H., KISSLINGER, J. A. & KOPAN, R. 1998. Notch-1 signalling requires ligand-induced proteolytic release of intracellular domain. *Nature*, 393, 382-6.
- SERNEELS, L., DEJAEGERE, T., CRAESSAERTS, K., HORRE, K., JORISSEN, E., TOUSSEYN, T., HEBERT, S., COOLEN, M., MARTENS, G., ZWIJSEN, A., ANNAERT, W., HARTMANN, D. & DE STROOPER, B. 2005. Differential contribution of the three Aph1 genes to gamma-secretase activity in vivo. *Proc Natl Acad Sci U S A*, 102, 1719-24.
- SHAH, S., LEE, S. F., TABUCHI, K., HAO, Y. H., YU, C., LAPLANT, Q., BALL, H., DANN, C. E., 3RD, SUDHOF, T. & YU, G. 2005. Nicastrin functions as a gamma-secretase-substrate receptor. *Cell*, 122, 435-47.
- SHAWBER, C., NOFZIGER, D., HSIEH, J. J., LINDSELL, C., BOGLER, O., HAYWARD, D. & WEINMASTER, G. 1996. Notch signaling inhibits muscle cell differentiation through a CBF1-independent pathway. *Development*, 122, 3765-73.
- SHERRINGTON, R., ROGAEV, E. I., LIANG, Y., ROGAEVA, E. A., LEVESQUE, G., IKEDA, M., CHI, H., LIN, C., LI, G., HOLMAN, K., TSUDA, T., MAR, L., FONCIN, J. F., BRUNI, A. C., MONTESI, M. P., SORBI, S., RAINERO, I., PINESSI, L., NEE, L., CHUMAKOV, I., POLLEN, D., BROOKES, A., SANSEAU, P., POLINSKY, R. J., WASCO, W., DA SILVA, H. A., HAINES, J. L., PERKICAK-VANCE, M. A., TANZI, R. E., ROSES, A. D., FRASER, P. E., ROMMENS, J. M. & ST GEORGE-HYSLOP, P. H. 1995. Cloning of a gene bearing missense mutations in early-onset familial Alzheimer's disease. *Nature*, 375, 754-60.
- SMOLARKIEWICZ, M., SKRZYPCZAK, T. & WOJTASZEK, P. 2013. The very many faces of presenilins and the gamma-secretase complex. *Protoplasma*, 250, 997-1011.
- STROOPER, D. 2003. Aph-1, Pen-2, and Nicastrin with Presenilin generate an active gamma-Secretase complex. *Neuron*, 38, 9-12.
- SU, B., WANG, X., NUNOMURA, A., MOREIRA, P. I., LEE, H. G., PERRY, G., SMITH, M. A. & ZHU, X. 2008. Oxidative stress signaling in Alzheimer's disease. *Curr Alzheimer Res*, 5, 525-32.
- TAKASUGI, N., TOMITA, T., HAYASHI, I., TSURUOKA, M., NIIMURA, M., TAKAHASHI, Y., THINAKARAN, G. & IWATSUBO, T. 2003. The role of presenilin cofactors in the gamma-secretase complex. *Nature*, 422, 438-41.
- TAMBOLI, I. Y., PRAGER, K., THAL, D. R., THELEN, K. M., DEWACHTER, I., PIETRZIK, C. U., ST GEORGE-HYSLOP, P., SISODIA, S. S., DE STROOPER, B., HENKA, M. T., FILIPPOV, M. A., MULLER, U., VAN LEUVEN, F., LUTJOHANN, D. & WALTER, J. 2008. Loss of gamma-secretase function impairs endocytosis of lipoprotein particles and membrane cholesterol homeostasis. *J Neurosci*, 28, 12097-106.
- TANZI, R. E. 2005. The synaptic Abeta hypothesis of Alzheimer disease. *Nat Neurosci*, 8, 977-9.
- TERBACH, N., SHAH, R., KELEMEN, R., KLEIN, P. S., GORDIENKO, D., BROWN, N. A., WILKINSON, C. J. & WILLIAMS, R. S. 2011. Identifying an uptake mechanism for the antiepileptic and bipolar disorder treatment valproic acid using the simple biomedical model Dictyostelium. *J Cell Sci*, 124, 2267-76.
- THE UNIPROT, C. 2017. UniProt: the universal protein knowledgebase. *Nucleic Acids Res*, 45, D158-D169.
- TROJANOWSKI, J. Q. & LEE, V. M. 2005. Pathological tau: a loss of normal function or a gain in toxicity? *Nat Neurosci*, 8, 1136-7.
- UPADHYAY, S. & SHAW, B. D. 2008. The role of actin, fimbrin and endocytosis in growth of hyphae in *Aspergillus nidulans*. *Mol Microbiol*, 68, 690-705.
- VELTMAN, D. M., AKAR, G., BOSGRAAF, L. & VAN HAASTERT, P. J. 2009. A new set of small, extrachromosomal expression vectors for Dictyostelium discoideum. *Plasmid*, 61, 110-8.

- VINET, A. F., FIEDLER, T., STUDER, V., FROQUET, R., DARDEL, A., COSSON, P. & PIETERS, J. 2014. Initiation of multicellular differentiation in Dictyostelium discoideum is regulated by coronin A. *Mol Biol Cell*, 25, 688-701.
- WILLIAMS, R. S., BOECKELER, K., GRAF, R., MULLER-TAUBENBERGER, A., LI, Z., ISBERG, R. R., WESSELS, D., SOLL, D. R., ALEXANDER, H. & ALEXANDER, S. 2006. Towards a molecular understanding of human diseases using Dictyostelium discoideum. *Trends Mol Med*, 12, 415-24.
- WOESE, C. R. 2002. On the evolution of cells. *Proc Natl Acad Sci U S A*, 99, 8742-7.
- WOLFE, D. M., LEE, J. H., KUMAR, A., LEE, S., ORENSTEIN, S. J. & NIXON, R. A. 2013. Autophagy failure in Alzheimer's disease and the role of defective lysosomal acidification. *Eur J Neurosci*, 37, 1949-61.
- WOLFE, M. S., XIA, W., OSTASZEWSKI, B. L., DIEHL, T. S., KIMBERLY, W. T. & SELKOE, D. J. 1999. Two transmembrane aspartates in presenilin-1 required for presenilin endoproteolysis and gamma-secretase activity. *Nature*, 398, 513-7.
- WONG, C. C., TRAYNOR, D., BASSE, N., KAY, R. R. & WARREN, A. J. 2011. Defective ribosome assembly in Shwachman-Diamond syndrome. *Blood*, 118, 4305-12.
- XIA, W., ZHANG, J., OSTASZEWSKI, B. L., KIMBERLY, W. T., SEUBERT, P., KOO, E. H., SHEN, J. & SELKOE, D. J. 1998. Presenilin 1 regulates the processing of beta-amyloid precursor protein C-terminal fragments and the generation of amyloid beta-protein in endoplasmic reticulum and Golgi. *Biochemistry*, 37, 16465-71.
- XIONG, Q., UNAL, C., MATTHIAS, J., STEINERT, M. & EICHINGER, L. 2015. The phenotypes of ATG9, ATG16 and ATG9/16 knock-out mutants imply autophagy-dependent and -independent functions. *Open Biol*, 5, 150008.
- XU, H., FINKELSTEIN, D. I. & ADLARD, P. A. 2014. Interactions of metals and Apolipoprotein E in Alzheimer's disease. *Front Aging Neurosci*, 6, 121.
- YU, G., NISHIMURA, M., ARAWAKA, S., LEVITAN, D., ZHANG, L., TANDON, A., SONG, Y. Q., ROGAEVA, E., CHEN, F., KAWARAI, T., SUPALA, A., LEVESQUE, L., YU, H., YANG, D. S., HOLMES, E., MILMAN, P., LIANG, Y., ZHANG, D. M., XU, D. H., SATO, C., ROGAEV, E., SMITH, M., JANUS, C., ZHANG, Y., AEBERSOLD, R., FARRER, L. S., SORBI, S., BRUNI, A., FRASER, P. & ST GEORGE-HYSLOP, P. 2000. Nicastrin modulates presenilin-mediated notch/glp-1 signal transduction and betaAPP processing. *Nature*, 407, 48-54.
- ZHANG, M., HAAPASALO, A., KIM, D. Y., INGANO, L. A., PETTINGELL, W. H. & KOVACS, D. M. 2006. Presenilin/gamma-secretase activity regulates protein clearance from the endocytic recycling compartment. *FASEB J*, 20, 1176-8.
- ZHANG, Y. W., THOMPSON, R., ZHANG, H. & XU, H. 2011. APP processing in Alzheimer's disease. *Mol Brain*, 4, 3.
- ZHANG, Z., HARTMANN, H., DO, V. M., ABRAMOWSKI, D., STURCHLER-PIERRAT, C., STAUFENBIEL, M., SOMMER, B., VAN DE WETERING, M., CLEVERS, H., SAFTIG, P., DE STROOPER, B., HE, X. & YANKNER, B. A. 1998. Destabilization of beta-catenin by mutations in presenilin-1 potentiates neuronal apoptosis. *Nature*, 395, 698-702.
- ZHANG, Z., NADEAU, P., SONG, W., DONOVIEL, D., YUAN, M., BERNSTEIN, A. & YANKNER, B. A. 2000. Presenilins are required for gamma-secretase cleavage of beta-APP and transmembrane cleavage of Notch-1. *Nat Cell Biol*, 2, 463-5.
- ZHAO, G., LIU, Z., ILAGAN, M. X. & KOPAN, R. 2010. Gamma-secretase composed of PS1/Pen2/Aph1a can cleave notch and amyloid precursor protein in the absence of nicastrin. *J Neurosci*, 30, 1648-56.

## Appendices

---



```

H.sapiens_Aph-1a      MGAAVFEGCTFVAFGAFALFLITVAGDPLRVIIILVAGAFFWVMSLLLASVVMFVLHVHT 60
M.musculus_Aph-1a    MGAAVFEGCTFVAFGAFSLFLITVAGDPLRVIIILVAGAFFWVMSLLLASVVMFVLHVHT 60
X.tropicalis_Aph-1   MALAVFEGCTFVAFGAFSLFLITIAVDPLKVIIILVAGSFFWVMSLLSLIMFISVQIS 60
M.musculus_Aph-1b    MTAAVFEGCAFIAFGAFALALVFTTATDPLRVIFLIAGAFFWVMSLLSSVFMFLVRVIT 60
M.musculus_Aph-1c    MTLPVFEGCAFIAFGAFALYLFITATDPLRVIFLIAGAFFWVMSLLSSMFMFLVRVIT 60
H.sapiens_Aph-1b     MTAAVFEGCAFIAFGAFALYVFTTATEPLRIIFLIAGAFFWVMSLLISSLVFMFARVII 60
D.melanogaster_Aph-1 MTLPEFEGCTFIAFGFPFALVFVTTIANDPVRIIILIAAAFFWVMSLLISS-LWYALIPLK 59
C.sinesis_Aph-1      MTLGGFGGCGALIGLGCISLFLVLTACDPLKVIVLTAGGFFWVMSLLLTSLFVLAFFSSVL 60
A.thaliana_Aph-1     MTVAAGIGYALVALGSLSLFVSVISRKPFILITVLSSTLLWVMSLLIILSGLRPFPLPK 60
P.patens_Aph-1       MGVVVGIGYFLIALGHALTIFSSIAKPKPFLTLTVLASALIYLVSLVAAAIIRAFPLGP 60
D.discoideum_Aph-1   MTQVLFYSCLFITFSEILAFFFMVIAKNSQLVILTIGGSFFWVMSILIAAIWYIIPPMR 60
*      *      : : : * : : : : : : : : : : : : : : : *

H.sapiens_Aph-1a      DRSDARLQYGLLIFGAAVSMLIQEVEFRFAYYKLLKK----- 96
M.musculus_Aph-1a    DRSDARLQYGLLIFGAAVSMLIQEVEFRFAYYKLLKK----- 96
X.tropicalis_Aph-1   NKNDANLQYGLLIFGAAVSMLIQEVEFRFAYYKLLKK----- 96
M.musculus_Aph-1b    DNRDGPVQNYLLIFGVLLSVCIQELFRLAYYKLLKK----- 96
M.musculus_Aph-1c    NNRDESQVNYLLIFGALLSVCIQELFRLAYYKLLKK----- 96
H.sapiens_Aph-1b     DNKDGPQKYLLIFGAFVSVYIQEMFRFAYYKLLKK----- 96
D.melanogaster_Aph-1 E-----FLAFGVVFSVCEQEAFFYIIRILRS----- 86
C.sinesis_Aph-1      SN-----LALSFLVAVASQELLRFAFFKLIIL----- 87
A.thaliana_Aph-1     AN-----VWWPYALLVITSVCEGLRFLFWKVYKR----- 91
P.patens_Aph-1       S-----WVFLMLLATAVFIQEVTRIFVWRFFLK----- 88
D.discoideum_Aph-1   EH-----WWFIISFSMLIQEIFSYIFRFLYSYGFNDRPSLNQIKETQHQMALDSMR 111
:      :      *      *      *      *      : :

H.sapiens_Aph-1a      -----ADEGLASLSEDGRSPIS----- 113
M.musculus_Aph-1a    -----ADEGLASLSEDGRSPIS----- 113
X.tropicalis_Aph-1   -----ADEGLATISEDGRSPIS----- 113
M.musculus_Aph-1b    -----ASEGLKSINPEE-TAPS----- 112
M.musculus_Aph-1c    -----ASEGLKSINPEEDIAPS----- 113
H.sapiens_Aph-1b     -----ASEGLKSINPGE-TAPS----- 112
D.melanogaster_Aph-1 -----TEQGLHAVAEDTRVTDN----- 103
C.sinesis_Aph-1      -----ADNGLRVIAISAQTPVAPVVATRPPTGQPTDGLSNTAALR 127
A.thaliana_Aph-1     -----LEDVLSDFADRI SRPRLFLT----- 111
P.patens_Aph-1       -----TEKYLNVLAVKLSKPQLNFV----- 108
D.discoideum_Aph-1   KRKQAQQQKQPPTNEIESINNEIIDTTNNNTNNNNNNNNNNINDDDNKEITEEEKEKRKI 171
.. :

H.sapiens_Aph-1a      -----IRQMAYVSGLSFGIISGVFSVINILADALGPGVVGVIHG 151
M.musculus_Aph-1a    -----IRQMAYVSGLSFGIISGVFSVINILADALGPGVVGVIHG 151
X.tropicalis_Aph-1   -----IQQMAYVSGFSFGIISGVFSVINILADALGPGIVGVHIG 151
M.musculus_Aph-1b    -----MRLLAYVSGLGFGIMSGVFSFVNTLSNSLGGPGTVGIHG 150
M.musculus_Aph-1c    -----MRLLAYVSGLGFGIMSGVFSFVNTLSNSLGGPGTVGIHG 151
H.sapiens_Aph-1b     -----MRLLAYVSGLGFGIMSGVFSFVNTLSNSLGGPGTVGIHG 150
D.melanogaster_Aph-1 -----KHILAYVSGLGFGIISGMFALVNVLADMSGPGTGMGLKG 141
C.sinesis_Aph-1      DPSNQDGGVLPSTKLTGNDGLDHRIVAVVSGLGFGIMTCTIFELLRLIDAWGPGIGFEVW 187
A.thaliana_Aph-1     -----DKLQIALAGGLGHGVAHAFVFCLSLLTPAFGPAATFYVER 150
P.patens_Aph-1       -----DRLEVSFGSGVGHGVAHAIFFGLSVIAPAFGPATYYTES 147
D.discoideum_Aph-1   EKQKQREIEINARLETLSARPNTLSSAAGVSGVAYGFMFGSILWESTGPGTLFSPA 231
:      * .. * : : : : : : : : : : : : : : : * ..

H.sapiens_Aph-1a      DSPY-YFLTSAFLTAAILLITFWGVVFFDACERRRYWALGLVGSLLTSGTLFLNP-- 208
M.musculus_Aph-1a    DSPY-YFLTSAFLTAAILLITFWGVVFFDACERRRYWALGLVGSLLTSGTLFLNP-- 208
X.tropicalis_Aph-1   DSQY-YFLTSAFLTMAIVFLITFWGIVFFACEKRKPLHIIGVLSHLVASGLTFLNP-- 208
M.musculus_Aph-1b    DSPQ-FFLNSAFMTLVVIMLVFWGVVFFDGCEKNKWTLLTLLTLVLTSTQTFLSP-- 207
M.musculus_Aph-1c    DSPQ-FFLNSAFMTLVVIMLVFWGVVFFDGCEKNKWTLLTLLTLVLTSTQTFLSP-- 208
H.sapiens_Aph-1b     DSPQ-FFLYSAFMTLVIILVFWGVVFFDGCEKKKGILLIMLTLTLVLSAQTFISS-- 207
D.melanogaster_Aph-1 GTEL-FFVTSAAQALSIIILLTFWSVIFSNADFNTNNYIHIGYVFSFLVSLITLLNANE 200
C.sinesis_Aph-1      EAKT-FYLVAAFQVMCTSLMHI FWSVILFAAFERRDYVLLVLMYATHLAVPYLSFLNRLH 246
A.thaliana_Aph-1     CSKVPFPLISALIALAFVTITFTFSMVIAPFEGYAKGNKVDQIIMPVILHTAGMLTLVNF-- 208
P.patens_Aph-1       CKEMPFFLVSAALLTLAFFLLITFTFSMVIAPFNAYTHGVGSQKLFMPVMLGASFLTINL-- 205
D.discoideum_Aph-1   CPSVNLFLSSIITFLMTLLHVYNVLAEGYRSKKYHLVAFMITHFVTYTLTLNLP-- 290
: : : : : : : : : : : : : : : : : : : : : : : : : : : :

H.sapiens_Aph-1a      WYEASLLPIYAVTVSMGLWAFITAGGSLRSIQRSLLCRRQEDSRVMVYSALRIPPED--- 265
M.musculus_Aph-1a    WYEASLLPIYAVTVSMGLWAFITAGGSLRSIQRSLLCRRQEDSRVMVYSALRIPPED--- 265
X.tropicalis_Aph-1   MYEASLPIYIITLGMALWAFVAAAGNYQNRKCLACAR----- 247
M.musculus_Aph-1b    YVEVNLVTAYIIMVLMGIWAFYVAGGSCRSCLKCLLCQDKD---FLLYNQRSR----- 257
M.musculus_Aph-1c    YVEVNLVTAYIIMVLMGIWAFYVAGGSCRSCLKCLLCQDKD---FLLYNQRSR----- 258
H.sapiens_Aph-1b     YYGINLASAFIILVLMGTWAFVLAAGGSCRSCLKCLLCQDKN---FLLYNQRSR----- 257
D.melanogaster_Aph-1 LYTTTLINLYLVITLTVGLAFRVAGGTSRSFRKFITCQ----- 238
C.sinesis_Aph-1      PPWPPELVCLFYMVVLVGLAIVARCVTGKRFCCGVQPPQAIADDET----- 293
A.thaliana_Aph-1     ASEGCVIGVPLLYLVASLTIVHCGKVMVWQR-----LLESRNQSSASR----- 250
P.patens_Aph-1       LPNGCIVGVPLVFLCTLVMTVYGDRIWENTDPNLFNHSSLSQSMHSGSSL----- 255
D.discoideum_Aph-1   ---TKTTCVSGSILPITGIITVFSVSGFCIFSLKSDSITKIH----- 328

```

**Appendix 1 Full alignment of *Dictyostelium* Aph-1 against human, animal, and plant Aph-1 proteins.** Black boxes indicate conserved domains or motifs across all species. Asterisks represent identical amino acids, colons represent highly similar amino acids and full stops represent similar amino acids.

O.sativa	MGGGSTAPLLAAAFACVFLAVFPFVAS--GDAATLESVPDLVKAMYINVES	48
A.thaliana_Ncstn	MAMGLIRLLSIAFTLVLLSILPLHLSLADEITSIESVPDLQKLMYVAVDG	50
P.patens_Ncstn	-----MAAIARAWGLLLLLLLLPWLA---HGSSIKSVPELESRMYSASLAG	42
M.musculus_Ncstn	----MATTRGGSGDPDPSRGRL-LLSFSVVLAGLCGGNSVERKIYIPLNK	45
R.norvegicus_Ncstn	----MATARGGSGDPDPSRGRL-LLSFSVVLAGLCGGNSVERKIYIPLNK	45
H.sapiens_Ncstn	----MATAGGGSGADPDSRGRLRLLSFCVLLAGLCRGNSVERKIYIPLNK	46
X.tropicalis_Ncstn	--MAVRTACCVRMMGEAYRGWRGLGLVALLAVVCGGNSVERKIYIPLNS	48
A.darlingi_Ncstn	-----MNPATRRNRNCWMLLPGLLLLLLALLDDVQCQRIKDNMYVRVTG	43
C.quinquefasciatus_Ncstn	-----MGSPQVTNLRQWPTLLLLLVIAASVQNADSQRIKDNMYASISG	43
D.melanogaster_Ncstn	-----MEMRLNAASIWLILSYGATIAQGERTRDKMYEPIGG	37
C.elegans_Ncstn	-----MKKWLVIVLIIAGIRCDGFSQVFTLFIGEGN	33
N.americanus_Ncstn	-----	
D.discoideum_Ncstn	-----MKIKNYFIIVFIIIVLSTDVISSQSSIEDKMYTSLNS	37
O.sativa	-FPCVRLNLNHSQVGCSSNP--GHDKVIAPIVRFGNRNDQ-----L	85
A.thaliana_Ncstn	-FPCVRLNLNLSGEIGCSSNP--GINKVVAPIIKLKDVKD-----L	86
P.patens_Ncstn	-FPCVRLNLNLTEIGCANP--GHGAVSAPILRMGDALD-----	77
M.musculus_Ncstn	TAPCVRLNLNATHQIGCQSSISGDTGVIHVVEKEEDLKWV-----LTDGP	89
R.norvegicus_Ncstn	TAPCVRLNLNATHQIGCQSSISGDTGVIHVVEKEEDLKWV-----LTDGP	89
H.sapiens_Ncstn	TAPCVRLNLNATHQIGCQSSISGDTGVIHVVEKEEDLQWV-----LTDGP	90
X.tropicalis_Ncstn	TAPCVRLNLNATHQIGCQSSKNGDTGVIHVVEQEDDLQWV-----LESGP	92
A.darlingi_Ncstn	-AHCFFRLNGTHVTGCSSEYGGSVGVLHWIERKEDIDFL-----VNKHP	86
C.quinquefasciatus_Ncstn	-AHCFFRLNGTHVTGCSRRQGSIGVHLVRSVADIDFV-----VEQHP	86
D.melanogaster_Ncstn	-ASCFFRLNGTHVTGCSSTYSGSVGVLHLINVEADLEFL-----LSSFP	80
C.elegans_Ncstn	--ACYRTFNKTHEFGCQANRENENGLIVRIDKQEDFKNLDSCWNSFYPKY	81
N.americanus_Ncstn	-----MSEAKSMILGFSKEDYNG---VVVFLKEDELKQLRDCWRERFKDY	41
D.discoideum_Ncstn	-YPCTRIMTLNGQIGCSSSHGGDSGILYLIDSDESYHNY-----FSYNQ	80
O.sativa	VQPSAVLLPLNQMTDFFLRVSNDEPELYRKIAGVLVEANG-----VDNML	129
A.thaliana_Ncstn	VQPHITILVTADEMEDFFTRVSTDLSFASKIGGVLVESGSNF---QQKLK	132
P.patens_Ncstn	-SPATVLVPAESFEFVDRFGDD---KNVVGVLVENGSG-----QAPGF	116
M.musculus_Ncstn	NPPYMVLLLEGKLFTRDVMKLGKTTSRIGLAVTLAK-----PNSTS	131
R.norvegicus_Ncstn	NPPYMVLLLEGKLFTRDIMEKLGKTTSRIGLAVTLAK-----PNSTS	131
H.sapiens_Ncstn	NPPYMVLLLESKHFTRDLMKLGKTTSRIGLAVSLTK-----PSPAS	132
X.tropicalis_Ncstn	HPPYMVVLEASLLRRDTMQKLGST-RVSGIAVTFSQ-----TGPA	133
A.darlingi_Ncstn	SPPYAPILSPALYTRENVLRLRDEAAPYISALVLINN-----VTGMQ	128
C.quinquefasciatus_Ncstn	AGPYAPVIPPHLFTRENILRLRDQGGEHVSAVVLINN-----ASELV	128
D.melanogaster_Ncstn	SPPYAPMIPPHLFTRNLMRLKEAGPKNISVVLINN-----TNQMK	122
C.elegans_Ncstn	SGKYWALLFPVNLIRDTISQLKSSKCLSGIVLYNSGES----IHPGDEST	127
N.americanus_Ncstn	FGKYHVVLSTNSINRVVDSILESSCIAGLIVIDSESE----LDPTER--	85
D.discoideum_Ncstn	QKDIIIVFDSNYFNKTLVLEMYSKKKMNGALVLTDIG-----KTY	120
O.sativa	EFSPDRKEFQQAFAFYS-----NLSHHWNPTGSGIMWNK	163
A.thaliana_Ncstn	GFSPDKREFQAQFSPYE-----NVEYKWNASASSIMWRN	166
P.patens_Ncstn	GASDDARFQQAFAFYPY-----NQSWVWNPFGSGMMHRR	150
M.musculus_Ncstn	SFSPSVQCFNDGFGIYSNSYGPEF-----AHCKKTLWNLGNGLAYED	174
R.norvegicus_Ncstn	SFSPSVQCFNDGFGIYSNSYGPEF-----AHCKKTLWNLGNGLAYDD	174
H.sapiens_Ncstn	GFSPSVQCFNDGFGVYSNSYGPEF-----AHCREIQWNSLGNGLAYED	175
X.tropicalis_Ncstn	GFSPDPQCFNDGFGLYTSDHGPF-----AHCNHTTNPLGSGISYED	176
A.darlingi_Ncstn	HFSQEAECFNEYSSLLFSLGSDSSSEDRCSADRPESKSWNPWGSGLLQEE	178
C.quinquefasciatus_Ncstn	QYSQESRCFNFQFSLIS--GTPDS-----CSVERPERSWNPWGTGLLED	171
D.melanogaster_Ncstn	QFSHELNCENQYSGLNS--TSET-----CDASNPAKNWNPWGTGLLED	164
C.elegans_Ncstn	AASHDAECFNAASDYLLQDKNEEY-----CERKINSRGAITRDGLMKID	171
N.americanus_Ncstn	-FSDHGACFNPNSDTYNDGCS-----SATAWNHDGYILFEGLRNI	125
D.discoideum_Ncstn	PYSPEDQYFIKQFGLYP-----DSNLNWNPNPDGFGTYMN	154
O.sativa	YDFPVFLLSE-ESTQTLQNLADKNEKSANGYLANVAEFDLVMQTTKAGTH	212
A.thaliana_Ncstn	YNFPVYLLSE-SGISAVHEILSKKKMKHGTYSVDAEFNMVMMETTKAGTH	215
P.patens_Ncstn	LNFPVFFLSSPENIELARRLASQNVKSGSRPANVVEFNDVMQTTKTGTP	200
M.musculus_Ncstn	FSFPIFILLEDENETKVIKQCYQDHNLGQNGSAPSFPLCAMQLFSHMHAVI	224
R.norvegicus_Ncstn	FSFPIFILLEDENETKVIKQCYQDHNLGQNGSAPSFPLCAMQLFSHMHAVI	224
H.sapiens_Ncstn	FSFPIFILLEDENETKVIKQCYQDHNLSQNGSAPTFFPLCAMQLFSHMHAVI	225
X.tropicalis_Ncstn	FQFPFIFFLREENETEVIKQCYREHNMPQNGSAPQYPLCAMQLSSFMYGVT	226
A.darlingi_Ncstn	FPFPIIYVFETSEVEKLRCYFKFNAHDLENQNGRSLCSIEVKAFMSAAV	228
C.quinquefasciatus_Ncstn	FPFPIIYVPHPEEIQKMVDCFAKFNNFDLENQHRRSLCSIEIKSFMSAAV	221
D.melanogaster_Ncstn	FPFPIIYIADLDQVTKLEKCFQDFNNHNYETHALRSLCAVEVKSFMMSAAV	214
C.elegans_Ncstn	WRIQMVFIDNSTDLIEIEKCYSMFNKPKEDGSGYPYCGMSFRLANMAAG	221
N.americanus_Ncstn	WKMQILYVYNDSSIEIKKVYNASSKLPDNS-----	156
D.discoideum_Ncstn	FPFPMFALELKTSIIIR-----NLSTINRDGKYPAYGAELDSFMQGA	197

O.sativa  
A.thaliana\_Ncstn  
P.patens\_Ncstn  
M.musculus\_Ncstn  
R.norvegicus\_Ncstn  
H.sapiens\_Ncstn  
X.tropicalis\_Ncstn  
A.darlingi\_Ncstn  
C.quinquefasciatus\_Ncstn  
D.melanogaster\_Ncstn  
C.elegans\_Ncstn  
N.americanus\_Ncstn  
D.discoideum\_Ncstn

DSESLR-----EQSCLPLGGQSVWTSPLPISNSSSTK 244  
NSEACLQ-----EGTCLPLGGYSVWSSLPPISVSSSN 247  
TTESCLG-----ELSCLPLGGYSVMSTFPVNVSHPL 231  
STATCMRRSFIQSTFSINP-----EIVCDPLSDYNVWSMLKPINTSSGVL 268  
STATCMRRSFIQSTFSINP-----EIVCDPLSDYNVWSMLKPINTSSGVL 268  
STATCMRRSSIQSTFSINP-----EIVCDPLSDYNVWSMLKPINTTGTTL 269  
NTVTCMRRNSLQSSFSLS-----AGVCDTIIVHNWSSSLKPINTTGTTL 269  
SSANCIRRSNFYSSVIPT-----TKFCDPLQGNVYATLFRTTQAVT 271  
DSRVCLARSIFFNINP-----VKFCDPLQGNVYATLFRVQVKLE 263  
NTEVCMRRNTNFINNLLG-----SKYCDPLEGRNVYATLPRKPAIEN 256  
NSEICYRRGKNDALFQMNIDSGDAPQLCGAMHSDNIFAFPTPIPTSPTN 271  
-----  
NAETCLR-----RGFCEPVGQSIWSSSFSEVIDQS-- 227

O.sativa  
A.thaliana\_Ncstn  
P.patens\_Ncstn  
M.musculus\_Ncstn  
R.norvegicus\_Ncstn  
H.sapiens\_Ncstn  
X.tropicalis\_Ncstn  
A.darlingi\_Ncstn  
C.quinquefasciatus\_Ncstn  
D.melanogaster\_Ncstn  
C.elegans\_Ncstn  
N.americanus\_Ncstn  
D.discoideum\_Ncstn

H-----QKPIIMVTASQDSASFFRDRSLGADSPISGLIALLTAVDA 285  
N-----RKPVVLTVASMDTASFFRDKSPGADSPISGLVALLGAVDA 288  
T-----VKPVVLMASVDSATFFRDVAPGADSPMSGVIALLAAYDA 272  
E-----PDVRVVVAATRLDSRSFFWNVAPGASAVASFVTLAAAEA 310  
E-----PDVRVVVAATRLDSRSFFWNVAPGASAVASFVTLAAAEA 310  
K-----PDDRNVVVAATRLDSRSFFWNVAPGASAVASFVTLAAAEA 311  
P-----PEEQIVVAAARADSHSFFWNLAPGADSTVSGFVTLAAAEA 311  
DESGARVRDARERIVVCTRTDTTTMFDGVGLGAMDSDVVPFVAVAVHF 321  
D-----RKVDLNERIILVSSRMDTTMFDGVGLGAMDSDVVPFVAVVSHF 309  
N-----LETVHTNEKIFILVTCRLDTTTMFDGVGLGAMDSDVVPFVAVVSHF 303  
E-----TIITSKYMMVTARMDSPGMIPISVGEVSVLTSIISVLAARS 315  
-----YLILSARMDSPGLIPEISVGEVSVLTSIISVLAARS 193  
-----KPIILVMLPIDATAFFRDLATGTDQSGYALTVLLSMLNT 266  
:: : \*

O.sativa  
A.thaliana\_Ncstn  
P.patens\_Ncstn  
M.musculus\_Ncstn  
R.norvegicus\_Ncstn  
H.sapiens\_Ncstn  
X.tropicalis\_Ncstn  
A.darlingi\_Ncstn  
C.quinquefasciatus\_Ncstn  
D.melanogaster\_Ncstn  
C.elegans\_Ncstn  
N.americanus\_Ncstn  
D.discoideum\_Ncstn

LSHLHDIS-----NLKKQLVFAVFNCEAWGYLSSRKFLQELDQGDAS-- 327  
LSRVDGIS-----LKKQLVFLVLTGCTWGYLSSRRFLHEDLDHSDA-- 330  
LSHVPDFD-----SFLKRLVFLVFTGEARGYLSSRQFLAQLKKGAF-- 314  
LHKAPDVT-----TLNRNVMFVFFQGETFDYIISSRMVYDMENGKFP-- 352  
LHKAPDVT-----TLNRNVMFVFFQGETFDYIISSRMVYDMENGKFP-- 352  
LQKAPDVT-----TLNRNVMFVFFQGETFDYIISSRMVYDMENGKFP-- 353  
LHKRNDP-----DLPRNIMFVFLQCEVYDYIISSRMVYDMENGKFP-- 353  
LAKVLPR-----SERAPNVVFMFFNGESYDYIGSRFVYDLQGTGAF-- 363  
LAKILPKRL-----QDDNPNVLFMFFNGESYDYIGSRFVYDLQGTGAF-- 353  
LKQLLPPQ-----SKDLHNVLFVTFNGESYDYIGSRFVYDMENKQFP-- 346  
MGTOIEKWQKASNTSRNVFFAFFNGESLDYIGSGAAAYQMGENGKFP-- 364  
IGSHAFAFEAAIISNKYILIALFDGGSFENIGSSDAAYSMTIEAFPRK-- 242  
LQGVDKTK-----WDKEVIFAMWNSERWGYVGSNTFVNDLLNFNCTSLD 310  
: : : \*

O.sativa  
A.thaliana\_Ncstn  
P.patens\_Ncstn  
M.musculus\_Ncstn  
R.norvegicus\_Ncstn  
H.sapiens\_Ncstn  
X.tropicalis\_Ncstn  
A.darlingi\_Ncstn  
C.quinquefasciatus\_Ncstn  
D.melanogaster\_Ncstn  
C.elegans\_Ncstn  
N.americanus\_Ncstn  
D.discoideum\_Ncstn

-----VNGISSLLIDQVLEIGS-VGKAIS-----QGY 353  
-----VAGLSNTSIETVLEIGS-VGKGLS-----GGI 356  
-----DYGLT-----SIHQILEVGS-VGQASE-----ATF 338  
-----VRLENIDSFVELGQVALRTSLDLW-----MHT 379  
-----VRLENIDSFVELGQVALRTSLDLW-----MHT 379  
-----VQLENVDSFVELGQVALRTSLDLW-----MHT 380  
-----VSLGNIHSFVELNQVALRNDLFLW-----VHT 380  
-----SRST-QTKPISLDNIELLIELGTL-----DDL 389  
-----TKGG-LTNPLSLDNIDLMIDLGTFF-----DDP 379  
-----TEST-GTPPIAFDNIDFMDLIGTL-----DDI 372  
-----IRSD-RTHIHPIRPNELDYILEVQOIGVAKGRK 396  
-----LKSVSVPQLDLIGIPQLDAIIEVQQLGTGDGST 275  
SNNQNSCSPMPLDLTFEQIKFENIYAIIEFNQIGRPVNSGKKTPNKLDI 360  
: : \*

O.sativa  
A.thaliana\_Ncstn  
P.patens\_Ncstn  
M.musculus\_Ncstn  
R.norvegicus\_Ncstn  
H.sapiens\_Ncstn  
X.tropicalis\_Ncstn  
A.darlingi\_Ncstn  
C.quinquefasciatus\_Ncstn  
D.melanogaster\_Ncstn  
C.elegans\_Ncstn  
N.americanus\_Ncstn  
D.discoideum\_Ncstn

PLFYAHAAGNSSISMKMVDALQSASESLGSDNVKVPKPAASSNPGVPPSSL 403  
NTFFAHKTRVSSVTNMTLDALKIAQDSLASKNIKILSDADANPGIPPPSSL 406  
-FVHKQATAAAVDTOQIIDALYLSASSTDS--TVKLANEDNPGIPPPSSL 384  
DPMSQKNESVKNQVEDLLATLEKSG--AGVPEVVLRLRAQSQA-LPPSSL 426  
DPMSQKNESVKNQVEDLLVTLQSG--ADTPQVLSRLVQSQA-LPPSSL 426  
DPVSQKNESVRNQVEDLLATLEKSG--AGVPAVILRRPNQSQ-LPPSSL 427  
DPISRTNETVNATVQEVVDSLVAAS--QGS-NVTIQEVDRSQ-LPPSSL 426  
TELQVYHAAPQPMATKMEVEVLKVNKAFNFNITTKPSKQTTN-LPPVSA 438  
NNLRIYHASELATVPQIAQAIDQINRKWNLVNTAEAP-ILTKN-LPPVSS 427  
SNIKHLALNGTTLAQQILERLNNYAKSPRYGFNLNIQSEMSAH-LPPISA 421  
YVHVVDGERYQONKTQTDRIIDRIERGLRSHAFLEKPSGSGDRVPPASW 446  
LNLADGEQFQSDKLKN--MLDSLARGAEAVGGSNLNYPTAS-SRMPSSSW 322  
YNLVFHPNGGAG-ANQLMDVFSQSTQSYEN--STIQFQKTQNELPPSS 407  
: : \*

O.sativa  
A.thaliana\_Ncstn  
P.patens\_Ncstn  
M.musculus\_Ncstn  
R.norvegicus\_Ncstn  
H.sapiens\_Ncstn  
X.tropicalis\_Ncstn  
A.darlingi\_Ncstn  
C.quinquefasciatus\_Ncstn  
D.melanogaster\_Ncstn  
C.elegans\_Ncstn  
N.americanus\_Ncstn  
D.discoideum\_Ncstn

MSFLGKNSS-----TPGLVLEDFDSQFSNRFYHSTLDGPNVNSSS-- 444  
MAFMRKNPQ-----TSAVVLEDFDTNFVNKFYHSHLDLNLNINSS-- 447  
MTFVHNDPT-----VAGVVEEFDTAFNKKYNSVDDNSSNVNLP-- 425  
QRFLRARN-----ISGVVLADHSGSFHNRYYQSIYDTAENINVTYPEP 469  
QRFLRARN-----ISGVVLADHSGSFHNRYYQSIYDTAENINVTYPEP 469  
QRFLRARN-----ISGVVLADHSGAFHNKYYQSIYDTAENINVTYPEP 470  
QRFLRVRN-----IPGVVLTDHRTAYSNRYHSHVYDTADNIMHRYPEG 469  
NSFLRENA-----SFPAILINSP--VRNRYHSHVYDGAKNLNRYRNH 479  
NSFLRENA-----SFPVVVTS--PGNRYHSHYDDSENLFKVYGNH 468  
QSFLRRDP-----FNALILNAR--PTNKYYHSIYDDADNVDFTYANT 462  
HSFAKADAH-----VQSVLLAPYGKEYEYQRVNSILDKNEWTEDE-- 488  
HSFARSR-----IKGVVLAFFSNKYECRRINSMLDRVNVNTAEQRS-- 364  
MSFIKEINKKSAPNFIGTLVITDHDYQYNNPYFGDEQDNSGNINTTTS-- 455



O.sativa	-----IAAAAALIARSLYLASAD-LPIDLITLN	472
A.thaliana_Ncstn	-----VVAAASVVARTLYILASDN-KDTSNSALG	475
P.patens_Ncstn	-----LVVAASLVARSVLVLLASDNNLRFDSPIFE	454
M.musculus_Ncstn	Q-----SPEEDLNFTDTAKALANVATVLARALYELAGGTNFSS	508
R.norvegicus_Ncstn	Q-----SPEEDLNFTDTAKALADVATVLARALYKLAGGTNFNN	508
H.sapiens_Ncstn	L-----SPEEDLNFTDTAKALADVATVLGRALYELAGGTNFSD	509
X.tropicalis_Ncstn	L-----TKDEELKYVTDARSLAGVATVLANSLYRLAGGK-STE	507
A.darlingi_Ncstn	SKLYDF*QLENLRERKDLWD*DSLQMRIRNVSS*IGMSIYELLEGNAYTP	529
C.quinquefasciatus_Ncstn	SRTDRFTELENLQQTIVDFPTNSIQMRLRNVSTLLGMTLYELVTKTAYPG	518
D.melanogaster_Ncstn	S--KDFTQLTEVNDFKSLNP--DSLQMKVRNVSSIVAMALYQ*ITGKEYTG	509
C.elegans_Ncstn	-----KAIQEI*EAVSTAILAAAADYVG*VET--DEV	516
N.americanus_Ncstn	-----AAISEITLAASSLLYAAADHVRNLSSANI	393
D.discoideum_Ncstn	-----TLFDMVQVFSKSIDLLAGGN---G	476
:		
O.sativa	TIKVNVS*LV*EELIGCLLKCDPGLSCGIVKSFISPSNSCPSHYVGVFQDLP	522
A.thaliana_Ncstn	SIHVNAS*FVEELLTC*LLACEPGLSCNLVKDYISPTNTCPGNYAGVILGEP	525
P.patens_Ncstn	SIQVNMS*LV*EEMVNCFFGTSPGMRC*SLVESLMTASHDVANHYVGVFQADP	504
M.musculus_Ncstn	SIQADPQT*VTRLLYGFLVKANNSWFQ*SLKHDLRSYLD*DRPLQHYIA---	555
R.norvegicus_Ncstn	SIQADPQT*VTRLLYGFLVRANNSWFQ*SLRHDLRSYLD*DGPLQHYIA---	555
H.sapiens_Ncstn	TVQADPQT*VTRLLYGFLKANNSWFQ*SLRQDLRSYLD*DGPLQHYIA---	556
X.tropicalis_Ncstn	EIKADPNT*VTQMLYGFLKMSNNSWFQ*SIIRDEWRNVLEATQ*QYYMTGTI	557
A.darlingi_Ncstn	EYGANSVLID*EFLHCFLEASDCPLFRATIRPEASINEFAGPPARYISVYS	579
C.quinquefasciatus_Ncstn	TLGTSPYLID*EFLYCLFQ*SDCPLFMAAVKPD*FPR--PFPIS*PQRYISVHS	567
D.melanogaster_Ncstn	TKVANPLMA*DEFLYCLFQ*SDCPLFKAASYPG*SQL--TNL*P*MYRISVLG	557
C.elegans_Ncstn	VAKVDKKLIT*TIIFDCLITSNFW*DCDFMQKLDGGRYHKLFNSYGFNQKST	566
N.americanus_Ncstn	SLEIDRDFVSVLV*ECFIDSPNWIECDFK*MDLSQHIRPG-----MWDL	437
D.discoideum_Ncstn	TVKVDDLFIREIN*VCLTQ*SITCNVWTKLMSTFPYNFIPNFYSGVYGVSPV	526
:		
O.sativa	AGTQ--FPSYADDISRFIWNFLADRTSSLAGNSSSCT-----GQCH	561
A.thaliana_Ncstn	SSKP--YLGYVG*DVSRFLWNFLADKTSVQKGN*TT*SVCSK-----GVCS	566
P.patens_Ncstn	SVSPNSM*EVIDD*TRFVWNFLADRTALPREDLHEKCT-----LVCK	546
M.musculus_Ncstn	---VSSPTNTTYV*VQYALANLTGKATNLTRE*QCQDPSKVPN*ESKDL*EYS	602
R.norvegicus_Ncstn	---VSSPTNTTYV*VQYALANLTGKVTNLTQE*QCQDPSKVPN*ESKDL*EYS	602
H.sapiens_Ncstn	---VSSPTNTTYV*VNLTR*EQCQDPSKVPN*ESKDL*EYS	603
X.tropicalis_Ncstn	K*TSREPN*SPARLLAVFANLTGAVVNLTK*E*CN*PDKID*DENKELY*YT	607
A.darlingi_Ncstn	SITAEATY*VTYQVLGLLVGQ*RVEN---VTKEECLARH-----LPYQ	617
C.quinquefasciatus_Ncstn	TLFSEASSWTIRLLGFLIGQ*LP*NDTNTSRAD*CALH-----LPYN	608
D.melanogaster_Ncstn	GS-QESSGYTYRLLGYLLSQ*LPD---IHRD*NC*TD-----LPLH	592
C.elegans_Ncstn	YISMESHTA*FPTVLH*WLTIFALGSDKETLNVKSEKSCSHLGG*FQAFQMYT	616
N.americanus_Ncstn	CLSLELVERVSPRRQ*TLQLLLHSSRLDPI*WKN-----VYY	473
D.discoideum_Ncstn	NHITPIETRFIFRMATYLTQ*HRTNATNCTSDND*CDTS-----	563
:		
O.sativa	DEGEICVGAEEV*GGGRV*VSTTRYVPAYSTR*LFKFED--NVVHVLFPVNSSD	609
A.thaliana_Ncstn	KTDEVCIKAESNKEGT*CVVSTTRYVPAYSTR*LFKYND--GAWTILPQNSSD	614
P.patens_Ncstn	NPDEVCGATQSQ*LGQCRVSSTRYVPAYSP*RLKFHD--YWWQLLPLEAGD	594
M.musculus_Ncstn	WVQGPWNSN*RT*ERLP*QCVRS*TVRLARALSPAFELS---QWSSTEYS---	645
R.norvegicus_Ncstn	WVQGPWNSN*KT*ERLP*QCVRS*TVRLARALSPAFELS---QWSSTEYS---	645
H.sapiens_Ncstn	WVQGPLHSN*ET*DLR*P*CVRS*ARLARALSPAFELS---QWSSTEYS---	646
X.tropicalis_Ncstn	WVQGPLDGN*STSR*LP*PCVRS*ATHSHV*ABSPAFELD---QWDSTEYS---	650
A.darlingi_Ncstn	WMAG-----YSGEGMCLLTQNTSLAISP*AF*LN*ET---YDWT*SYRYS---	656
C.quinquefasciatus_Ncstn	WFAG-----YSGHGECLRTQNF*SQASSPAFL*DDD---YDFRS*GRYS---	647
D.melanogaster_Ncstn	YFAG-----FNNIGECRLTQNYSHALSP*AF*LDG---YDWS*SGMYS---	631
C.elegans_Ncstn	YTWQP---NPYTGNFSCLKSAIVKKVMVSP*AVDSQ*TP--EEM*NNTRY*---	659
N.americanus_Ncstn	YIWQV---DPNSGIRH*CV*RT*PVSLFEV*VSPAFQ*IKG---YNF*TNNTFS---	515
D.discoideum_Ncstn	-----SSICVNKVC*LYSNTHYHNAISLAFSPD*NSKSSWTIVNTS---	602
:		
O.sativa	PFSAADPVWTESFWNTIGLRVYAVQATS*YD*WLVL*LGIIITVAS*YFAVIV	659
A.thaliana_Ncstn	SMGMVDPVWTESNWD*TLRVH*VYTVQHSAYD*NAV*LVAGITV*TLAYIGILA	664
P.patens_Ncstn	KMGAADPVYTESFWNSISIRSYQKEDS*WYEELILF*IGVFVTFV*VSI*LT*YC	644
M.musculus_Ncstn	-----TWAESRWKDIQARIFLIASKKLEFITLIVGFSILFVSLIVTYC	688
R.norvegicus_Ncstn	-----TWAESRWKDIQARIFLIASKELEFITLIVGFSILFVSLIVTYC	688
H.sapiens_Ncstn	-----TWTESRWKDIRARIFLIASKELELITLVGFGILFSLIVTYC	689
X.tropicalis_Ncstn	-----TWTESRWKEIKARIFLVPSHELEVITLVVGIAVLLVSLLT*TYF	693
A.darlingi_Ncstn	-----TWTESTWSEMSARIFLRPSPAHETL*TL*SIGIVVMV*ISFLLVFL	699
C.quinquefasciatus_Ncstn	-----TWTESTWREMSARIFLQPAASHETL*TL*SIGFVVM*LLSFVLLVFL	690
D.melanogaster_Ncstn	-----TWTESTWSQFSARIFLRPSNVHQV*TL*SVGIVVLI*ISFCLVYI	674
C.elegans_Ncstn	-----TWMESVYIIESVNL*YL*MEDASFEYTMILIAVISALLSIFAVGR	702
N.americanus_Ncstn	-----TWTESHYRIENLR*LYLVIDTSFEYIMFGIGIAFLIVSFLIVGR	558
D.discoideum_Ncstn	-----Y*PVFVESNWDYTTVRLFQVGSYANEI*WFLVSG*LI*ELL*SVGIIFY	647
:		
O.sativa	GRSYISKIKRD-----	671
A.thaliana_Ncstn	AKSIITKALKQD-----	676
P.patens_Ncstn	STSLLRKRLKRA-----	656
M.musculus_Ncstn	INAKADVL*FVAPREP*GAVSY-----	708
R.norvegicus_Ncstn	INAKADVL*FVAPREP*GAVSY-----	708
H.sapiens_Ncstn	INAKADVL*FIAPREP*GAVSY-----	709
X.tropicalis_Ncstn	INAKADIL*FTNTQDS-DVAY-----	712
A.darlingi_Ncstn	INRSRDVL*FNQGGSS*TIPIATQPTQC	725
C.quinquefasciatus_Ncstn	INRSSEVL*FNQCGASTVP-----	708
D.melanogaster_Ncstn	ISSRSEVL*FEDLPASNAALFG-----	695
C.elegans_Ncstn	CSETTFIVDEGEPA*EGGEPL-----	723
N.americanus_Ncstn	CND*DTFMIKAREHSSEGE-----	576
D.discoideum_Ncstn	IKKYL*SKRYKLL-----	659

**Appendix 2 Full protein alignments of *Dictyostelium* Nicastrin against human, animal, and plant Nicastrin proteins.** Black boxes indicate conserved motifs and domains across all species. Asterisks represent identical amino acids, colons represent highly similar amino acids and full stops represent similar amino acids.

```

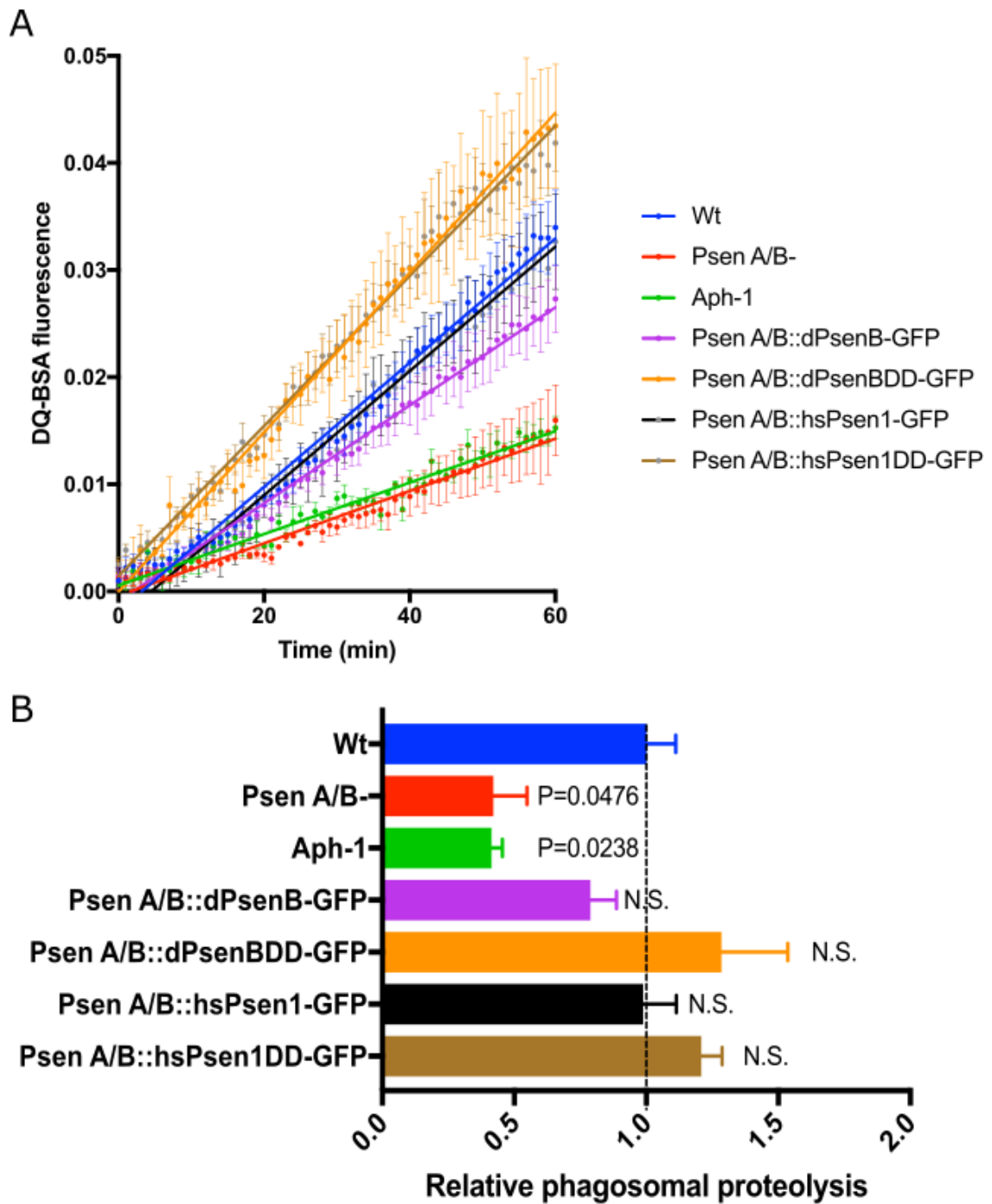
H.sapiens_Pen-2      -----MNLE-----RVSNEEKLNLCR 16
M.musculus_Pen-2    -----MNLE-----RVSNEEKLNLCR 16
R.norvegicus_Pen-2  -----MNLE-----RVSNEEKLNLCR 16
D.rerio_Pen-2       -----MNLE-----RIPNEEKLNLCR 16
X.tropicalis_Pen-2  -----MNLE-----RVPNEEKLQLCR 16
D.melanogaster_Pen-2 -----MDIS-----KAPNPRKLELCR 16
C.elegans_Pen-2     -----MDIS-----KLTDVKKVDLCK 16
D.discoideum_Pen-2  -----MLIPEDD---KLDDEKMINIAK 19
A.thaliana_Pen-2    MEATRSDDPSLNPIRNRPNPNPNPLSTIISSAQVWPTIDG---PLGLTEEASVDYAR 57
C.clementina_Pen-2 MDASQSDN-----RIPNPNPRGNNGNSITLSTPVWPTIDG---PLGLTEDDSLSYAR 49
P.patens_Pen-2      -----WPTIDG---PLGVYHEEAVNLAK 20
G.aurea_Pen-2       MENEPNNYADAGAVTGFLPTTVSAGNPSSIGRLNRAEWLTIDG---PLGLSNEESLVYAR 57
                                     : . : ..

H.sapiens_Pen-2      KYYLGGFAFLPFLMLVNIWFEEFREAFLVPAYTEQSQIKGVWRSVAVGFLFWVIVLTSMIT 76
M.musculus_Pen-2     KYYLGGFAFLPFLMLVNIWFEEFREAFLAPAYTEQSQIKGVWRSVAVGFLFWVIIATWIT 76
R.norvegicus_Pen-2   KYYLGGFAFLPFLMLVNIWFEEFKEAFFAPAYTEQSQIKGVWRSVAVGFLFWVIVLTWIT 76
D.rerio_Pen-2        RYYLGGFAFLPFLMLVNIWFEEFKEAFLKPAYTEQPQIKSVKKSALGLLLWVAVLTTWIT 76
X.tropicalis_Pen-2   KYYLGGFAFLPFLMLVNIWFEEFKEAFFKPAYTEQPLIQSVKRSALGLFWVIVLTWIS 76
D.melanogaster_Pen-2 KYFFAGFAFLPFLVNIWFEEFTEAFHKPPFSEQSQIKRVVIYSVAVGTLFWLIVLTAWII 76
C.elegans_Pen-2      KYFLIGACFLPLVNIWFEEFSDAFCKPINAHRRQIRKVIASIVGSIFWIIIVLSAMEI 76
D.discoideum_Pen-2   KLWFIQFFFLPFWVNLINILYFIP--YRNSLN---DKVKWMLKFSLIGFLGYSTIFMGWVG 74
A.thaliana_Pen-2     RFYKFGFALLPFLVNIWFEEFVWPVLR--HSR-AFPQIRNVVRSVAVGFSVFTALLSAAWAL 114
C.clementina_Pen-2  KFYQFGFALLPFLVNIWFEEFVWPVLR--HSA-SFPRIRHVVLGSAVGFVAVTVVLLSWAL 106
P.patens_Pen-2       SFYYVGFGLCLPFLVNIWFEEFVWPVLR--NSR-SDPLIRPVVVKSGIGFLVCGSLLLSWAL 77
G.aurea_Pen-2        RFFKFGFGLCLPFLVNIWFEEFVWPVLR--NSR-SDPLIRPVVVKSGIGFLVCGSLLLSWAL 117
                                     : * ** : * : * : * : * : * : * : * : *

H.sapiens_Pen-2      IFQIYRPRWG--ALGDYLSFTIPLGTP----- 101
M.musculus_Pen-2     IFQIYRPRWG--ALGDYLSFTIPLGTP----- 101
R.norvegicus_Pen-2   IFQIYRPRWG--ALGDYLSFTIPLGTP----- 101
D.rerio_Pen-2        VFQHFRAQWG--EVGDYLSFTIPLGTA----- 101
X.tropicalis_Pen-2   VYQTHRAGWG--ATGDYLSFTIPLGIP----- 101
D.melanogaster_Pen-2 IFQTNRTAWG--ATADYMSFIIPLGSA----- 101
C.elegans_Pen-2      FFQHYRAQGL--VWTDFTLTFVPTGRV----- 101
D.discoideum_Pen-2   IYLVNRNKWG--AFGDDISITIPFG----- 97
A.thaliana_Pen-2     TFSIGGEQLFGPLYDKLVMYNVADRLGLSLGLA 146
C.clementina_Pen-2  TFAIGGEHLFGSVWDKLVMYNVVAERLGLTGWS 138
P.patens_Pen-2       TFAYGGEGLLGPSSWKHLAVYDIANK----- 102
G.aurea_Pen-2        TFAIGGEKLFGHAWQDLVMYNVADKYGLTGWI 149
                                     : . : ..

```

**Appendix 3. Full protein alignments of *Dictyostelium* Pen-2 against human, animal, and plant Pen-2 proteins.** Black boxes indicate conserved motifs and domains across species. Asterisks represent identical amino acids, colons represent highly similar amino acids and full stops represent similar amino acids.



**Appendix 4 DQ-BSA acidification in  $\gamma$ -secretase null mutants.** A) Fluorescence of phagocytically engulfed DQ-BSA during phagosomal acidification in wild-type, PsenA<sup>-</sup>/B<sup>-</sup>, Aph-1<sup>-</sup>, PsenA<sup>-</sup>/B<sup>-</sup>::PsenB-GFP, PsenA<sup>-</sup>/B<sup>-</sup>::PsenBDD-GFP, PsenA<sup>-</sup>/B<sup>-</sup>::hPsen1-GFP, PsenA<sup>-</sup>/B<sup>-</sup>::hPsen1DD-GFP cells. PsenA<sup>-</sup>/B<sup>-</sup> cells and Aph-1<sup>-</sup> cells exhibit a decrease in fluorescence upon uptake and acidification (error bars = SEM). B) Rate of uptake shows a significant decreased ( $p < 0.05$ ) in proteolysis in Aph-1<sup>-</sup> and PsenA<sup>-</sup>/B<sup>-</sup> cells compared to wild-type cells which is rescued upon expression of *Dictyostelium* or human Presenilin. Additionally, catalytically inactive mutants (PsenBDD, hPsen1DD) are capable of restoring acidification to wild-type levels ( $p > 0.05$ ).